Flux Performance and Silver Leaching From In-Situ Synthesized Silver Nanoparticle Treated Reverse Osmosis Point of Use Membranes

by

Sean Zimmerman

A Thesis Presented in Partial Fulfillment
of the Requirements for the Degree
Master of Science

Approved October 2017 by the
Graduate Supervisory Committee:

Paul Westerhoff, Chair
Francois Perreault
Shahnawaz Sinha

ARIZONA STATE UNIVERSITY
December 2017

ABSTRACT

Drinking water filtration using reverse osmosis (RO) membranes effectively removes salts and most other inorganic, organic, and microbial pollutants. RO technologies are utilized at both the municipal and residential scale. The formation of biofilms on RO membranes reduces water flux and increases energy consumption. The research conducted for this thesis involves In-Situ coating of silver, a known biocide, on the surface of RO membranes. This research was adapted from a protocol developed for coating flat sheet membranes with silver nanoparticles, and scaled up into spiral-wound membranes that are commonly used at the residential scale in point-of-use (POU) filtration systems. Performance analyses of the silver-coated spiral-wound were conducted in a mobile drinking water treatment system fitted with two POU units for comparison. Five month-long analyses were performed, including a deployment of the mobile system. In addition to flux, salt rejection, and other water quality analyses, additional membrane characterization tests were conducted on pristine and silver-coated membranes.

For flat sheet membranes coated with silver, the surface charge remained negative and contact angle remained below 90°. Scaling up to spiral-wound RO membrane configuration was successful, with an average silver-loading of 1.93 μg-Ag/cm^2. Results showed the flux of water through the membrane ranged from 8 to 13 liters/m^2*hr. (LMH) operating at 25% recovery during long-term of operation. The flux was initially decreased due to the silver coating, but no statistically significant differences were observed after 14 days of operation ($P < 0.05$). The salt rejection was also not effected due to the silver coating ($P < 0.05$). While 98% of silver was released during long-term

studies, the silver release from the spiral-wound membrane was consistently below the secondary MCL of 100 ppb established by the EPA, and was consistently below 5 ppb after two hours of operation. Microbial assays in the form of heterotrophic plate counts suggested there was no statistically significant difference in the prevention of biofouling formation due to the silver coating ($P < 0.05$). In addition to performance tests and membrane characterizations, a remote data acquisition system was configured to remotely monitor performance and water quality parameters in the mobile system.

DEDICATION

I dedicate this thesis to my family, friends, and colleagues who were always there for support, motivation, commiseration, and to enjoy libations with when necessary. While work can be enjoyable, during research, data analysis, and writing, it was easy to become frustrated and unmotivated with the routine and meticulous nature of it all. Without my friends and family reminding me to step back and remain focused on the reason I was pursuing a Master's Degree, it would have been much easier not to put in the time and effort necessary to complete the degree. Thank you to everyone who provided me with the drive and focus to achieve my goals.

ACKNOWLEDGMENTS

The first person I would like to thank is my advisor Dr. Paul Westerhoff, for providing me with the opportunity to advance my knowledge and reignite my passion to pursue a career in environmental engineering. Without Dr. Westerhoff recognizing my personality type as a "hands-on" researcher and employing me in the pilot-scale drinking water treatment sector, I would not be as prepared as I am today for a career in consulting. The next person I would like to thank is my mentor Dr. Shahnawaz Sinha, who took the time and effort to explain to me in detail the reasons and theories behind the experiments we conducted, and was there for me every day to answer any questions I had and to keep me on track. Without Dr. Sinha's knowledge and guidance, I would not have completed the work necessary to compose a M.S. Thesis. I would also like to thank my other committee member Dr. Francois Perreault, who took the time to provide me with supplementary means to gain the knowledge (and lab results) in a field in which I had little to no experience, microbiology. Additionally, I would like to thank those who provided further understanding and lab work for my research, including Yuqiang Bi for running (a lot of) ICP-MS, and Doug Rice for helping me through the microbiology work conducted. Finally, I would like to thank my family, friends and colleagues who provided me with support, motivation, and further understanding needed to complete my work, including Harsh Ashani, Omar Alrehaili, Emmy Pruitt, Madelyn Pandorf, Stephanie Bone, and Sepideh Hakim-Elahi. This work was partially funded through the Nano-Enabled Water Treatment Technologies Nanosystems Engineering Research Center by the National Science Foundation (EEC-1449500). Partial funding was also provided from the US Environmental Protection Agency through the STAR program (RD83558001).

TABLE OF CONTENTS

Page

LIST OF TABLES viii

LIST OF FIGURES ix

CHAPTER

1 INTRODUCTION 14

2 MATERIALS AND METHODS 17

2.1 Flat Sheet Membranes 17

Membrane Coating Procedure 18

Membrane Characterization 19

Permeability Tests 19

Surface Charge 21

Scanning Electron Microscope & Energy Dispersive X-Ray 22

Static Leaching Tests 23

2.2 Spiral-Wound Membranes 26

Membrane Coating Procedure 27

Membrane Characterization 30

Silver Loading on Spiral-Wound RO Membrane 31

Dynamic Leaching Test 32

Contact Angle Measurements 33

Mobile NEWT Testbed 35

Point of Use Configuration 37

Run 1: Baseline Unit Comparison 39

CHAPTER Page

Run 2: Pristine Membrane vs. Silver-Coated Membrane 39

Run 3: Contaminant Removal Efficiency of Hexavalent Chromium40

Run 4: Induced Fouling Test 42

Run5: Deployment to Chandler Water Treatment Plant..... 43

3 RESULTS 48

3.1 Flat Sheet Membranes 48

Permeability Tests..... 48

Microfiltration Membranes 48

Ultrafiltration Membranes..... 51

Reverse Osmosis Membranes 54

Static Leaching Tests..... 56

Microfiltration Membranes 56

Ultrafiltration Membranes..... 58

Reverse Osmosis Membranes 60

Scanning Electron Microscope & Energy Dispersive X-Ray..... 62

Microfiltration Membranes 63

Ultrafiltration Membranes..... 66

Reverse Osmosis Membranes 71

Surface Charge..... 73

3.2 Spiral-Wound Membranes..... 76

Membrane Characterization 76

Silver Loading on Spiral-Wound RO Membrane..... 76

CHAPTER Page

Contact Angle Measurements 77

Dynamic Leaching Test..... 79

Mobile NEWT Testbed 82

Run 1: Baseline Unit Comparison..... 82

Run 2: Pristine Membrane vs. Silver-Coated Membrane 89

Run 3: Contaminant Removal Efficiency of Hexavalent Chromium 96

Run 4: Induced Fouling Test..... 105

Run5: Deployment to Chandler Water Treatment Plant..... 114

Remote Data Acquisition 126

4 DISCUSSION 132

Permeability Tests..... 132

Static Leaching Test..... 133

Scanning Electron Microscope & Energy Dispersive X-Ray..... 134

Silver Loading on Spiral-Wound RO Membrane 134

Mobile NEWT Testbed..... 135

5 SUMMARY AND CONCLUSIONS 141

Future Research For This Project 144

REFERENCES 145

LIST OF TABLES

Table Page

2.1: Membrane Product Specifications 17

2.2: Static Leaching Test membrane Transfer Time 26

3.1: Flat Sheet membrane Average Flux Summary (LMH) 55

3.2: Cumulative Silver Leached 62

3.3: Membrane Average Performance Summary from testbed Runs 130

3.4: Silver Remaining on Spiral Wound Membranes After Use and Percent Released Based upon Initial Loading..... 131

4.1: Silver Loading and Release Comparison..... 139

LIST OF FIGURES

Figure Page

2.1: Bench-Scale Flat Sheet Membrane Filtration Configuration 20

2.2: Static Leaching Test Configuration After Commencement 25

2.3: Spiral-Wound Membrane Silver-Coating Setup Configuration 28

2.4: Spiral-Wound RO Membrane Coupon Punch Locations for Digestion 31

2.5: Contact Angle Measurement on Reverse Osmosis Membrane 34

2.6: Mobile NEWT Testbed at Arizona State University 36

2.7: Two POU Units with Water Storage Tanks and Solenoid Valves with Timer in Mobile NEWT Testbed (Unit 1 right, Unit 2 left) 38

2.8: Hexavalent Chromium Spike Setup; Dosing Pump, Feed Tank, Check Valve, and Static Mixer Pictured 41

2.9: Remote Data Acquisition Sensor Module Configuration 44

2.10: LabVIEW Data Remotely Viewed Using Google Chrome Remote Desktop Application and a Smartphone Title Here 46

3.1: Permeability/Flux Test Results for (a) Nylon and (b) PVDF Flat Sheet Microfiltration Membranes 50

3.2: Permeability/Flux Test Results for (a) Regenerated Cellulose and (b) PES Flat Sheet Ultrafiltration Membranes 53

3.3: Permeability/Flux Test Results Polyamide Flat Sheet Reverse Osmosis Membrane 55

3.4: Static Leaching Test Results for (a) Nylon and (b) PVDF Flat Sheet Microfiltration Membranes 58

Figure Page

3.5: Static Leaching Test Results for (a) Regenerated Cellulose and (b) PES Flat Sheet Ultrafiltration Membranes 60

3.6: Static Leaching Test Results for Polyamide Flat Sheet Reverse Osmosis Membrane 61

3.7: SEM/EDX Images of Silver-Coated Nylon Microfiltration Membrane at (a) 1,000x, (b) 10,000x, (c) 25,000x, (d) 25,000x magnification in backscatter mode, and (e) EDX at 10,000x magnification 63

3.8: SEM/EDX Images of Silver-Coated PVDF Microfiltration Membrane at (a) 1,000x, (b) 10,000x, (c) 25,000x, (d) 25,000x magnification in backscatter mode, and (e) EDX at 10,000x magnification 65

3.9: SEM/EDX Images of Silver-Coated Regenerated Cellulose Ultrafiltration Membrane at (a) 1,200x, (b) 10,000x, (c) 10,000x magnification in backscatter mode, and (e) EDX at 1,500x magnification 67

3.10: SEM/EDX Images of Silver-Coated PES Ultrafiltration Membrane at (a) 1,000x, (b) 10,000x, (c) 25,000x, (d) 25,000x in backscatter mode, (e) 65,000x, (f) 65,000x in backscatter mode, (g) 120,000x, and (h) EDX at 10,000x magnification 70

3.11: SEM/EDX Images of Silver-Coated Polyamide Reverse Osmosis Membrane at (a) 3,500x, (b) 12,000x in BSE mode,(c) 25,000x, (d) 100,000x magnification in backscatter mode, and (e) EDX at 10,000x magnification 72

Figure Page

3.12: Surface Charge Results for Pristine and Silver-Coated (a) Nylon Microfiltration, (b) Regenerated Cellulose Ultrafiltration, and (c) Polyamide Reverse Osmosis Membranes 75

3.13: Silver Loading Results from Reverse Osmosis Membrane Digestion, Before and After 51 Days of Use in Point of Use System..... 77

3.14: Spiral-Wound Polyamide RO Membrane Contact Angle, Before and After 51 Days of Use..... 78

3.15: Dynamic Leaching Test Results Over (a) 34 Days and (b) 24 hours 79

3.16: Operating Conditions During the Dynamic Leaching Test in Metrics of (a) Flow Rate and (b) Pressure 81

3.17: Baseline Unit Comparison Results for (a) Flow Rates, (b) Flux Rates, and (c) Normalized Flux Rates Over 26 Days 83

3.18: Water Quality Measurements During Baseline Unit Comparison for (a) Temperature and (b) pH 85

3.19: Baseline Unit Comparison Measurements for (a) Conductivity and (b) Calculated Salt Rejection 87

3.20: Pristine vs. Silver-Coated Membrane Comparison Results for (a) Flow Rates, (b) Flux Rates, and (c) Normalized Flux Rates Over 37 Days..... 90

3.21: Water Quality Measurements During Pristine vs. Silver-Coated Membrane Comparison for (a) Temperature and (b) pH 92

3.22: Pristine vs. Silver-Coated Membrane Comparison Measurements for (a) Conductivity and (b) Calculated Salt Rejection..... 94

Figure Page

3.23: HPC Results from Pristine Membrane and Silver-Coated Membrane After Testbed Shut Down 95

3.24: Contaminant Removal Comparison for Pristine vs. Silver-Coated Membrane Results for (a) Flow Rates, (b) Flux Rates, and (c) Normalized Flux Rates Over 51 Days 97

3.25: Water Quality Measurements During Contaminant Removal Comparison for Pristine vs. Silver-Coated Membrane for (a) Temperature and (b) pH 99

3.26: Contaminant Removal Comparison for Pristine vs. Silver-Coated Membrane 101

3.27: Silver Released Over 51 Days of Operation During the Contaminant Removal Comparison for Pristine vs. Silver-Coated Membranes 103

3.28: Chromium Concentrations and Removal Efficiency Comparison of (a) Pristine in Unit 1 vs. (b) Silver-Coated Membrane in Unit 2 104

3.29: Induced Fouling Test Results for (a) Flow Rates, (b) Flux Rates, and (c) Normalized Flux Rates Over 36 Days 106

3.30: Water Quality Measurements During Induced Fouling Test for Pristine vs. Silver-Coated Membrane for (a) Temperature and (b) pH 108

3.31: Induced Fouling Test Measurements for (a) Conductivity and (b) Calculated Salt Rejection 110

3.32: Induced Fouling Tests Organic Measurement Results for (a) UV-254 and (b) TOC 112

Figure Page

3.33: HPC Results from Pristine Membrane and Silver-Coated Membrane After Testbed Shut Down 113

3.34: Testbed Deployment Test Results for (a) Flow Rates, (b) Flux Rates, and (c) Normalized Flux Rates Over 34 Days..... 115

3.35: Water Quality Measurements During Testbed Deployment in Chandler, AZ for (a) Temperature and (b) pH..... 117

3.36: Testbed Deployment Measurements for (a) Conductivity and (b) Calculated Salt Rejection 119

3.37: Silver Released Over 34 Days of Operation During the Contaminant Removal Comparison for Pristine vs. Silver-Coated Membranes 121

3.38: Testbed Deployment in Chandler Water Treatment Plant Organic Measurement Results for (a) UV-254 and (b) TOC..... 122

3.39: Multiple Constituent Removal Efficiencies of the (a) Pristine and (b) Silver-Coated Membrane During the Testbed Deployment at the Chandler Water Treatment Plant..... 124

3.40: HPC Results After Testbed Shutdown in Chandler Water Treatment Plant . 125

3.41: Flux Data and Salt Rejection Data from the Remote Data Acquisition System Over 34 Days of Operation at Chandler Water Treatment Plant 126

3.42: Remote Data Acquisition System Data from (a) Temperature, (b) Conductivity, and (c) Pressure Sensors 128

CHAPTER 1

INTRODUCTION

Water sources are becoming more scarce as population continues to grow exponentially. With population growth comes increased industry and agriculture, which in turn produce high volumes of waste water (Fritzmann et al. 2007). Many municipalities are moving towards desalination technologies to produce clean drinking water from salt water. Reverse osmosis (RO) membrane filtration is an effective method of removing salts and other monovalent ions from water, with salt rejection rates as high as 99.7 – 99.8% (Greenlee et al., 2009). While municipalities are increasingly using RO membranes or similar technologies to produce clean drinking water, these technologies can also be applied at a residential scale, in point of use (POU) system.

Advanced POU system uses a multi-step process in which water is filtered through a sediment filter to remove suspended solids, followed by carbon blocks to remove organic material such as natural organic matter, and finally through the RO membrane element. Despite these pretreatment steps, contaminants can still reach the membrane surface and have undesirable effects on the membrane performance. When a membrane is impacted by constituents in water, it is referred to as fouling. There are different types of fouling, depending on the constituents present and the location at which they bind to the membrane. For RO membranes, fouling only occurs on the surface, since RO membranes do not have pores, but instead operate through diffusion (Greenlee et al., 2009). Depending on the type of foulant, fouling can be classified as inorganic scaling, organic fouling, or biofouling (Jiang et al., 2017). All types of fouling of a membrane can lead to an increase in operating pressure, a decrease in water recovery, and ultimately a

decrease in membrane lifespan (Jiang et al., 2017). To save time, energy and money, methods of controlling and preventing fouling have been studied. The purpose of the research conducted for this thesis was to investigate the feasibility of conducting an In-Situ silver-coating procedure on spiral-wound RO membranes, and to monitor the long-term performance of these membranes in terms of flux, salt rejection, and silver-leaching.

The concept of biofouling involves the attachment of a microorganism on an inhabitable surface, and the subsequent growth and multiplication of microorganisms due to the release of extracellular polymeric substances (EPS) (Deng et al., 2016). There are many ways to prevent biofouling on a membrane surface. A common way of increasing the anti-fouling properties of a membrane is to add an antifoulant, such as copper, in a layer-by-layer fashion to coat the membrane surface. However, this can lead to a decrease in the hydrophilicity of the membrane if too many layers are required, causing the membrane performance to suffer (Wang, Wang, Han, Wang, & Wang, 2017). Another common method of mitigating biofouling is to deposit or coat inorganic materials onto a membrane surface, such as titanium dioxide or silver nanoparticles (Kochkodan & Hilal, 2015). The research conducted for this thesis was based on a silver nanoparticle In-Situ coating procedure developed at Yale University for flat sheet RO membranes (Ben-Sasson et al., 2014).

In this study, the feasibility of scaling up the flat sheet In-Situ coating procedure to spiral-wound RO membranes for POU systems was investigated. A silver nanoparticle coating for RO membranes at the POU scale has not been conducted before, meaning extensive performance studies needed to be undertaken. The performance, efficacy,

safety, and sustainability of these nano-enabled membranes was tested in a modular mobile drinking water treatment system called the Mobile NEWT Testbed.

The National Science Foundation-funded Nanotechnology-Enabled Water Treatment (NEWT) Engineering Research Center focuses on enhancing drinking water treatment technologies using nanoparticles. The Mobile NEWT Testbed was used to compare a standard POU system to a POU system containing a silver nanoparticle-coated RO membrane. Five long-term studies were conducted, including a baseline unit comparison, a membrane comparison, a contaminant rejection comparison by spiking with hexavalent chromium, an induced fouling test, and a testbed deployment to the Chandler Water Treatment Plant in Arizona. In addition to deploying the testbed, a remote data acquisition (DAQ) system was configured to monitor performance remotely using a smart phone. This thesis investigates the performance and membrane characterization results of the silver-coated spiral-wound RO membrane, and discusses key findings and challenges associated.

CHAPTER 2

MATERIALS AND METHODS

2.1 Flat Sheet Membranes

The feasibility of performing an In-Situ silver coating process on spiral-wound RO membranes was assessed, based upon the silver coating procedure developed at Yale University (Ben-Sasson et al., 2014) . Five types of flat sheet membranes were tested, including two types of microfiltration (MF) membranes, two types of ultrafiltration (UF) membranes, and one type of RO membrane. Table 2.1 below describes the types of membranes used and their product specifications.

Table 2.1: Membrane Product Specifications

Membrane Type	**Composition**	**Pore-Size**	**Brand**	**Model/Catalog Number**
MF	Nylon	0.2 μm	Whatman	7402-004
MF	Polyvinylidene Fluoride (PVDF)	0.2 μm	Sterlitech	PVDF0247100
UF	Regenerated Cellulose	3 kDa = 6 x 10^{-5} μm	Millipore	PLBC04310
UF	Polyetherlsulfone (PES)	10 kDa = 2 x 10^{-4} μm	Sterlitech	YMUF103001
RO	Polyamide Active Layer, PES Support	Semi-Permeable	Applied Membranes Inc.	M-T1812A24

The RO membrane listed above was supplied by Applied Membranes Inc. and was sent in a spiral-wound configuration, meaning flat sheets coupons needed to be punched out from the membrane for analyses. The membrane used was a 12-inch long, 1.75-inch diameter polyamide membrane element capable of producing 24 gallons per day.

Membrane Coating Procedure

All flat sheet membranes were coated following the procedure developed at Yale University, which can be found in the article titled, "In situ formation of silver nanoparticles on thin-film composite reverse osmosis membranes for biofouling mitigation" (Ben-Sasson et al., 2014). Briefly, a 44.5 mm-diameter flat sheet membrane was placed in a Millipore brand 50 mL Amicon cell. The cell was fitted with a magnetic stir bar that was rotated on the lowest setting of a Thermolyne brand magnetic stir plate throughout the process. First, the flat sheet membrane was wetted with nanopure water to rinse off any preservatives or binding agents on the membrane. Secondly, 50 mL of 3mM silver nitrate ($AgNO_3$) was added to the cell and allowed to stir for 10 minutes, as per the coating protocol. Thirdly, the $AgNO_3$ solution was discarded, leaving a thin layer of solution on the membrane surface. Fourth, 50 mL of 3mM sodium borohydride ($NaBH_4$) was added to the cell and allowed to stir and react for another 5 minutes. The $NaBH_4$ acts as a reducing agent, leaving silver nanoparticles (Ag-NPs) uniformly on the membrane surface. Finally, the membrane could again be rinsed with nanopure water to remove any loose particles from the surface. At this point, the membrane was ready for use.

Membrane Characterization

After the coating protocol was completed, the silver-coated membranes were analyzed and compared to pristine membranes to insure they did not lose their functionality. Physical and chemical properties of the membranes were analyzed. These tests included permeability tests, surface charge analyses, contact angle analyses, scanning electron microscope images, and elemental analyses using energy dispersive x-ray techniques.

Permeability Tests

Permeability and flux tests were conducted at the bench-scale for the five different types of flat sheet membranes to compare the performance of pristine membranes and silver-coated membranes. All membranes were tested first with nanopure water to obtain a baseline flux rate, then with tap water to observe the flux decline caused by inorganic fouling. First, a 5-liter stainless steel Millipore pressure vessel, fitted with quick-connect hose connectors was filled to the "maximum fill" line, which was approximately 5-liters of water. The 44.5 mm-diameter membranes were placed into a 50 mL Millipore brand Amicon cell, fitted with a rubber O-ring, magnetic stir bar, and inlet/outlet quick-connect ports. The Amicon cell was then filled with 50 mL water and sealed. The inlet hose was connected to the pressure vessel, and the outlet hose led to a 2000 mL beaker on a Mettler Toledo brande digital scale. The digital scale was connected to a computer that had a LabVIEW program configured to measure the mass over time. The LabVIEW program also converted the mass into a flux rate of units of liter per square meter per hour (LMH) using the membrane diameter and the

mass/volume of water over time. Manual measurements and calculations to determine the flux rate were also performed to insure accuracy of the program.

To begin the test, the magnetic stir bar was set to the lowest setting on the stir plate, the LabVIEW program was set to "RUN", and the pressure vessel was pressurized to the desired pressure (psi) using compressed nitrogen gas. For the MF membranes, 20 psi was used, and for both the UF and RO membranes, 50 psi was used. The lock on the lid of the Amicon cell was left open briefly while the pressure was building to purge any excess air within the cell. Under pressure, the water began to filter through the membrane using dead-end filtration and flowed out of the outlet tube into the beaker. The digital scale could then measure the mass of water as it flowed into the beaker. Figure 2.1 below illustrates the configuration of the bench-scale set up.

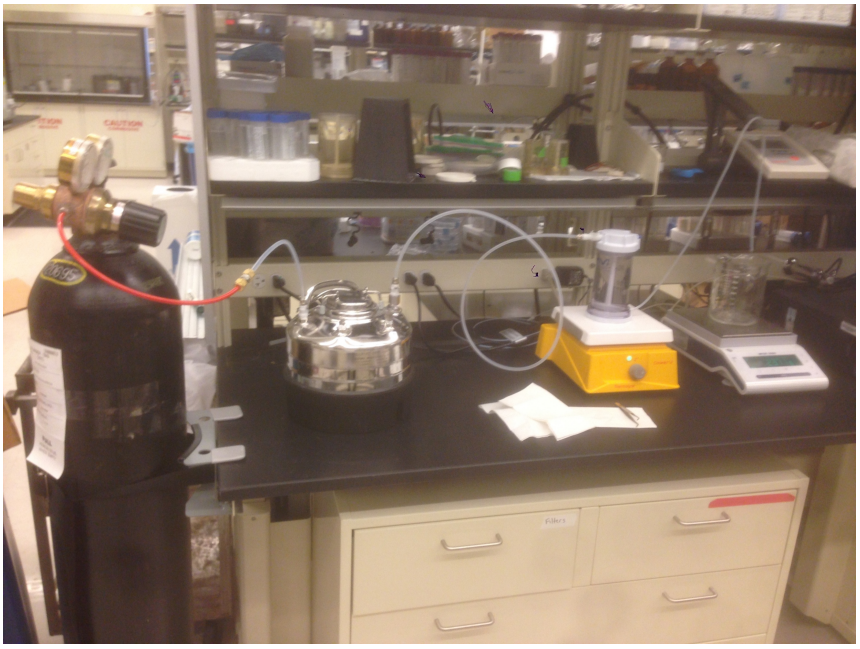

Figure 2.1: Bench-Scale Flat Sheet Membrane Filtration Configuration

As the test was being conducted, manual readings were taken every minute, and the LabVIEW program took readings every second. The LabVIEW program also was set

to convert the reading on the scale to volume of water, where one gram is equal to one mL of H_2O, which could then be converted to a flow rate in mL/min, and ultimately to a flux rate in units of LMH. This process was performed four times for each membrane type, filtering nanopure water and tap water through both pristine membranes and silver-coated membranes for the duration of time required to fill the 2000 mL beaker.

Surface Charge

The surface charge of the membranes was measured using a ZetaCAD Surface Zeta Potential analyzer. Surface charge is an important parameter of membrane characteristics because the type and quantity of fouling that occurs on a membrane surface is related to surface charge. For example, most microorganisms and organic matter are negatively charged and are attracted to positively charged surfaces. Therefore, a negative surface charge of the membrane would repel microorganisms and natural organic matter. Conversely, a positively charged membrane surface would attract microorganisms and promote biofouling. It was important that the surface charge of the membranes was not altered due to the silver-coating, so that the membranes would not lose their functionality.

To conduct the surface charge measurements, both the pristine and silver-coated flat sheet membranes had two coupons cut to 75mm x 75 mm. The coupons were mounted in an acrylic cell using double-sided and tape, at which point the cell was screwed together to maintain a gap between the two coupons ranging from 250 – 450 μm. One liter of electrolyte solution was then prepared using 1 mM KCl aand 0.1 mM $KHCO_3$. The pH was adjusted for each surface charge measurement to 3, 5, 7, and 9 using KOH and HCl. The cell containing the membrane coupons was then fixed to the

analyzer, and the electrolyte solution was used to fill the two attached jars to 500 mL each. A glass shield was then lowered and a lever switched to seal the system away from atmospheric conditions. The ZetaCAD software was then configured and run, to insure continuous flow between the two electrolyte jars. The direction of flow was configured in the software, either from jar 1 to jar 2, or vice versa, so that flow was uninterrupted and no air was allowed in the system.

The theory behind in the surface charge analyzer is to force the solution through a capillary between the membranes using a pressure gradient. As the solution flows through the capillary, excess charges from the membrane surface are carried in the liquid and accumulate downstream. After the charges have accumulated, an electric current is formed and flows upstream, where steady state is achieved (Utilisateur, 2017). The potential across the capillary is measured in mV, called the streaming potential. This process is repeated after adjusting the pH of the electrolyte solution for both the pristine and silver-coated membranes.

Scanning Electron Microscopy & Energy Dispersive X-Ray

Scanning Electron Microscopy (SEM) images were taken to observe the surface topography of the membranes, as well as observe and measure the size of the silver particles deposited on the membrane surfaces. SEM is a powerful microscope that utilizes a focused beam of electrons that generate a signal when they come into contact with a solid surface. The signal generated by the electrons in contact with the surface is read by the instrument and can determine the texture, structural orientation, and chemical makeup of a sample. The high-resolution images generated by SEM make it a powerful tool for this application because it can easily observe modifications made to membranes on the

nano-scale. SEM images are also useful when observing pristine membranes to determine physical characteristics, such as pore size and shape.

To obtain the SEM images, a FEI XL30 Environmental SEM was used. Membrane samples were mounted to a metal sample holder, approximately 1 cm in diameter, using carbon tape. The samples were all coated with carbon using carbon-sputtering, so the highly-conductive silver particles did not become charged during the imaging, mobilizing the particles thus making them difficult to detect and measure. The samples were then inserted into a vacuum chamber where the detector is located, so that no interference from outside sources was observed. High-resolution images of each membrane were then obtained at different magnification levels ranging from 100x to 120,000x. Most images were shot using the secondary electron (SE) detector, which is useful for obtaining surface topography images. However, some images were taken in back scatter electron (BSE) mode, which acquires compositional images that penetrate deep into the membrane.

During the imaging, the system was operated under backscatter mode, where the intensity of the electrons backscattered could be correlated to their atomic number. In this fashion, an elemental analysis of the membrane surfaces was conducted to obtain the elemental makeup of the membranes.

Static Leaching Tests

Static, or diffusion-based leaching tests were conducted on the flat sheet membranes to determine the kinetics of silver leaching from the membranes over time due to different pH conditions. This was an important test to determine how well the

silver was bound to each membrane type, and determine the safety and feasibility of using these membranes in real-world applications.

To conduct the static leaching test, four flat sheet membranes were weighed before and after they were coated with silver. The membranes were then fastened to nylon clips, which were suspended from a stand. In a 2000 mL Erlenmeyer flask, 1500 mL of 5mM $NaHCO_3$ in nanopure water solution was made. This $NaHCO_3$ solution provided buffer capacity, so the pH could subsequently be adjusted accordingly. The pH of this solution was intended to be around 8.0 ± 0.1, which was measured and confirmed after mixing the solution using a magnetic stir bar. The solution was then transferred into eight glass jars, filled to 60 mL each and placed in a straight line. The pH of the remaining $NaHCO_3$ solution was then adjusted using 70% HNO_3, targeting pH 6.0 ± 0.1. Approximately 50 μL of 70% HNO_3 was added at a time, checking the pH after each addition. The final ratio of 70% HNO_3 to 5 mM $NaHCO_3$ solution to achieve pH 6.0 ± 0.1 was 225 μL to 1000 mL, respectively. The pH 6.0 solution was then transferred into eight glass jars, filled to 60 mL each and placed in a straight line adjacent to the pH 8.0 solution jars. The remaining 500 mL of pH 6.0 solution in the Erlenmeyer flask was then pH-adjusted using 70% HNO_3, targeting pH 2.0 ± 0.1. The volume of acid required to achieve pH 2.0 was approximately 500 μL in 500 mL of remaining solution. The pH 2.0 solution was then transferred into 8 glass jars with 60 mL in each jar, and placed into a straight line adjacent to the pH 6.0 solution. The static leaching test was then ready to commence. Figure 2.2 below illustrates the configuration of the static leaching test, with membranes fully submerged in pH 8.0, pH 6.0, and pH 2.0 solutions in glass jars.

Figure 2.2: Static Leaching Test Configuration After Commencement

As illustrated in Figure 2.2 above, the membranes were fully submerged into their respective pH jars simultaneously. After reacting for a specified amount of time, the membranes were removed from the pH solutions, allowed to drain for 10-seconds, and then placed into the subsequent jars simultaneously. The process was then repeated after the membranes reacted for a specified amount of time. The transfer times for the static leaching test is illustrated in Table 2.2 below.

Table 2.2: Static Leaching Test Membrane Transfer Time Table

Sample ID	Interval Duration (min)	Interval Duration (hr)	Cumulative Time (hr)	pH 8	pH 6	pH 2
T1	1	-	0.02	X	X	X
T2	4	-	0.08	X	X	X
T3	10	-	0.25	X	X	X
T4	20	-	0.58	X	X	X
T5	25	-	1.0	X	X	X
T6	-	1	2.0	X	X	X
T7	-	4	6.0	X	X	X
T8	-	24	30.0	X	X	X

The membranes were transferred from jar to jar at different time intervals, with a cumulative experiment time of 30 hours. Dissolved silver was then measured at the end of the test using ICP-MS. The results of this test provided the kinetics for silver released from the MF, UF, and RO membranes under ambient pH conditions (pH 8.0), slightly acidic pH conditions (pH 6.0), and highly acidic conditions (pH 2.0) that may be experienced during membrane clean in place (CIP) treatment processes.

2.2 Spiral-Wound Membranes

After completing the physical and chemical characterizations as well as the permeability and flux tests for the flat sheet membranes, the next challenge was to scale up the procedure to spiral-wound RO membrane elements. The membrane used for all spiral-wound tests was supplied by AMI, model number M-T1812A24, which is a 12-inch long, 1.75-inch diameter membrane element capable of producing 24 gallons per

day. The membrane is composed of a PES support layer beneath a polyamide active layer. The characterization performed for the spiral-wound membrane utilized the same methods described for the flat sheet membranes, with the addition of contact angle and a different type of leaching test. This section will discuss the materials and methods used to coat, characterize, and utilize the spiral-wound membrane elements.

Membrane Coating Procedure

The silver-coating procedure for the spiral-wound RO membrane was adapted from the flat sheet membrane coating protocol. The chemicals used to coat the spiral-wound RO membrane were the same used in the flat sheet coating procedure (i.e. 3mM $AgNO_3$ and 3mM $NaBH_4$), however larger quantities were required for the larger membrane surface area. Additionally, rather than allowing the solutions to mix over the submerged flat sheet membrane, for the spiral-wound membrane solutions were recirculated over the membrane surface in cross-flow mode. The experimental setup configuration is illustrated in Figure 2.3 below:

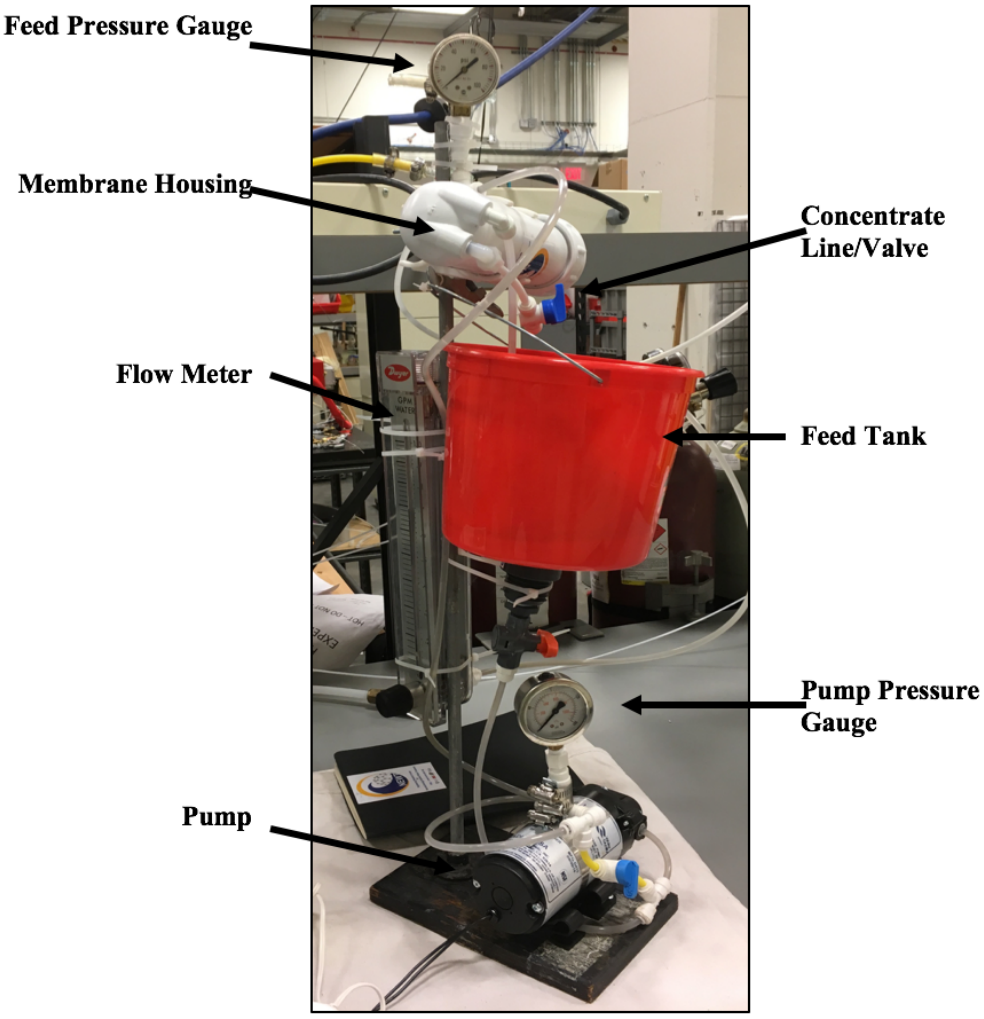

Figure 2.3: Spiral-Wound Membrane Silver-Coating Setup Configuration

As observed in Figure 2.3 above, the setup consisted of the aforementioned spiral-wound polyamide RO membrane element contained within a standard membrane housing supplied by AMI (Model Number PV2012PME), a solution feed tank, flow and pressure gauges, an Aquatec brand pump rated to 125 psi (Model Number CDP 6800) and several valves and other fittings. The system was configured so the solution from the feed tank was pumped to the membrane housing, and the concentrate line of the membrane housing was fed back into the feed tank so the solution was permitted to recirculate. Valves were

fitted onto the permeate line, the concentrate line, and the solution feed tank. The valve on the permeate line was kept in the OFF position so only the concentrate line would experience any flow. This was determined to be the ideal operating condition after attempting to coat the membrane with both the permeate and concentrate valves in the open position and observing an inoperable buildup of pressure and loss of flux. The valve on the concentrate line was kept approximately half open to maintain the ideal operating pressure of about 8 psi. This pressure was again determined after trial and error, where greater pressure caused the Aquatec pump to fail, and less pressure resulted in lower silver-coating efficacy.

The first step of the protocol was to pour one liter of nanopure water into the feed tank to rinse and prime the membrane for coating. The feed tank valve was then opened and the pump was turned on. The operating conditions (i.e. flow and pressure) were set by adjusting the concentrate valve. The nanopure water rinse period also served as a time to check that feed pressure and flow were maintained around 8 psi and approximately 945 mL/min, respectively. The rinse period was performed for 10 minutes, where the pressure and flow data was recorded every minute to insure stable operating conditions. Once the operating conditions were optimized and stable, the valve positions were not adjusted and the nanopure water could be discarded from the solution feed tank. At this point, the pump was turned off and the feed tubing was removed from the membrane housing. The membrane housing was then removed from the stand and the cap was unscrewed using a strap wrench. All the water was then drained from the system, including the membrane housing, which required the membrane element to be removed from the membrane housing for maximum drainage. The membrane was then placed back into the membrane

housing and the cap was reattached using the strap wrench before placing the housing back onto the stand. Now, the feed tubing was reattached into the membrane housing, and one liter of 3mM $AgNO_3$ solution was poured into the feed tank. Again, the pump was turned on and the solution could recirculate for 10 minutes while recording flow and pressure every minute. After 10 minutes, the solution from the feed tank was discarded into a hazardous waste vessel. Then, the tubing from the membrane housing was removed and the remaining solution was permitted to completely drain from the housing into a hazardous waste vessel. The housing was then placed back onto the stand with the tubing reattached. One liter of 3mM $NaBH_4$ solution was then poured into the feed tank the valve was opened, and the pump was turned on. The $NaBH_4$ reducing solution was recirculated for five minutes, again recording pressure and flow every minute. After five minutes, the membrane housing was removed and the solution was drained from both the housing and the feed tank into a hazardous waste vessel. The membrane housing was then placed back onto the stand and the tubes were reattached. The membrane and the system could then be flushed with one liter of nanopure water for one minute to remove any loosely-bound silver particles. After one minute, the membrane element was removed from the membrane housing using a strap wrench and needle-nose pliers and was stored for either membrane characterization analyses or use in performance studies.

Membrane Characterization

Upon successfully coating several spiral wound RO membrane elements, a membrane characterization was performed to compare the results with those of the flat sheet membrane coating procedure. The comparison included a digestion test, leaching

test, SEM imaging, elemental analyses, surface charge measurements, and contact angle measurements.

Silver Loading on Spiral-Wound RO Membrane

To quantify the amount of silver loaded on the spiral-wound RO membrane, a digestion of the membrane was performed. Once the membrane was coated, the O-rings, outside labels, adhesive tape, and membrane spacer was removed. The membrane was then unfurled and laid flat on a clean cutting surface. A "top" and a "bottom" of the membrane was determined, where the top was the side of the membrane envelope that curled upwards, and the bottom was the side of the membrane envelope that curled downwards. Nine evenly-distributed coupons were then punched out from each side of the membrane for a total of 18 coupons, 44.5 mm in diameter each. The coupons were taken from strategic locations around the membrane to see if the mass of silver loaded varied due to location on the membrane. Figure 2.4 below illustrates the fashion and locations in which the coupons were punched from each side of the membrane.

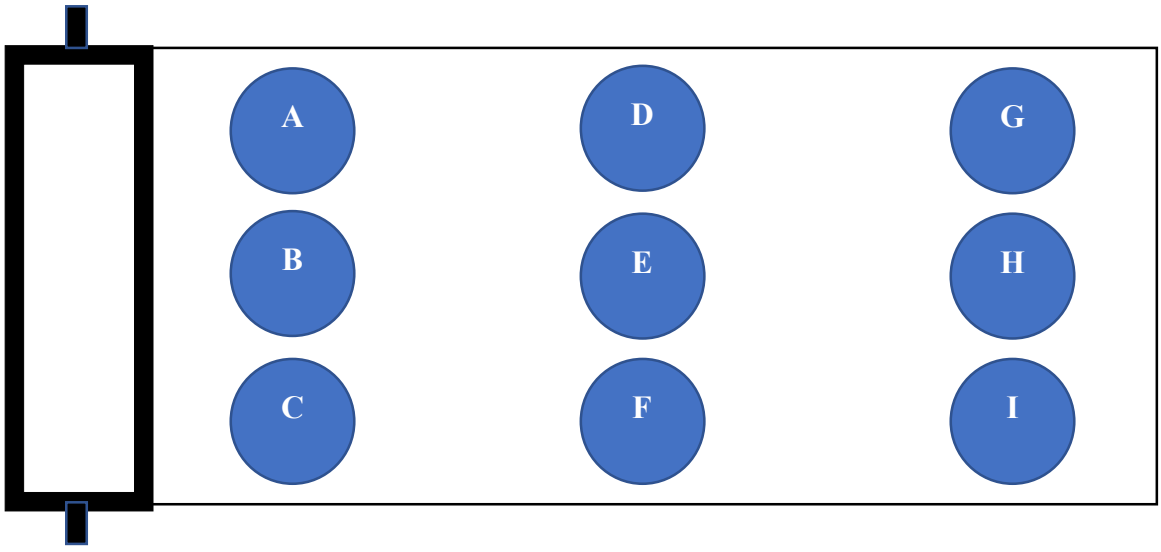

Figure 2.4: Spiral-Wound RO Membrane Coupon Punch Locations for Digestion

As illustrated in Figure 2.4 above, the membrane coupons were labeled "A – I" for each membrane side. Coupons A through C were designated as the inside of the membrane, D through F was the middle, and G through I was the outside. Once the 18 coupons were obtained, each coupon was cut in half to undergo a different method of digestion. This was to ensure that results for the mass-loading of silver were consistent, regardless of the method used to digest the membrane. Each membrane half was then fashioned to a plastic clip, placed into a plastic 50-mL centrifuge tube, and labeled. The purpose of the plastic clip was to ensure the membrane would remain stationary during the digestion, so all surfaces would remain exposed to the acid solution.

For both digestion methods, the centrifuge tubes were filled with 35 mL of 2% HNO_3, which was the necessary volume of acid to completely submerge the membrane. For each coupon, half was digested in a bath sonicator and the other half was digested by agitation using a shaker table at 160 rpm. The temperature of the shaker table setup was set to 23°C, and the sonicator was operated at room temperature, or approximately 23°C as well. Both digestion methods were conducted for 24 hours, and the silver concentrations in the acid solution were measured using ICP-MS to determine a mass of silver loaded per area (ug/cm^2). The process was then repeated after 51 days of use to measure the amount of silver remaining on the membranes.

Dynamic Leaching Test

To test the safety and sustainability of silver-coated spiral-wound RO membranes for home use, a leaching test was conducted over a period of 34 days. To simulate the fashion in which these membranes are utilized at the residential scale, a point-of-use (POU) system was replicated in the lab using the City of Tempe municipal tap water

supply. The POU system consisted of three cartridge filters used as pretreatment before the spiral wound membrane element. The cartridge filters used was a sediment filter, followed by two carbon filters. The dimensions, pore-size, and model numbers of the filters used will be discussed later in this thesis, under the Mobile NEWT Testbed section of this chapter. After the pretreatment step, the water was fed into the RO membrane element. Samples were collected from the permeate and concentrate flow streams of the RO membrane into 50-mL plastic centrifuge tubes, as well as from the raw tap water and after the cartridge filters.

To develop a plot of the kinetics of silver released from the membrane, samples were initially taken every five-minutes for the first half hour, then every 10-minutes during the next half hour, then once per hour for three hours, and eventually once per day for 34 days. The samples were then acidified using 70% HNO_3 to preserve them and analyzed for silver concentrations using ICP-MS. During the leaching test, performance data such as pressure and flow through the system was monitored, and water quality parameters such as pH, temperature, and conductivity were occasionally measured as well.

Contact Angle Measurements

An additional parameter tested on the spiral-wound RO membrane was for the hydrophobicity of the membrane using contact angle measurements. For this analysis, four spiral-wound membranes were taken apart so 44.5 mm diameter coupons could be punched out at different locations, analogous to the digestion method described earlier. The four membranes used were a pristine membrane, an unused silver-coated membrane, a membrane after one month of use, and a silver-coated membrane after one month of

use. These membranes were selected to determine if the hydrophobicity of the membrane was altered due to the silver coating or after being used in a POU configuration. Three coupons from each membrane were analyzed for contact angle, all from the same locations on every membrane.

The method in which contact angle was measured was the Sessile Drop method. An Attension Theta Optical Tensiomter created by Biolin Scientific was used for the measurements. To perform the analysis, membrane coupons were mounted on a level surface next to a camera. A syringe and needle filled with DI water was mounted approximately one cm above the membrane, A drop approximately 5 μL in volume is then pressed out of the needle and suspended above the membrane. The contact angle software was then set to record, at which point the drop was pressed off the needle and onto the membrane. The software then takes collects images for about 500 frames, which takes approximately 10 seconds. During this time, the angle at which the drop is in contact with the membrane is measured, and a mean contact angle can be obtained. Figure 2.5 below illustrates the angle of the drop measured during this analysis.

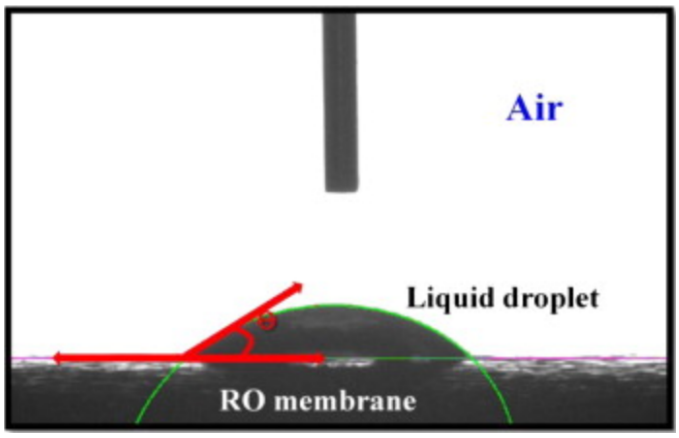

Figure 2.5: Contact Angle Measurement on Reverse Osmosis Membrane (Baek, Kang, Theato, & Yoon, 2012)

Multiple drops were measured on each membrane coupon to ensure measurements were consistent with each other. When contact angle measurements are greater than 90°, the membrane is considered to be hydrophobic. Conversely, when contact angle measurements were less than 90°, the membrane was hydrophilic (Baek et al., 2012). This test was repeated for all membranes to observe the changes in contact angle measurements caused by the silver coating and by one month of use.

Mobile NEWT Testbed

To test the performance of the coated spiral-wound membranes, two POU units were assembled inside the Mobile NEWT Testbed. The Mobile NEWT Testbed is designed as a modular drinking-water treatment system contained in a dual-axle trailer that can be deployed to rural communities or in emergency response situations. However, at ASU, it served as a pilot-scale experimental and educational vehicle, where different drinking water treatment technologies (i.e. silver-coated RO membranes) could be tested on a large scale. Figure 2.6 below depicts the Mobile NEWT Testbed trailer parked inside Arizona State University's Interdisciplinary Science and Technology Building (ISTB4), where most of the experiments were conducted.

Figure 2.6: Mobile NEWT Testbed at Arizona State University

Features on the Mobile NEWT Testbed that may not be visible pictured above include the following:

- Air conditioning
- 50 Amp electric panel
- Multiple breakers for lights and power-outlets
- Optional solar panels
- Multiple access doors and a large concession window for public demonstrations
- Power and water hookups to treat and perform tests from different water sources
- Three separate treatment units that can be run in parallel or in series
- Units fitted with flow meters, pressure gauges, and sampling ports

During the silver-coated RO membrane tests, two POU units designed to simulate RO systems at the residential scale were utilized.

Point of Use Configuration

A common POU configuration for residential-scale RO systems includes the use of a sediment filter, two carbon blocks, followed by the RO membrane element. Applied Membranes Inc. carries these pre-filters sold as a complete set (Model RFK-5-PRE), which was purchased for all Mobile NEWT Testbed runs. These pre-filters are all housed in standard 10-inch long plastic filter housings, and are easily replaced. The sediment pre-filter is a melt-blown polypropylene filter with a five-micron pore-size, designed to remove suspended solids such as fine clay or silt. The carbon block pre-filters are made from extruded carbon with a 10-micron pore-size and are designed to adsorb organic materials such as NOM or taste and odor compounds. After the cartridge filters, water was fed into the RO membrane element. The RO membrane operates in cross-flow mode, where approximately 75% of the feed water is discarded as the concentrate flow, and 25% of the feed water is recovered as drinking water in the permeate flow. Because the recovery rate of drinking water is only 25%, most residential POU RO systems utilize a pressurized permeate tank, where the treated drinking water is stored for later use, rather than treating water as it is needed. Both units in the Mobile NEWT Testbed utilized these pressurized permeate storage tanks. Additionally, both units were fitted with sampling ports for the feed water, cartridge-filter water, permeate flow, and concentrate flow so that samples could be taken and analyzed at all points of the treatment system. The units were fitted with flow and pressure gauges to monitor performance during the experiments. To further simulate POU systems in the residential scale, the system was

connected to two solenoid valves set on a timer, where 12-hours during the day it turns on and off every 30-minutes, and at night it is kept off. This is to simulate an extreme case in which a small family may consume drinking water, requiring the system to generate water every 30-minutes (after the storage tank is depleted), while remaining off during sleeping hours. Figure 2.7 below depicts the two POU units in the Mobile NEWT Testbed.

Figure 2.7: Two POU Units with Water Storage Tanks and Solenoid Valves with Timer in Mobile NEWT Testbed (Unit 1 right, Unit 2 left)

Once the configuration of the Mobile NEWT Testbed was determined, long-term performance data for the spiral-wound membranes could be acquired. Performance measurements for all the tests described below included flow measurements, flux rate, pressure loss across the membrane (transmembrane pressure, or TMP), and water quality measurements such as pH, temperature, and conductivity. These performance measurements were taken three to four times daily. In addition to performance measurements, other analyses may have been performed depending on the type of test being conducted.

Run 1: Baseline Unit Comparison

The first analysis conducted on the Mobile NEWT Testbed was a baseline comparison of the two POU units. Because the units were configured identically other than their location within the testbed, it was expected that they would behave the same. However, the baseline run was used to see if there were any discrepancies between the units before any silver-coated membranes were tested, ruling out the unit configuration as a source of any variances. The baseline run was also utilized as a time to fix any leaks or other issue associated with the configuration of the testbed, as this was the first time any water was treated by the Mobile NEWT Testbed. The baseline run was conducted for 26 days, from September 28, 2016 to October 24, 2016.

Run 2: Pristine Membrane vs. Silver-Coated Membrane Comparison

After the baseline unit comparison was completed and any issues regarding the physical configuration of the system were resolved, the silver-coated RO membranes were ready to be tested. For this analysis and every analysis hereafter, the silver-coated spiral-wound RO membrane was loaded into Unit 2 (left) on the testbed, and analyzed in

comparison with a pristine, unmodified RO membrane in Unit 1 (right) on the testbed. The purpose of this analysis was to measure the performance of the silver-coated membrane against an unmodified membrane. This analysis was conducted for 37 days, from October 26, 2016 through December 2, 2016.

Run 3: Contaminant Removal Efficiency Using Hexavalent Chromium

The purpose of the third analysis conducted was to measure the affects the silver-coating had on contaminant removal. The contaminant chosen to spike in the testbed was hexavalent chromium, which has been detected in some of Phoenix's drinking water supply and continues to be an issue. To spike the feed water to the testbed, a Pulsatron brand electronic metering pump was purchased (model number LE02SA-KTCJ-XXX). The pump is a 0.60-amp pump, rated to a flow rate of 6 GPD and a pressure of 150 psi. A calibration of the dosing pump was performed to determine the flow rate (mL/min) achieved by adjusting the power and the stroke length of the pump. A stock solution of potassium dichromate ($K_2Cr_2O_7$) at a concentration of 5 mg/L or 5 ppm was mixed in a 30-gallon drum with DI water, which required 567 mg of $K_2Cr_2O_7$ in 30-gallons (113.4 L) of DI water. The target feed concentration of $K_2Cr_2O_7$ was 50 ppb, which resulted in a dose of about 8.3 mL/min of the stock solution into the feed water. The corresponding power and stroke length of the dosing pump was approximately 100% and 35%, respectively. The dosing pump was set on the same timer as the testbed itself to ensure it would turn on and off simultaneously with the testbed operation. Figure 2.8 below illustrates the configuration of the dosing pump and feed tank setup.

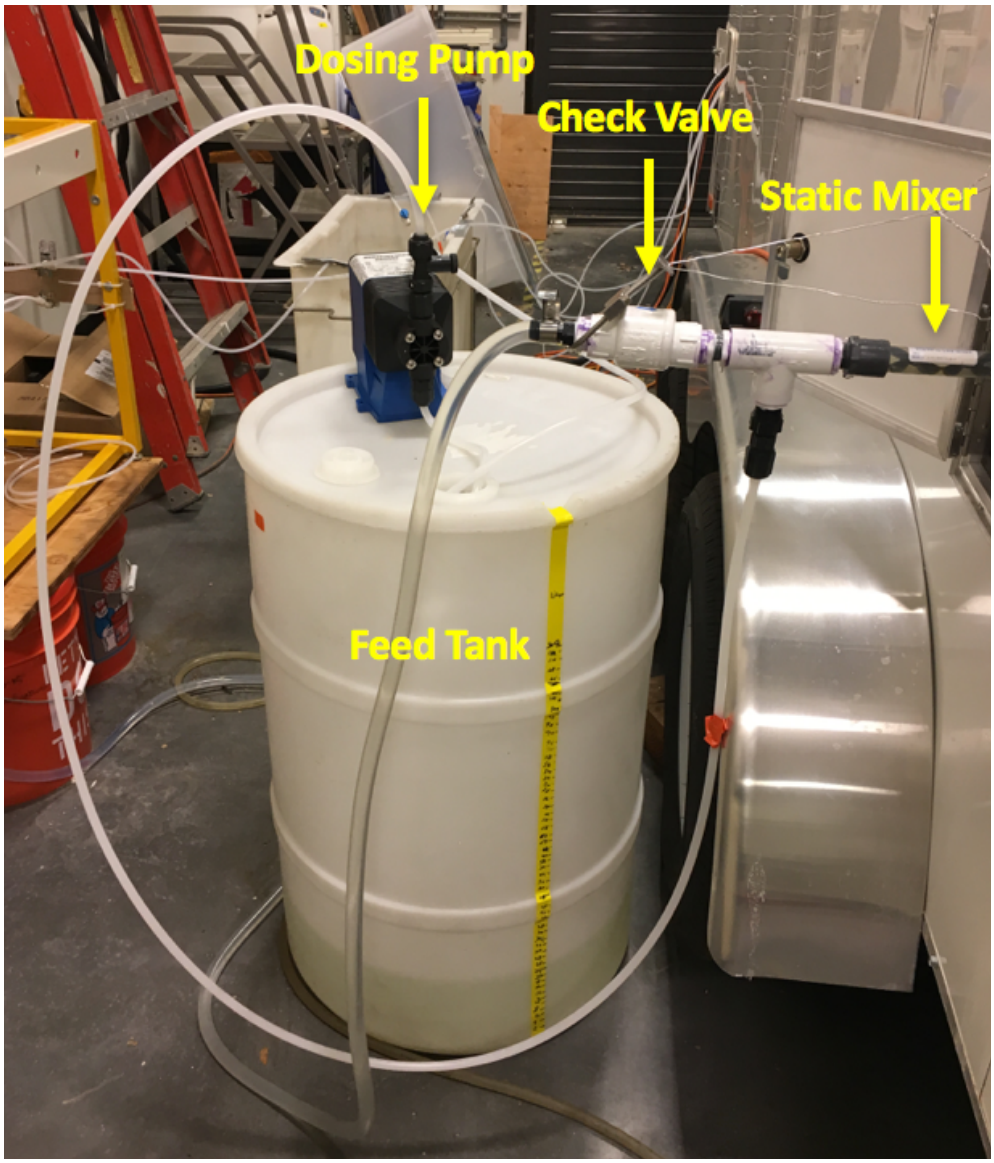

Figure 2.8: Hexavalent Chromium Spike Setup; Dosing Pump, Feed Tank, Check Valve, and Static Mixer Pictured

As illustrated in Figure 2.8 above, the dosing pump was attached to a T-shaped pipe-fitting. The feed water was fed into a check valve before the T-fitting. The check-valve would remain open under pressure when the feed water was flowing, but when the testbed was in "off" mode, the valve would close to prevent any $K_2Cr_2O_7$ solution from flowing back into the feed line. A static mixer was placed after the T-fitting to ensure a

homogenous mixture of feed water and $K_2Cr_2O_7$ solution was received by the POU units. Throughout the analysis, the level of the $K_2Cr_2O_7$ solution feed tank was monitored to check the flow rate into the testbed. The solution tank required refills of $K_2Cr_2O_7$ stock solution two times throughout the analysis. In addition to the standard performance measurements, samples from this analysis were analyzed for silver and chromium using ICP-MS, and organic measurements of TOC and UV-254 were taken using a Shimadzu TOC analyzer and DR-5000 spectrophotometer, respectively. The third analysis was conducted for 51 days, from March 1, 2017 to April 21, 2017.

Run 4: Induced Fouling Test

The purpose of the fourth analysis was to induce fouling on both membranes by increasing the permeate recovery rate from 20% to 30% This was achieved by adding a flow-restrictor to the concentrate lines of both units. The flow-restrictor allowed 150 mL/min of flow to pass through the concentrate line (previously 300 mL/min), forcing the remainder of the feed flow through the membrane to be produced as permeate flow. The theory behind this analysis was to observe the effects of the silver-coating on the formation of biofouling, due to the biocidal nature of silver. Additional analyses for biofouling were performed on the membranes after the run was complete, which included a heterotrophic plate count (HPC) and optical coherence tomography (OCT) images. The HPC and OCT analyses were performed immediately after the testbed run was terminated due to the nature of bacterial degradation once flow is shut off through the membrane. This testbed run was conducted for 36 days, from May 24, 2017 to June 29, 2017.

To perform the HPC, a 6 cm x 1 cm coupon was cut from the top and bottom of both the pristine and the silver-coated membranes for a total of four membrane coupons.

The coupons were sonicated for six minutes in 10 mL of 0.9% NaCl buffer solution to dislodge the bacteria from the membrane surface. A serial dilution was then performed into 0.9% NaCl buffer solution, resulting in dilution factors of 10^{-1}, 10^{-2}, 10^{-3}, and 10^{-4}. The dilutions were individually vortexed before and after diluting, to create homogenous mixtures. Once the dilutions were created, 100 μL of each dilution was pipetted onto R2A agar plates. R2A is a growth media that promotes bacterial growth of slow-growing species found in potable water. Cultures were developed using the spread plate technique on the R2A growth media. The plates were incubated at 28° C for 5 days before enumerating the amount of colony forming units (CFU) on each plate. The HPC is a common technique for quantifying biofilm formation on membrane surfaces.

Run 5: Deployment to Chandler Water Treatment Plant

The purpose of the fifth and final testbed run conducted was to deploy the testbed to treat a different source water and to test the remote data acquisition system newly installed in the testbed. The testbed was brought to the City of Chandler Water Treatment Plant (WTP). The testbed was hooked up to a tap where the water had gone all the treatment processes in the plant (i.e. coagulation, flocculation, sedimentation, and filtration), but had not yet been disinfected. This water quality was chosen over the finished water in hopes that biofouling on the membrane surfaces would again be induced by the source water, allowing for another comparison of the effects of the silver-coated membrane on biofouling formation. One challenge experienced in the deployment of the testbed was that the tap hookup was in a depressed portion of the WTP, approximately 15 feet below the trailer. This caused a pressure loss in the feed line to the testbed, resulting a feed pressure about 5 psi less than previously experienced by the testbed. For this

reason and to maintain the induced fouling procedure, the 150 mL/min flow restrictor was kept on the concentrate line to increase the permeate recovery rate. Another challenge associated with deploying the testbed was the frequency at which samples could be obtained. The WTP is located 20 miles from ASU's campus and has accessibility only during normal business hours. Therefore, performance measurements and samples were taken three days per week, three to four times per day. For this reason, the remote data acquisition (DAQ) system was very useful.

The remote DAQ system was configured and tested in the lab before deploying to the Chandler WTP. The DAQ system consisted of four National Instruments (NI) sensors, including a flow sensor, pressure sensor, conductivity probe, and temperature probe. The sensors were configured inside of a sensor module, as depicted in Figure 2.9 below.

Figure 2.9: Remote Data Acquisition Sensor Module Configuration

Five sensor modules pictured in Figure 2.9 were assembled at the lab. The sensors were connected to a 4-20mA George Fischer (GF) controller which relayed data to a desktop PC. The PC was configured with a LabVIEW program that was programmed to take continuous data measurements and both store them as well as report them graphically. For the LabVIEW program to function, a linear equation associated with each sensor was required. This meant that the sensors needed to be individually calibrated using varying parameters. For example, to calibrate the temperature sensor, four different water sources were recirculated through the sensor module with varying temperatures (i.e. 10°C, 15°C, 25°C, and 40°C). The resulting signal in mA was recorded for each known temperature and a graph plotting temperature vs. signal in mA could be developed. A linear equation with a slope and y-intercept was then found, and inputted into the LabVIEW program. The ranges of values selected for all sensors were expected to be the most extreme cases observed. To adjust the temperature, ice cubes were added or water was heated using a hot plate. The temperature was then measured using an infrared temperature sensor gun. The pressure values used in the calibration were 0, 5, 30, and 60 psi. Pressure was adjusted using a valve on the flow line, and measured using an attached manual pressure gauge. The flow was also adjusted using the valve on the flow line, which was measured using a manual flow meter. The target flow rates for the calibration were 25, 50, 100, and 500 mL/min. The conductivity values used for the calibration curve were 25, 100, 1000, and 2000 μS/cm, which was adjusted using conductivity salt calibration solutions. Conductivity was measured using a handheld conductivity meter. Once the calibrations were complete and the program was set up, the sensor modules were added to the feed line, the permeate lines, and the concentrate lines

of both POU units. Once the testbed was running, the LabVIEW was programmed to collect a data point every 15 minutes, so not to overpopulate the storage system with continuous data. In order to remotely monitor the system so performance could be observed from anywhere, the desktop PC was configured with the Google Chrome Remote Desktop application. This application allows the user to access any desktop with the same google chrome login credentials from another desktop, laptop, tablet, or smartphone. Since there was no internet connection at the WTP for the desktop to connect to, an internet hotspot was purchased and a monthly data plan was contracted through AT&T Wireless. Figure 2.10 below illustrates the data being viewed remotely using a smartphone.

Figure 2.10: LabVIEW Data Remotely Viewed Using Google Chrome Remote Desktop Application and a Smartphone

Maintaining remote access of the performance data generated at the WTP allowed for faster responses to any issues presented during the test. For instance, if the pressure differential across the membrane was greater than 5 psi and the cartridge filters needed to be changed, the remote DAQ could be configured with an alert system that to notify the user to change the cartridge filters. This became a valuable tool both educationally and applicably during this test.

The testbed was deployed for 34 days, from August 3, 2017 to September 6, 2017. In addition to the performance measurements taken throughout the analysis, TOC measurements and UV-254 measurements were taken. Additionally, the HPC analysis described in the Induced Fouling analysis was performed after the deployment as well.

CHAPTER 3

RESULTS

In this section, the results obtained from the analyses described in the Materials and Methods section of this thesis are illustrated and discussed. These results include the performance and characterization data obtained from both the flat sheet membranes and the spiral-wound RO membranes used in the Mobile NEWT Testbed.

3.1 Flat Sheet Membranes

Permeability Tests

Microfiltration Membranes

Figure 3.1 illustrates the flux for the microfiltration flat sheet membrane. The figures are plotted to show flux rate over time to illustrate any changes in flux rate experienced due to the silver coating or due to inorganic fouling. For these and all subsequent flux figures, flux initially increases to the maximum flux rate, due to the nature of turning the pressure regulator up to the desired pressure when initiating the experiment. Figure 3.1(a) shows the Nylon MF membrane, while Figure 3.1(b) shows the PVDF MF membrane. A pristine Nylon MF membrane reaches an average flux rate of 3931 ± 884 LMH, with a maximum flux rate of about 4,600 LMH under 20 psi of pressure when filtering nanopure water. After the silver coating is applied, the flux rate decreases to an average of 3784 ± 703 LMH, with a maximum of about 4,250 LMH when filtering nanopure water, which is a 4% decrease in average flux. When filtering tap water, both the pristine and coated Nylon MF membrane reach a maximum flux rate around 3,500 LMH, but have average flux rates of 3237 ± 610 LMH and 2722 ± 296

LMH, respectively. Both membrane flux rates then decline over time due to constituents in the tap water causing inorganic fouling. The average flux decline observed due to the silver coating in tap water was approximately 15% lower than the uncoated membrane.

As shown in Figure 3.1(b), a pristine PVDF MF membrane also reaches a maximum flux rate of about 4,600 LMH under 20 psi of pressure when filtering nanopure water, with an average flux rate of 4446 ± 455 LMH. After the silver coating is applied, the flux rate decreases to an average of 4065 ± 490 LMH, with a maximum flux rate of about 4,250 LMH when filtering nanopure water, which is a 9% decrease in average flux. When filtering tap water, a pristine membrane reaches a maximum flux rate of about 4,250 LMH, with an average flux rate of 3963 ± 247 LMH, and the silver-coated membrane reaches a maximum flux rate around 3,600 LMH with an average flux rate of 3504 ± 301 LMH. Both membranes then decline over time due to constituents in the tap water. The average flux decline observed due to the silver coating was approximately 12% lower than the uncoated membrane.

Comparing the performance of the two types of MF membranes yields consistent results. The silver-coating resulted in an average flux decline of 8-9% when filtering nanopure water and 12-15% when filtering tap water. Both the Nylon and the PVDF MF membranes experience flux decline due to constituents in the tap water for both the pristine and silver-coated membranes.

a)

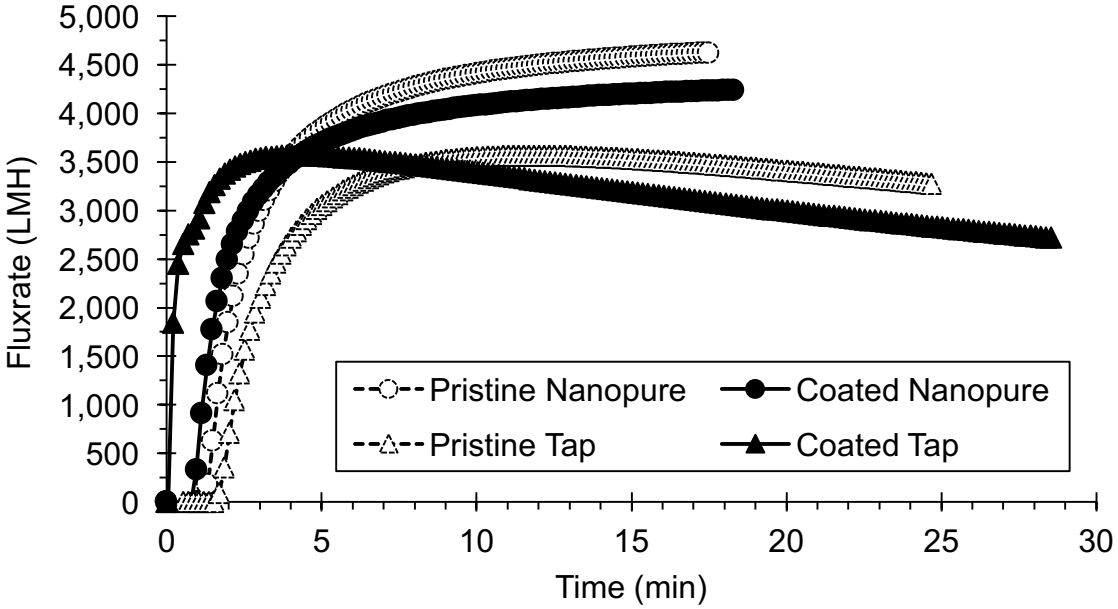

b)

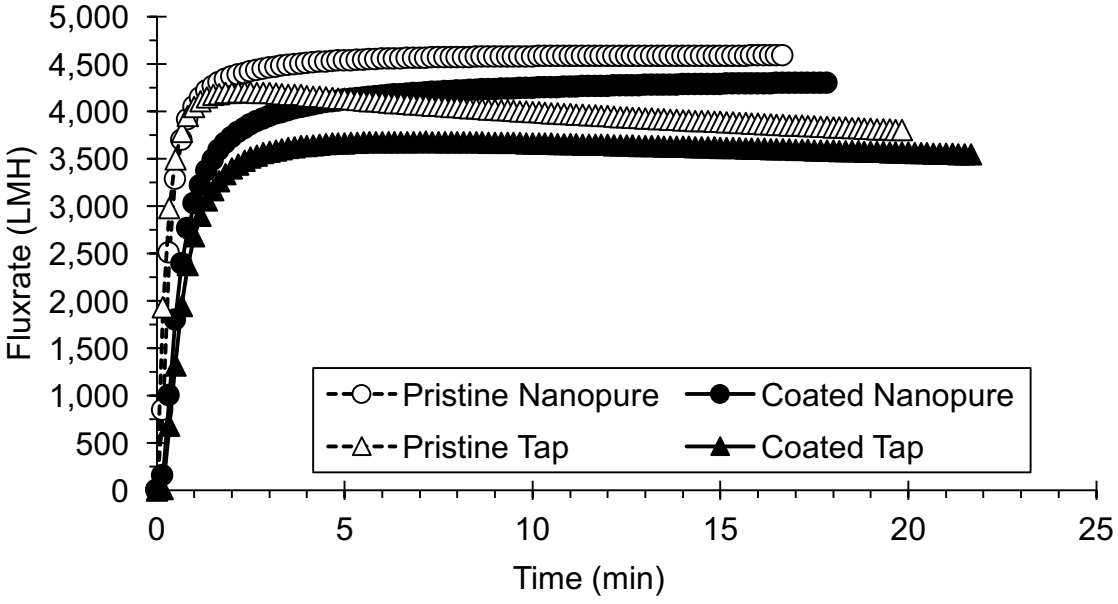

Figure 3.1: Permeability/Flux Test Results for (a) Nylon and (b) PVDF Flat Sheet Microfiltration Membranes

Ultrafiltration Membranes

Figure 3.2 below illustrates the flux results obtained from the ultrafiltration flat sheet membrane permeability tests. The figures are plotted to show flux rate over time to illustrate any changes in flux rate experienced due to the silver coating or due to inorganic fouling. Figure 3.2(a) shows the results observed in the Regenerated Cellulose UF membrane, while Figure 3.2(b) shows the results observed in the PES UF membrane. A pristine Regenerated Cellulose UF membrane reaches a maximum flux rate of about 33 LMH, with an average flux rate of 31 LMH under 50 psi of pressure when filtering nanopure water. After the silver coating is applied, the flux rate decreased to a maximum of about 30 LMH, with an average flux rate of 29 LMH when filtering nanopure water, which is approximately a 6% decrease in average flux. When filtering tap water, both the pristine and silver-coated Regenerated Cellulose UF membrane reach a maximum flux rate around 30 LMH, with an average flux rate of 29 LMH and 30 LMH, respectively. Both membranes then experience little to no flux decline caused by inorganic fouling. Other than the 6% decrease in flux caused by the silver coating, all Regenerated Cellulose flat sheet membrane achieve and maintain consistent flux rates around 30 LMH over time, which is slightly less than the 1 LMH/psi reported by the manufacturer (Millipore, 2008).

As shown in Figure 3.1(b), a pristine PES UF membrane reaches a maximum flux rate of about 360 LMH, with an average flux of 349 LMH under 50 psi of pressure when filtering nanopure water. After the silver coating is applied, the flux rate decreases to a maximum of about 340 LMH, with an average flux of 317 LMH, which is approximately

a 9% decrease in average flux. When filtering tap water, both the pristine membrane and silver-coated membrane reach a maximum flux rate of about 320 LMH, with an average flux rate of 252 LMH and 266 LMH, respectively. Both membranes then decline over time due to constituents in the tap water causing inorganic fouling. When inorganic fouling is a factor, the flux decline observed in the pristine membrane and the silver-coated membrane were aligned.

Comparing the performance of the two types of UF membranes yields consistent results. Due to the 0.06 nm pore-size in the Regenerated Cellulose membrane compared to the 0.2 nm pore-size in the PES membrane, higher flux rates are achieved in the PES membrane. The silver-coating resulted in a 3% greater average flux decline in the PES membrane compared to the Regenerated Cellulose membrane when filtering nanopure water. Both membranes experience little to no flux decline due to the silver coating when filtering tap water. The Regenerated Cellulose does not experience much flux decline due to inorganic fouling from tap water, while the PES membrane does for both the pristine and silver-coated membranes.

a)

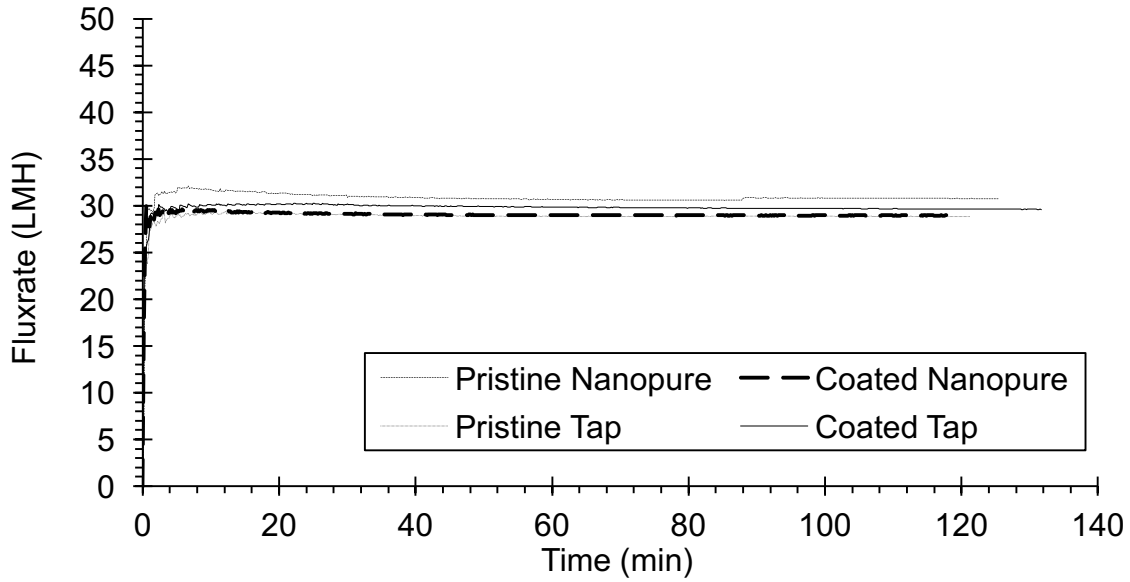

b)

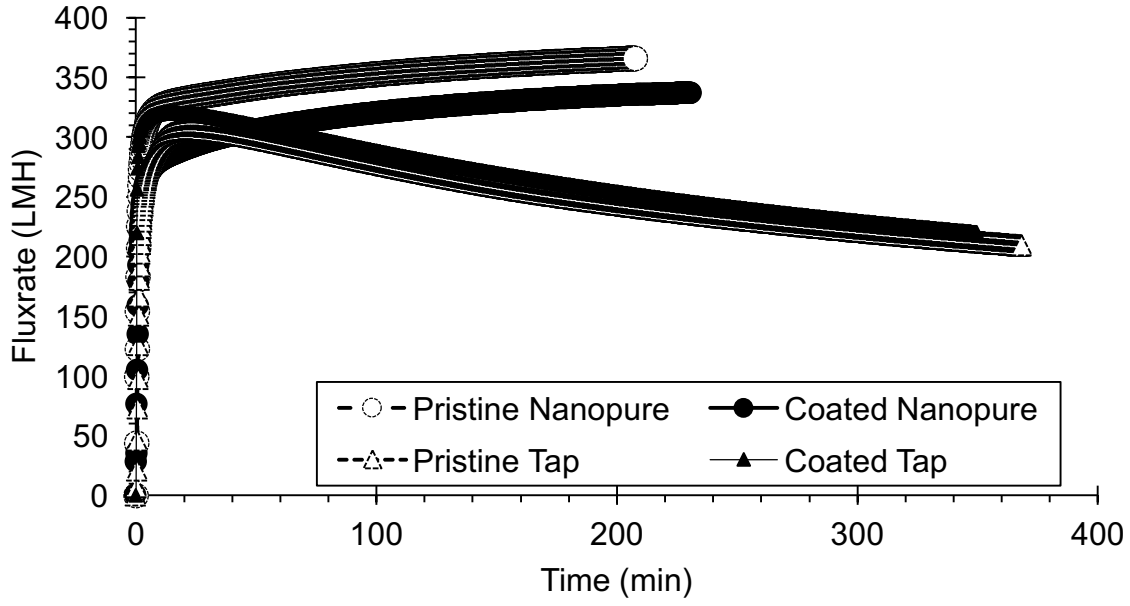

Figure 3.2: Permeability/Flux Test Results for (a) Regenerated Cellulose and (b) PES Flat Sheet Ultrafiltration Membranes

Reverse Osmosis Membrane

Figure 3.3 below illustrates the flux results obtained from the Polyamide RO flat sheet membrane permeability tests. The figure is plotted to show flux rate over time to illustrate any changes in flux rate experienced due to the silver coating or due to inorganic fouling. A pristine RO membrane reaches a maximum flux rate of about 33 LMH, with an average flux of 16 LMH under 50 psi of pressure when filtering nanopure water. The RO membrane quickly decreases to 15 LMH shortly after due to the compaction phenomenon experienced in RO membranes. After the silver coating is applied, the maximum flux rate decreased to about 15 LMH, with an average flux of 14 LMH when filtering nanopure water, which is approximately a 12% decrease in flux. When filtering tap water, the pristine membrane reaches a maximum flux rate around 15 LMH, with an average flux of 12 LMH after 6 hours. The silver-coated RO membrane reaches a maximum flux rate around 11 LMH, with an average flux of 10 LMH after 6 hours. When filtering tap water, the average flux decline after 6 hours of filtration is approximately 20% and 9% in the pristine and the silver-coated RO membranes, respectively. When filtering tap water, the average flux decline caused by the silver coating is approximately 25% when the test was initiated, but drops to about 16% after 6 hours of filtration.

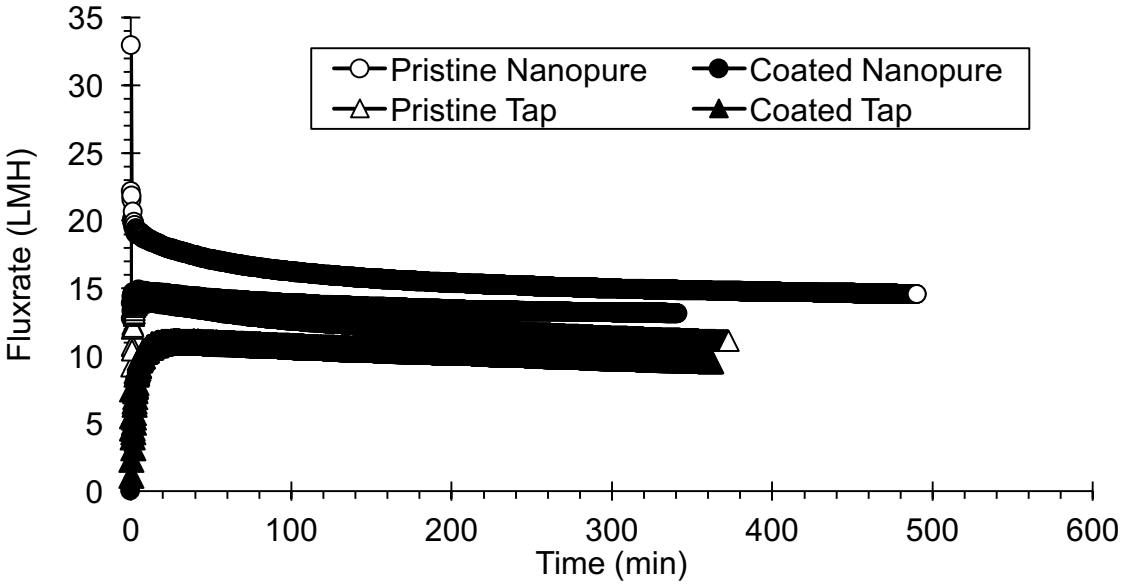

Figure 3.3: Permeability/Flux Test Results Polyamide Flat Sheet Reverse Osmosis Membrane

Table 3.1: Flat Sheet Membrane Average Flux Summary (LMH)

Membrane	**Pore-Size (µm)**	**Pristine Nanopure**	**Ag-Coated Nanopure**	**P-Value**	**Pristine Tap Water**	**Ag-Coated Tap Water**	**P-Value**
Nylon MF	0.2	3931 ± 884	3784 ± 703	0.24	3237 ± 610	2722 ± 296	0.10
PVDF MF	0.2	4446 ± 455	4065 ± 490	0.00	3963 ± 247	3504 ± 301	0.00
Regenerated Cellulose UF	6×10^{-5}	31 ± 1.0	29 ± 0.5	0.00	29 ± 0.6	30 ± 0.5	0.00
PES UF	2×10^{-4}	349 ± 21	317 ± 24	0.00	252 ± 32	266 ± 31	0.00
Polyamide RO	Semi-permeable	16 ± 1.1	14 ± 0.4	0.00	12 ± 0.9	10 ± 0.7	0.00

Static Leaching test

Microfiltration Membranes

Figure 3.4 illustrates the results obtained from the static silver-leaching test for MF flat sheet membranes. The initial silver-loading was found to be 1.9 ± 0.1 μg/cm^2, as described in the digestion section. In Figure 3.4(a), the leaching test for the Nylon membrane shows that after 4 hours of submersion in both pH 8.0 and pH 6.0 solutions, diffusion-based interactions release about 0.25 μg of silver per cm^2 of membrane, which occurs within the first 30 minutes of reaction. However, the pH 2.0 solution shows that 1.00 μg/cm^2 is released after 4 hours, 50% of which occurs within the first hour of reaction. This indicates that under ambient pH conditions experienced in tap water, the silver coating is not rapidly released, but in extreme pH conditions that may be experienced during clean-in-place procedures, silver can be released in much greater quantities.

In Figure 3.4(b), the leaching test for the PVDF membrane shows that after 4 hours of submersion in all pH conditions, diffusion-based interactions release greater than 0.5 μg of silver per cm^2 of membrane. It was hypothesized that the pH 2.0 solution would cause a significantly greater release of silver compared to the pH 8.0 and pH 6.0 solutions. However, results indicate that the pH 2.0 and pH 6.0 solutions both release around 0.5 μg/cm^2 is after 1 hour, while the pH 8.0 solution causes a release of 0.3 μg/cm^2. This indicates that silver is more loosely bound to PVDF membranes compared to Nylon membranes, as more silver is released under the same pH conditions. Additionally, for all MF membranes tested, approximately 50% of the silver released

occurs within the first 30 minutes of submersion in solution due to diffusion-based interactions.

a)

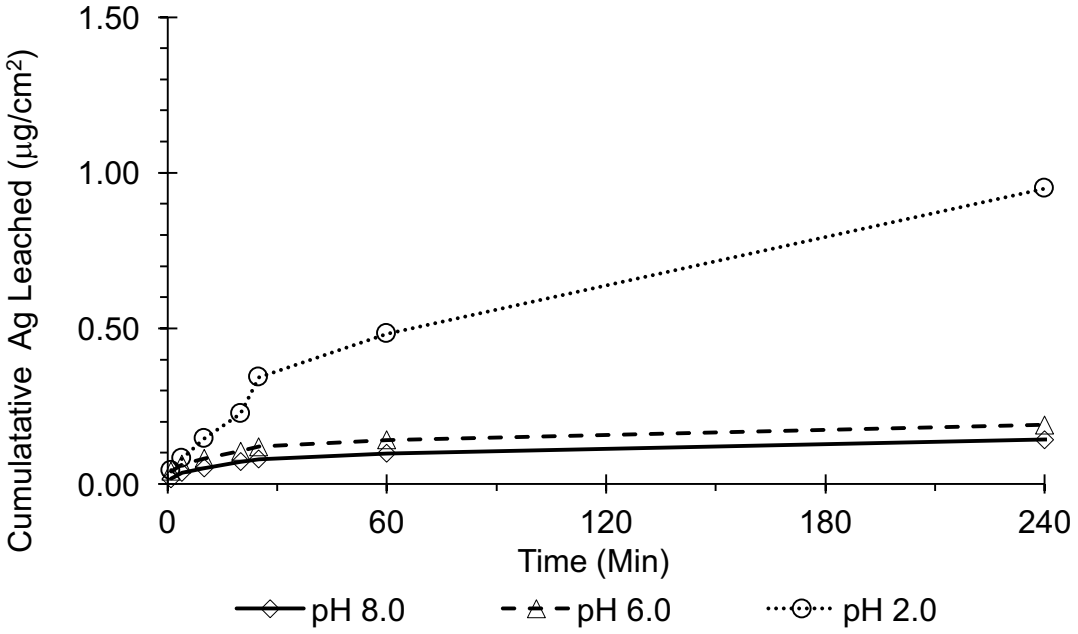

b)

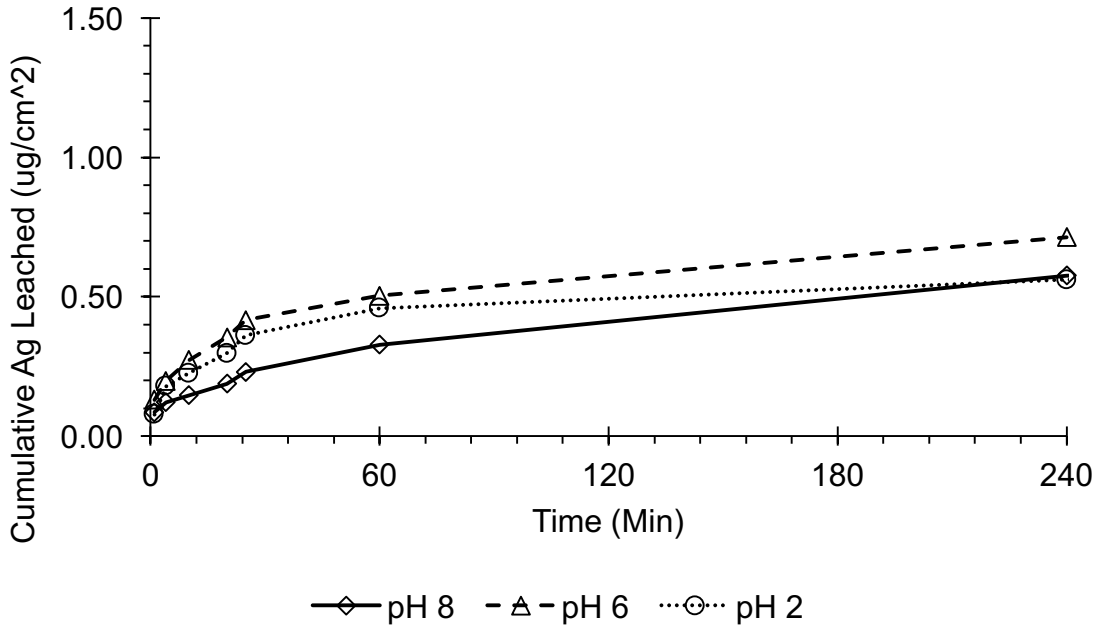

Figure 3.4: Static Leaching Test Results for (a) Nylon (Initial Loading 0.95 μg/cm^2) and (b) PVDF(Initial Loading 0.71 μg/cm^2) Flat Sheet Microfiltration Membranes

Ultrafiltration Membranes

Figure 3.5 illustrates the results obtained from the static leaching test for UF flat sheet membranes. In Figure 3.5(a), the leaching test for the Regenerated Cellulose membrane shows that after 4 hours of submersion in pH 8.0 and pH 2.0 solutions, the membranes released 0.4 and 0.7 μg/cm^2, respectively. The pH 6.0 solution released around 1.4 μg/cm^2 after 4 hours of submersion. In all pH solutions, around 50% of the silver released occurs within the first 30 minutes of reacting, and 90% occurs within the first two hours.

In Figure 3.4(b), the leaching test for the PES membrane shows a similar phenomenon, where the most silver release occurs in the pH 6.0 solution. After 4 hours of

submersion, the membranes released 1.4, 2.5, and 1.3 μg/cm^2 in pH 8.0, pH 6.0, and pH 2.0 solutions, respectively. For all solutions, around 50% of the total silver released occurred within the first 30 minutes, and around 80% of the silver released occurred within the first hour. For all UF membranes tested, further investigation may be required to determine the reason pH 6.0 solution causes the greatest amount of silver release.

a)

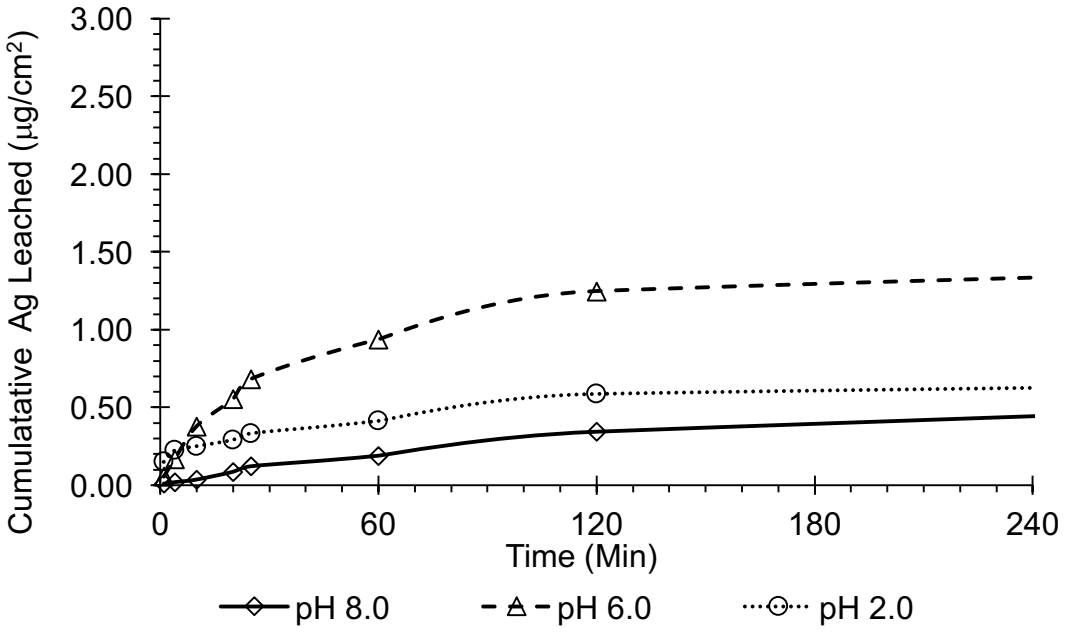

b)

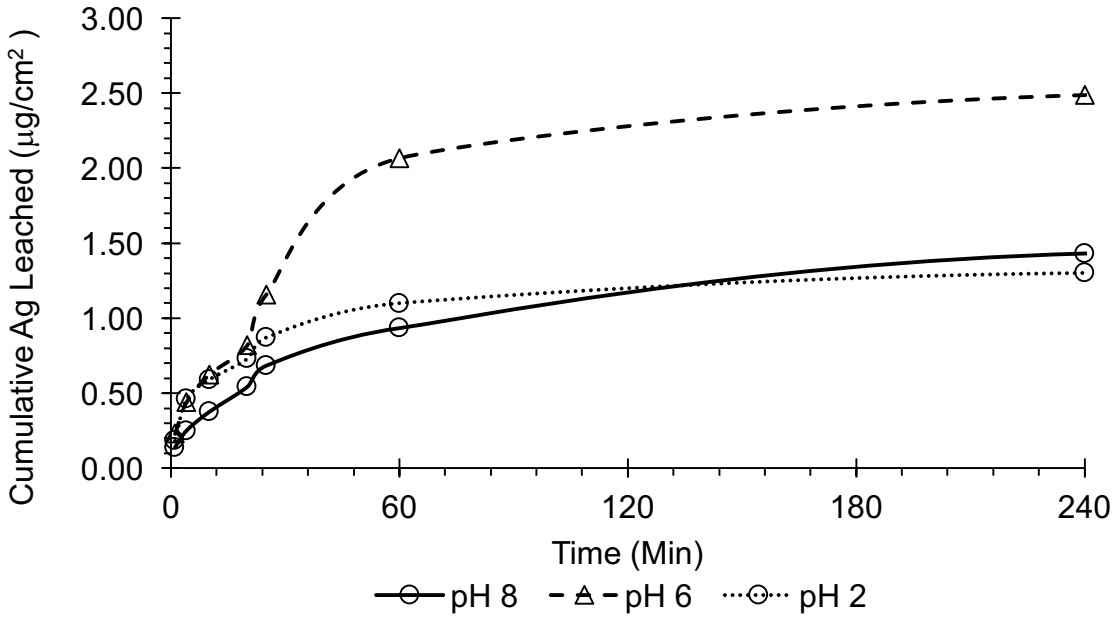

Figure 3.5: Static Leaching Test Results for (a) Regenerated Cellulose (Initial Loading 1.80 µg/cm^2) and (b) PES (Initial Loading 2.49 µg/cm^2) Flat Sheet Ultrafiltration Membranes

Reverse Osmosis Membrane

Figure 3.6 below illustrates the results obtained from the static leaching test for the polyamide RO flat sheet membrane. The results show that after one hour of submersion in pH 8.0, pH 6.0, and pH 2.0 solutions, the membranes released around 0.25, 0.20, and 0.50 µg/cm^2, respectively. For all pH solutions, around 50% of the total silver released occurred within the first 10 minutes, and 90% occurred within the first 30 minutes. These results indicate that in ambient pH conditions as well as conditions that may be experienced during CIP procedures, 90% of the silver released due to diffusion-based interactions will occur within the first 30 minutes for polyamide RO membranes.

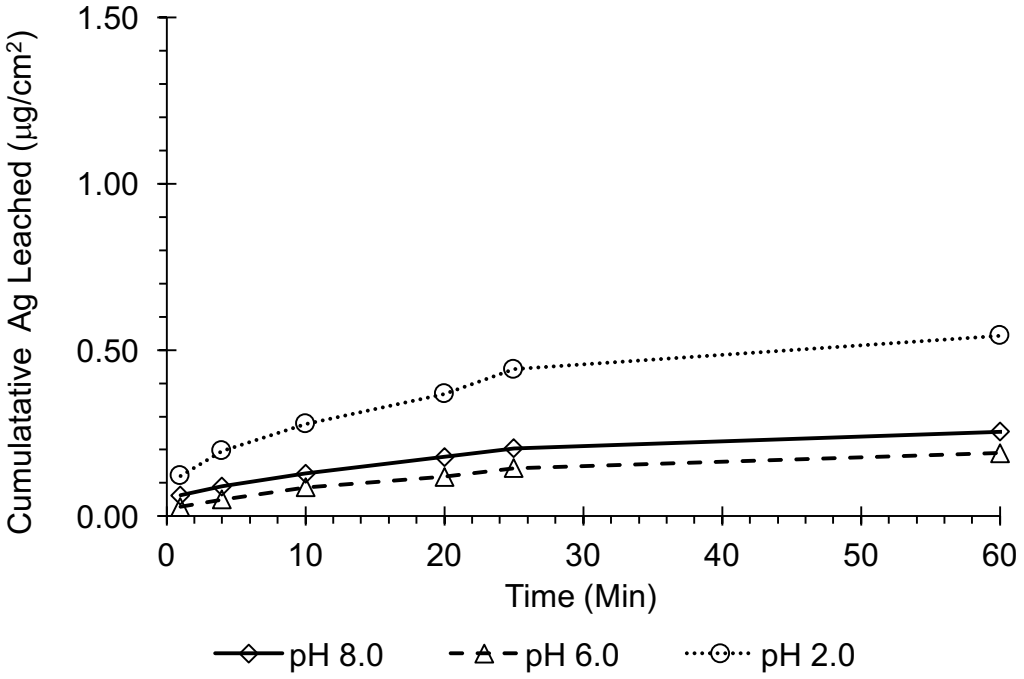

Figure 3.6: Static Leaching Test Results for Polyamide Flat Sheet Reverse Osmosis Membrane (Initial Loading 1.93 µg/cm^2)

Table 3.2 below summarizes the cumulative silver leached for each membrane type after 60-minutes of diffusion in each pH solution.

Table 3.2: Cumulative Silver Leached

		Silver Leached After 60 Minutes (μg/cm^2)		
Membrane Type	Initial Silver Loading (μg/cm^2)	pH 2.0	pH 6.0	pH 8.0
Nylon MF	0.95	0.48	0.14	0.10
PVDF MF	0.71	0.46	0.50	0.33
Regenerated Cellulose UF	1.80	0.41	0.94	0.19
PES UF	2.49	1.10	2.07	0.93
Polyamide RO	1.90	0.54	0.19	0.25

SEM/EDX

Figures 3.7 through 3.11 below display the images obtained from the SEM and EDX analyses of the silver-coated MF, UF, and RO membranes. The images serve to illustrate the surface topography, pore-size and structure of the membranes, the size of Ag-NPs coated on the membranes, and the elemental composition of the membranes.

Microfiltration Membranes

Figure 3.7 below illustrates the images obtained from the SEM and EDX analyses conducted on the Nylon MF membranes.

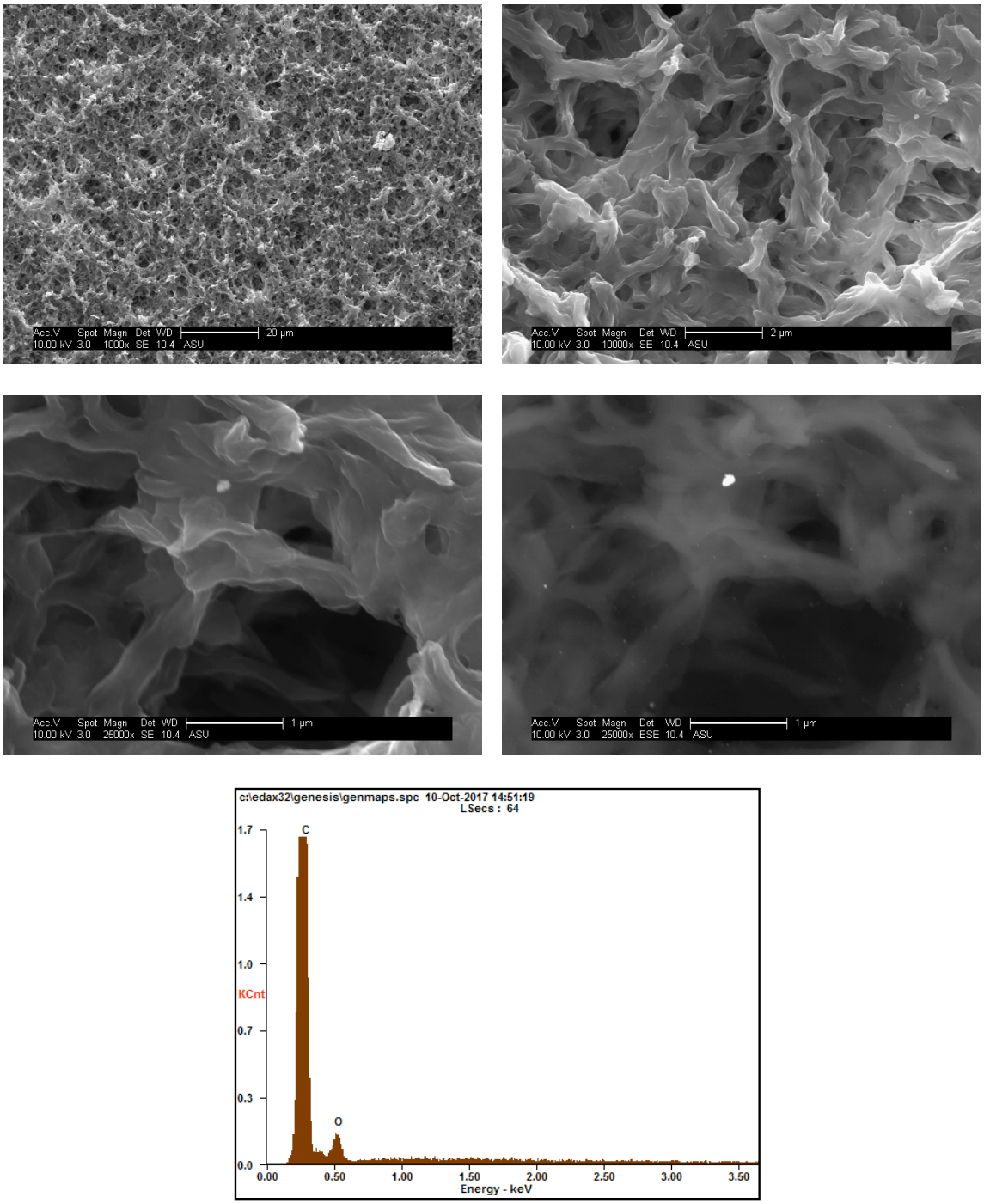

Figure 3.7: SEM/EDX Images of Silver-Coated Nylon Microfiltration Membrane at (a – Top Left) 1,000x, (b – Top Right) 10,000x, (c – Middle Left) 25,000x, (d – Middle Right) 25,000x magnification in backscatter mode, and (e - Bottom) EDX at 10,000x magnification

Figure 3.7(a) at 1,000x magnification shows the surface topography of the Nylon MF membrane is complex and highly porous. Figure 3.7(b) at 10,000x magnification illustrates the varying pore shapes and sizes within the membrane. Figure 3.7(c) at 25,000x magnification was chosen to observe an agglomeration of silver particles. Figure 3.7(d) is the same image but shot in BSE mode, where the silver agglomeration and surrounding nanoparticles can be observed. The agglomeration of silver was measured to be around 100 nm in diameter, and the surrounding bright spots were determined to be smaller Ag-NPs. The elemental analysis showed peak responses for carbon and oxygen, which was caused by the carbon sputtering and the nylon membrane, primarily composed of carbon, oxygen, hydrogen, and nitrogen.

Figure 3.8 below illustrates the images obtained from the SEM and EDX analyses conducted on the PVDF MF membranes.

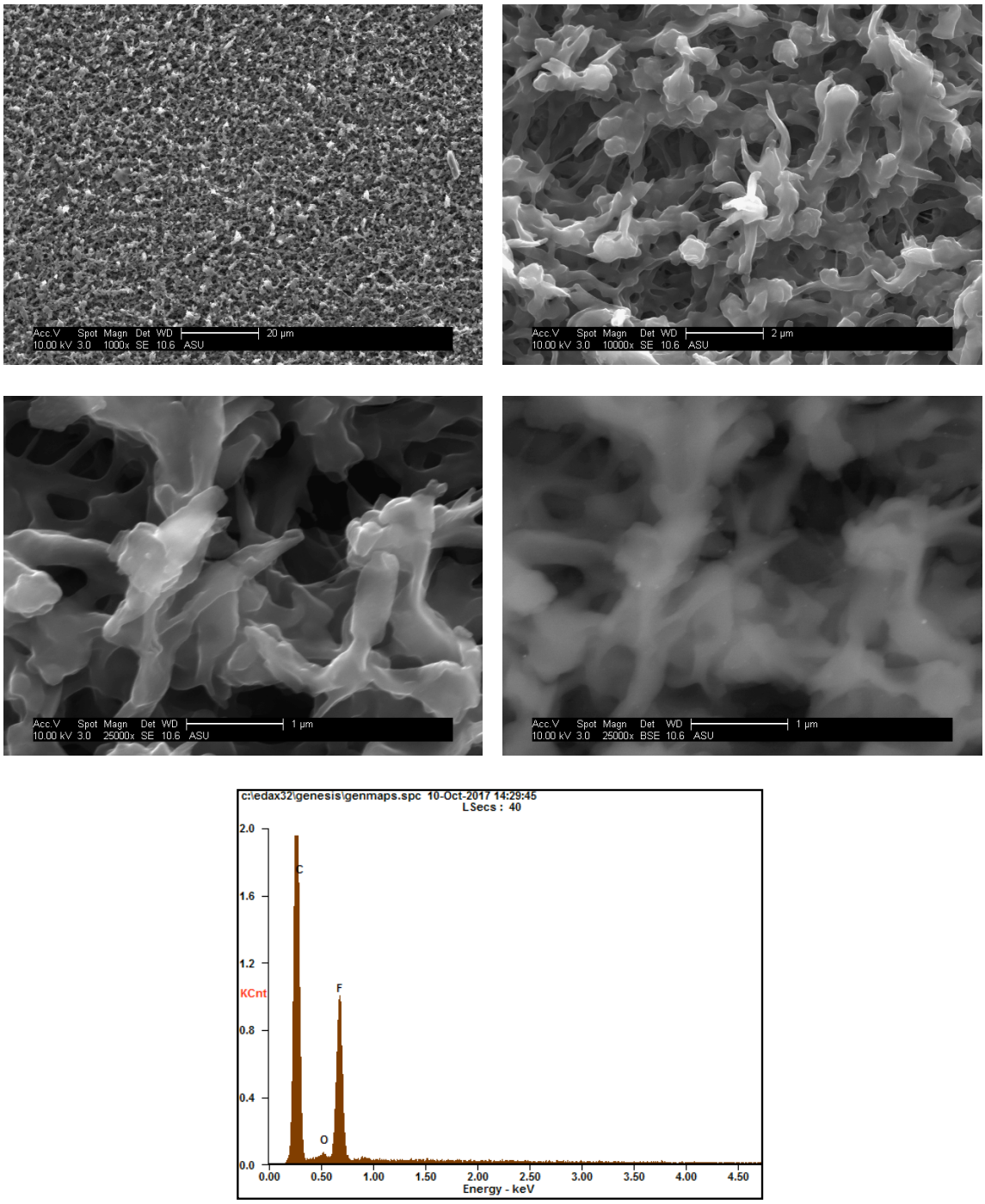

Figure 3.8: SEM/EDX Images of Silver-Coated PVDF Microfiltration Membrane at (a – Top Left) 1,000x, (b – Top Right) 10,000x, (c – Middle Left) 25,000x, (d – Middle Right) 25,000x magnification in backscatter mode, and (e - Bottom) EDX at 10,000x magnification

Figure 3.8(a) at 1,000x magnification shows the surface topography of the PVDF MF membrane is complex and highly porous. Figure 3.8(b) at 10,000x magnification illustrates the varying pore shapes and sizes within the membrane, as well as the more sharp, jagged edges as compared to the Nylon MF membrane. Figure 3.8(c) at 25,000x magnification was chosen to observe Ag-NPs embedded within the membrane matrix. Figure 3.8(d) is the same image but shot in BSE mode, where the Ag-NPs can be observed. The Ag-NPs measured were determined to be in the nanometer range, between 20 and 100 nm. The elemental analysis showed peak responses for carbon and fluorine, which was caused by the carbon sputtering and the PVDF membrane, primarily composed of carbon, hydrogen, and fluorine.

Ultrafiltration Membranes

Figure 3.9 below illustrates the images obtained from the SEM and EDX analyses conducted on the Regenerated Cellulosed UF membranes.

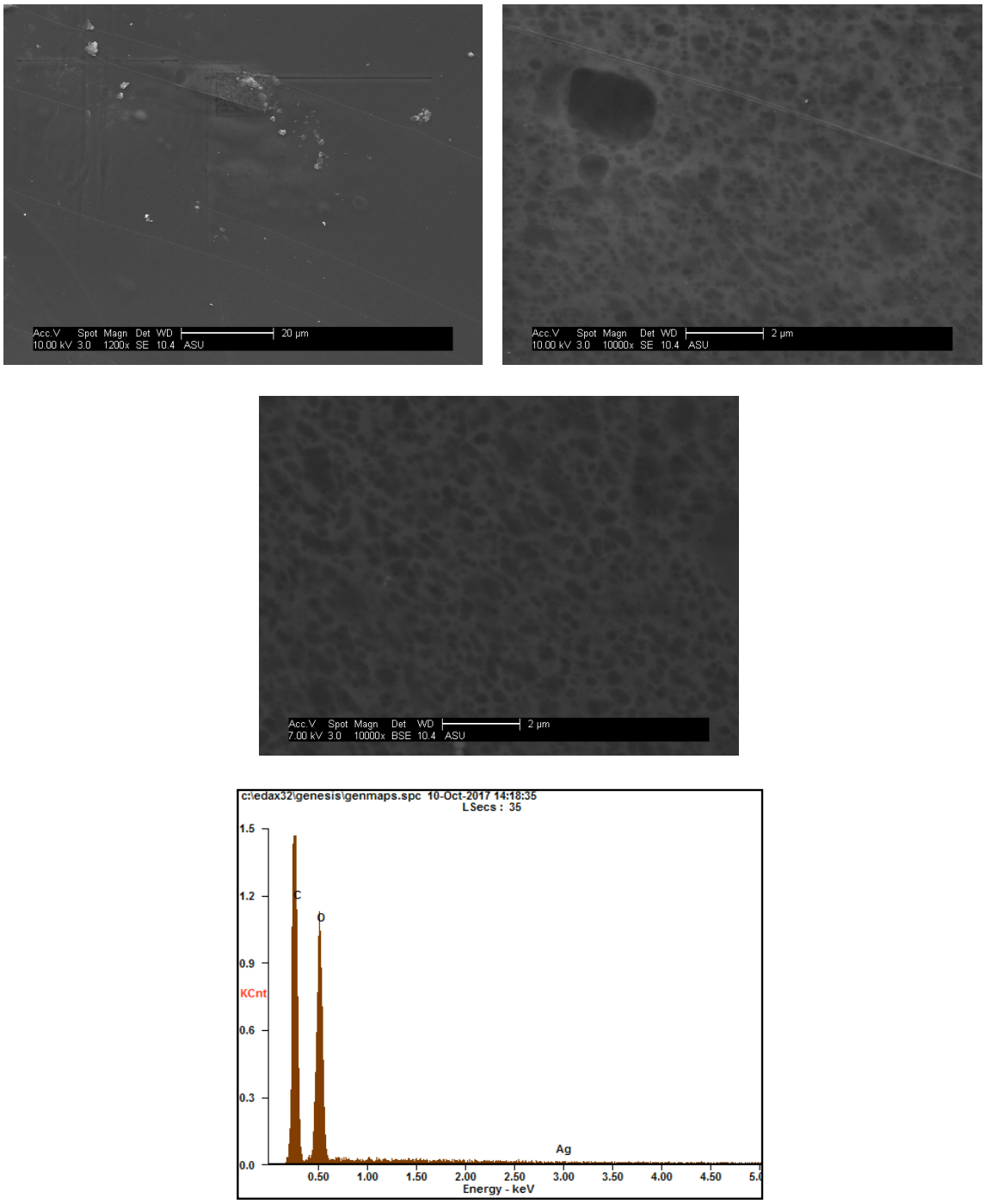

Figure 3.9: SEM/EDX Images of Silver-Coated Regenerated Cellulose Ultrafiltration Membrane at (a – Top Left) 1,200x, (b – Top Right) 10,000x, (c - Middle) 10,000x magnification in backscatter mode, and (e - Bottom) EDX at 1,500x magnification

Figure 3.9(a) at 1,200x magnification was the first attempt at obtaining SEM images of the regenerated cellulose UF membrane. The abnormalities on the membrane are locations where the electron beam damaged or penetrated the membrane. If left too long on one spot, the electron beam would burn off the spot in which it was penetrating. Therefore it was very difficult to obtain quality images of the regenerated cellulose membrane. However, the images above were obtained to show some surface features of the regenerated cellulose UF membrane. Figure 3.9(b) at 10,000x magnification illustrates the varying pore shapes and sizes within the membrane. Figure 3.9(c) was taken with the same 10,000x magnification, but at a different location and in BSE mode. Pore structures can be observed in both 10,000x magnification images. The elemental analysis showed peak responses for carbon oxygen, which was caused by the carbon sputtering and the regenerated cellulose membrane, primarily composed of oxygen and hydrogen.

Figure 3.10 below illustrates the images obtained from the SEM and EDX analyses conducted on the PES UF membranes.

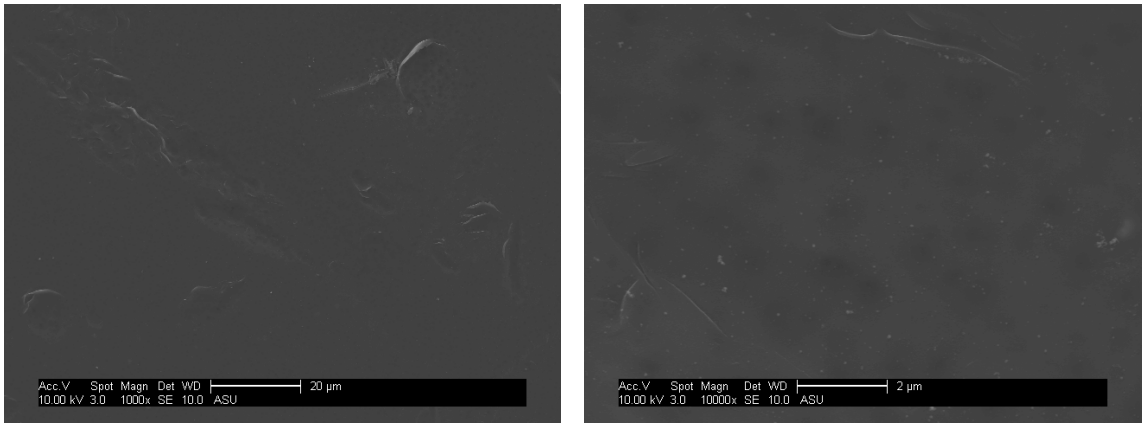

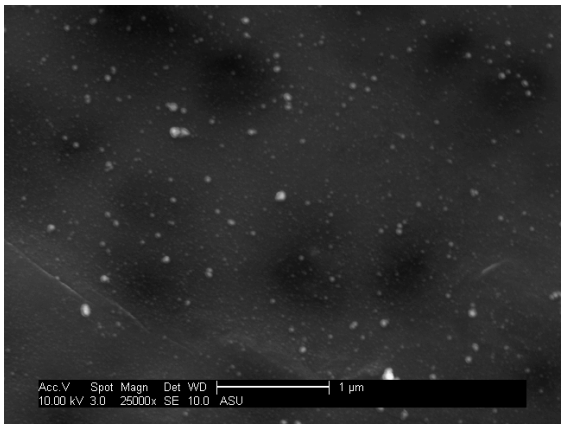
Acc.V Spot Magn Det WD 1 µm
10.00 kV 3.0 25000x SE 10.0 ASU

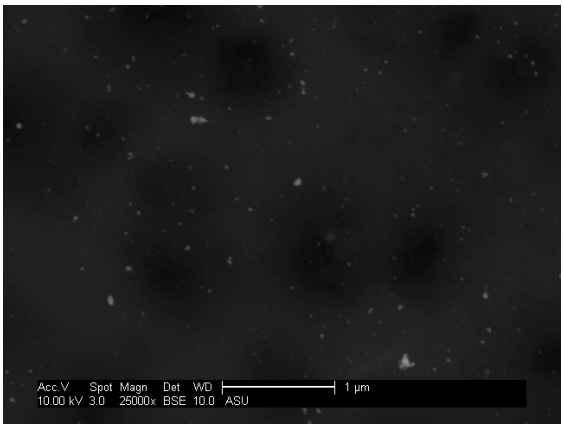
Acc.V Spot Magn Det WD 1 µm
10.00 kV 3.0 25000x BSE 10.0 ASU

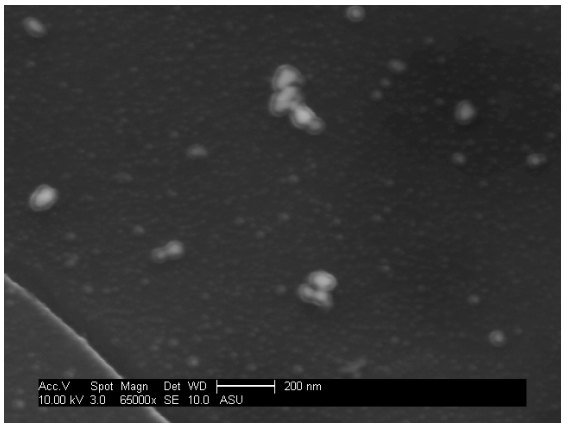
Acc.V Spot Magn Det WD 200 nm
10.00 kV 3.0 65000x SE 10.0 ASU

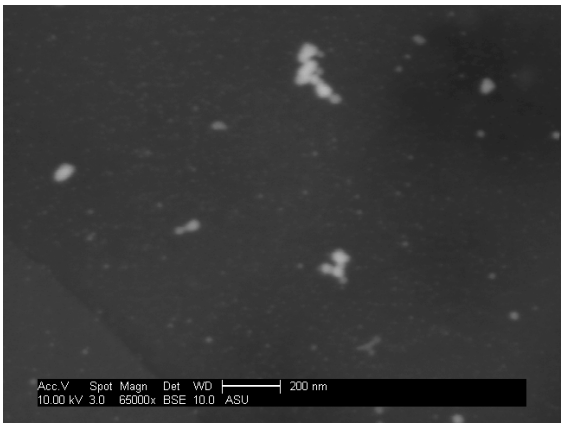
Acc.V Spot Magn Det WD 200 nm
10.00 kV 3.0 65000x BSE 10.0 ASU

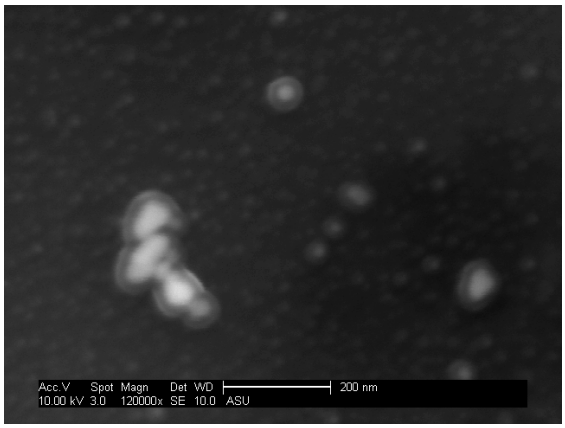
Acc.V Spot Magn Det WD 200 nm
10.00 kV 3.0 120000x SE 10.0 ASU

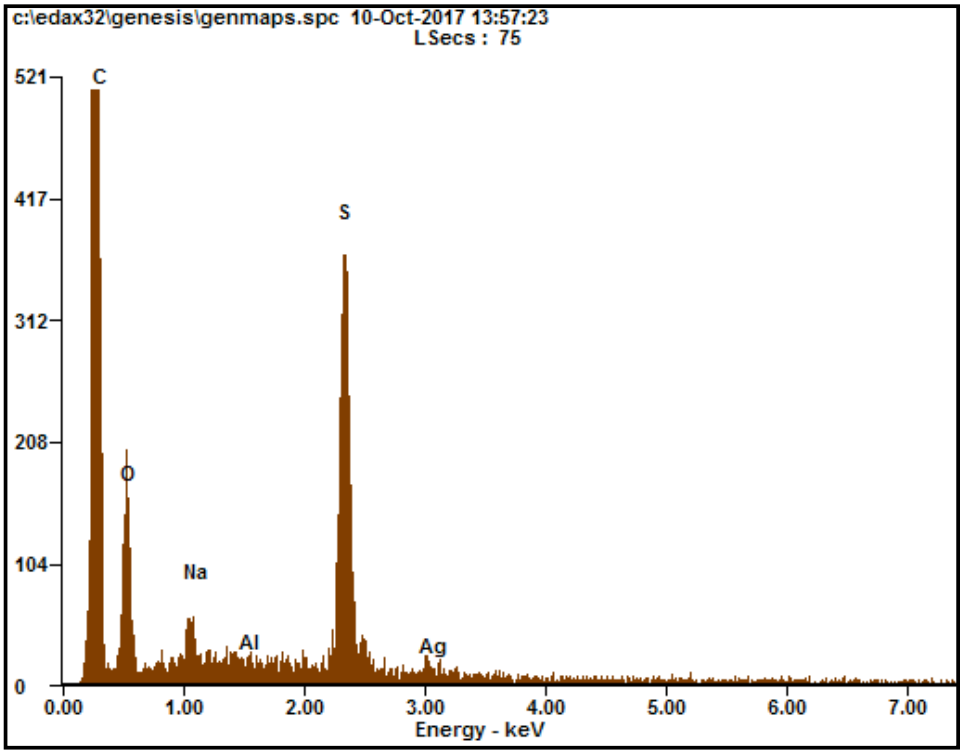

Figure 3.10: SEM/EDX Images of Silver-Coated PES Ultrafiltration Membrane at (a – Top Left) 1,000x, (b- Top Right) 10,000x, (c – Row Two, Left) 25,000x, (d – Row Two, Right) 25,000x in backscatter mode, (e – Row Three, Left) 65,000x, (f – Row Three, Right) 65,000x in backscatter mode, (g – Row Four) 120,000x, and (h - Bottom) EDX at 10,000x magnification

Figure 3.10(a) at 1,000x magnification shows the surface topography of the PES UF, which appears to be flat and amorphous. In Figure 3.10(b) at 10,000x magnification, Ag-NPs deposited on the surface can be distinguished as raised bumps, or white dots across the surface. Figure 3.10(c) at 25,000x magnification shows Ag-NPs of varying sized distributed across the surface. Figure 3.10(d) is the same image location but shot in BSE mode, where the Ag-NPs can be seen both embedded in the membrane and

distributed across the membrane surface. Figure 3.10(e) takes a closer look at the Ag-NPs at 65,00x magnification, where individual particles can be seen separately and together as agglomerations. Figure 3.10(f) shows the same image location and same 65,000x magnification, but in BSE mode, where the particles are more opaque and apparent. Figure 3.10(g) takes a closer look at an agglomeration and an individual Ag-NP at 120,000x in SE mode. At this magnification, it appears the Ag-NPs may have a solid core, surrounded by a more transparent shell. The Ag-NPs measured were determined to be in the nanometer range, between 20 and 100 nm. The elemental analysis showed peak responses for carbon, oxygen, and sulfur, which was caused by the carbon sputtering and the PES membrane, primarily composed of carbon, hydrogen, oxygen, and sulfur.

Reverse Osmosis Membrane

Figure 3.11 below illustrates the images obtained from the SEM and EDX analyses conducted on the Polyamide RO membranes.

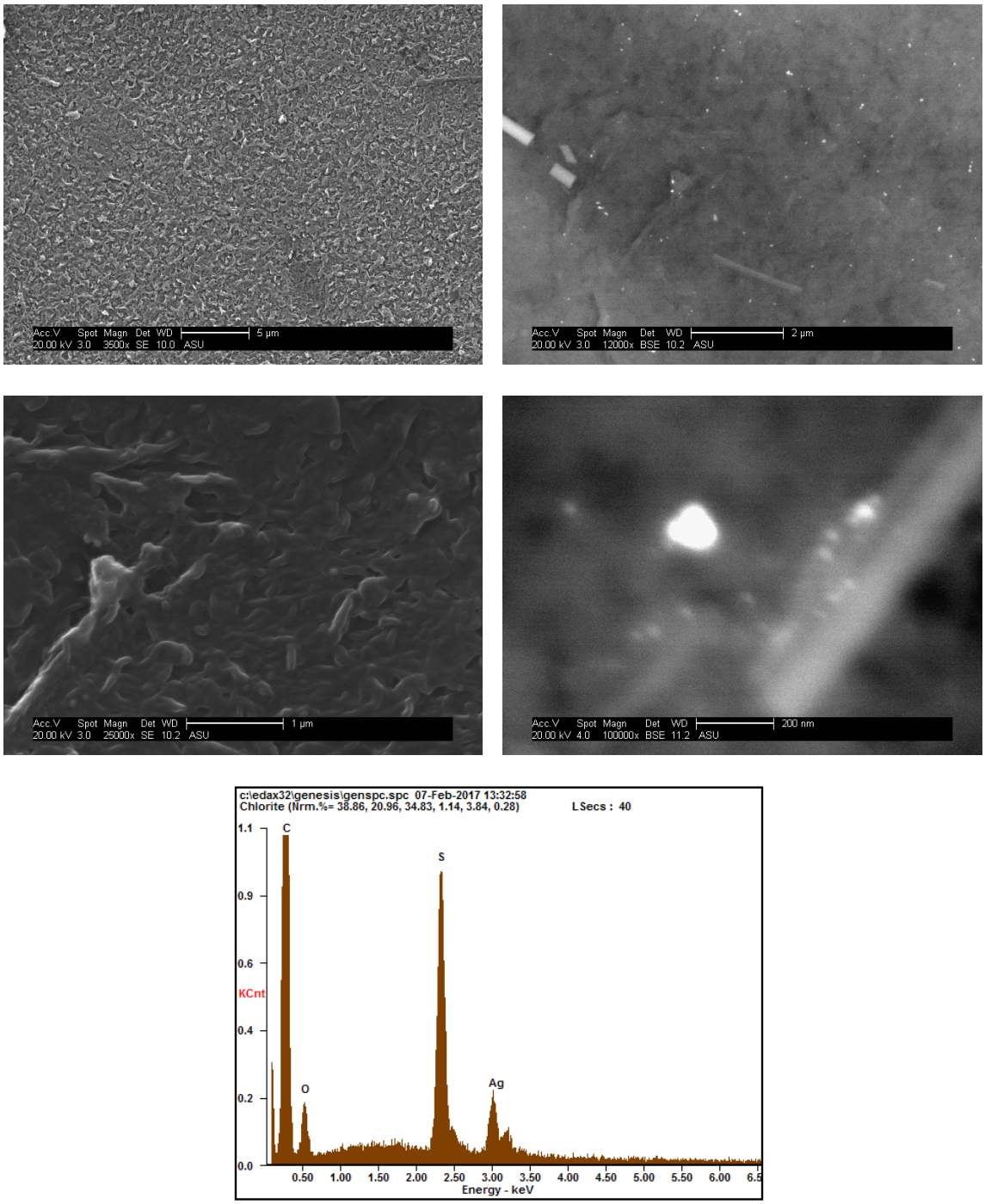

Figure 3.11: SEM/EDX Images of Silver-Coated Polyamide Reverse Osmosis Membrane at (a – Top Left) 3,500x, (b – Top Right) 12,000x in BSE mode,(c – Middle Left) 25,000x, (d – middle Right) 100,000x magnification in backscatter mode, and (e - Bottom) EDX at 10,000x magnification

Figure 3.11(a) at 3,500x magnification shows the surface topography of the polyamide RO membrane is complex, with no visible pores due to the semipermeable nature of the membrane. Figure 3.11(b) at 12,000x magnification in BSE mode illustrates the distribution of Ag-NPs across the membrane surface, which can be seen as the white dots spread across the membrane. Figure 3.11(c) at 25,000x magnification in SE mode takes a closer look at the polyamide active layer surface of the RO membrane. Figure 3.11(d) at 100,000x magnification in BSE mode shows a close look at a Ag-NP, which is the bright white circle illuminated in the center of the image. The Ag-NP was measured to be in the nanometer range, about 100 nm in diameter. The elemental analysis showed peak responses for carbon, oxygen, sulfur, and silver. These peaks were caused by the carbon sputtering and the polyamide active layer on top of the PES support layer of the membrane, which is primarily composed of carbon, hydrogen, oxygen, and sulfur. The silver peak was caused by the silver coating on the RO membrane.

Surface Charge

Figure 3.12 below illustrates the results obtained from the ZeataCAD streaming potential analyzer for the Nylon MF membrane, the Regenerated Cellulose UF membrane, and the polyamide RO membrane, both pristine and silver-coated for all types.

Microfiltration Membrane

a)

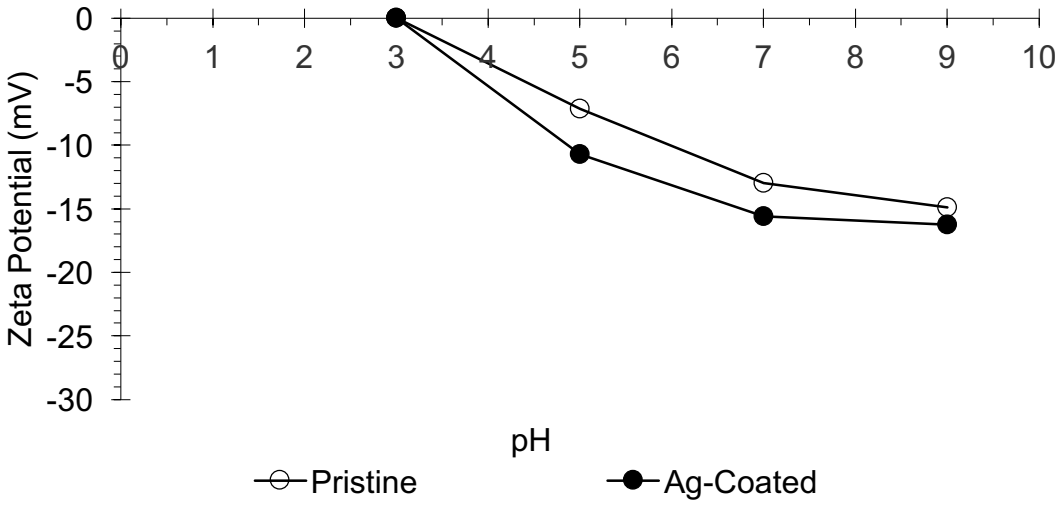

b)

Ultrafiltration Membrane

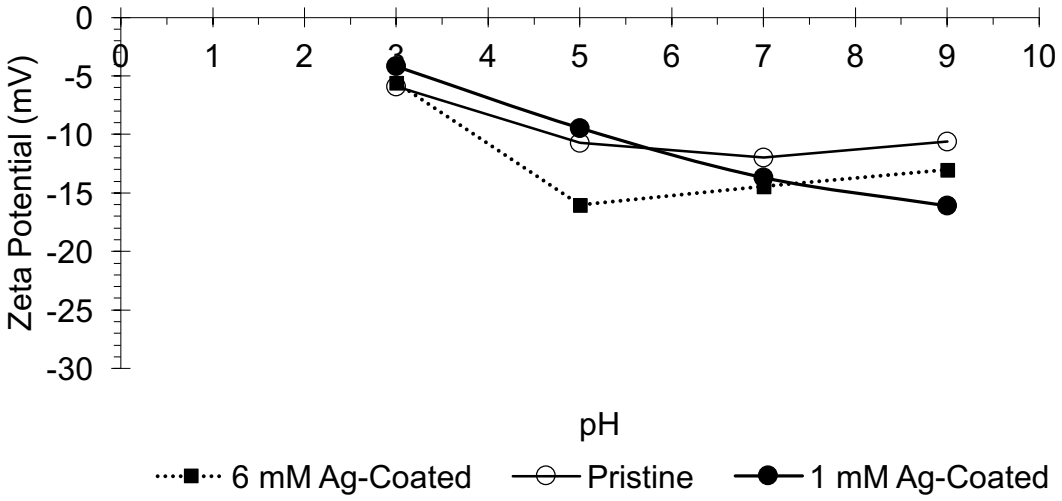

c)

Reverse Osmosis Membrane

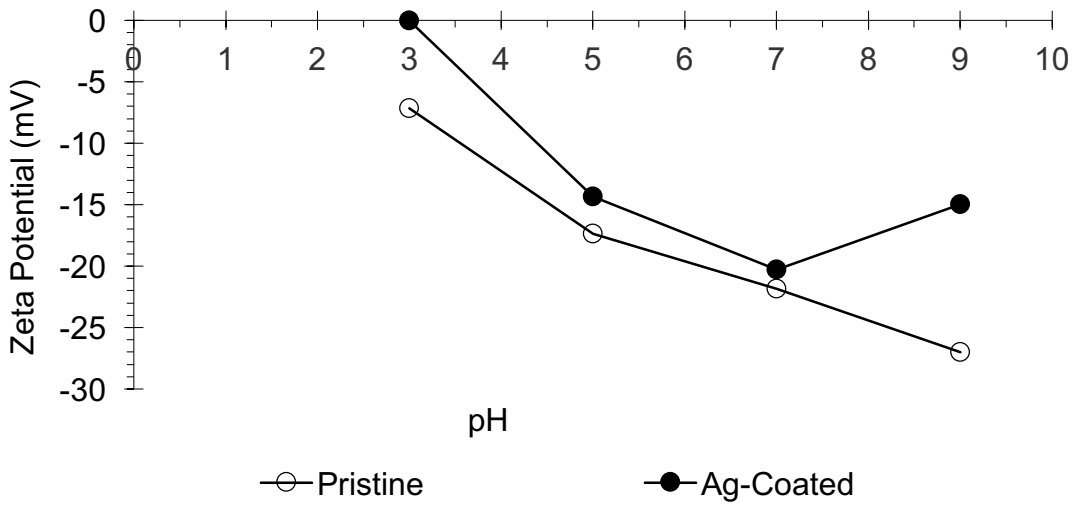

Figure 3.12: Surface Charge Results for Pristine and Silver-Coated (a) Nylon Microfiltration, (b) Regenerated Cellulose Ultrafiltration, and (c) Polyamide Reverse Osmosis Membranes

As illustrated in Figure 3.12 above, the pristine membranes and the silver-coated membranes experience similar streaming potential, or zeta potential responses in varying pH solutions for all membrane types. For the Nylon MF membrane, as pH decreases, the surface response increases. The point of zero charge (PZC) is at pH 3.0 for both the pristine and the silver-coated membranes. For the Regenerated Cellulose UF membrane, 1 mM and 6 mM silver-coated membranes both behave similarly to a pristine membrane. The zeta potential response at pH 9.0 ranges from -11 mV to – 16 mV between the pristine membrane and the 1 mM silver-coated membrane, respectively. The PZC was not obtained for the UF membrane, however all three UF membranes tested approached zero charge at pH 3.0, with -5 mV responses. For the polyamide RO membrane, there were

slight discrepancies between the pristine membrane and the silver-coated membrane. At pH 9.0, the pristine membrane showed a zeta potential response at -27 mV, while the silver-coated membrane had a zeta potential response at -15 mV. However, at pH 7.0 and pH 5.0, the responses were very similar, around -20 mV and -16 mV for both membranes, respectively. The PZC for the silver-coated membrane was at pH 3.0, and the pristine membrane remained negatively charged throughout the analyses.

3.2 Spiral Wound Membranes

Membrane Characterization

Silver Loading on Spiral-Wound RO Membrane

Figure 3.13 below depicts the results obtained from the membrane digestion for the polyamide RO membrane after being analyzed for silver-loading. The results were converted from μg/L to μg/cm^2, where 30 mL of sample was analyzed, and 7.78 cm^2 of membrane was digested. Equation 3.1 below shows the calculation performed for the results.

$$(X\ \mu g\ Ag\ /L)\ x\ (0.03\ L)\ \div\ (7.78\ cm^2 \text{ per membrane})\ =\ Y \mu g\ Ag/\ cm^2\ membrane \qquad (3.1)$$

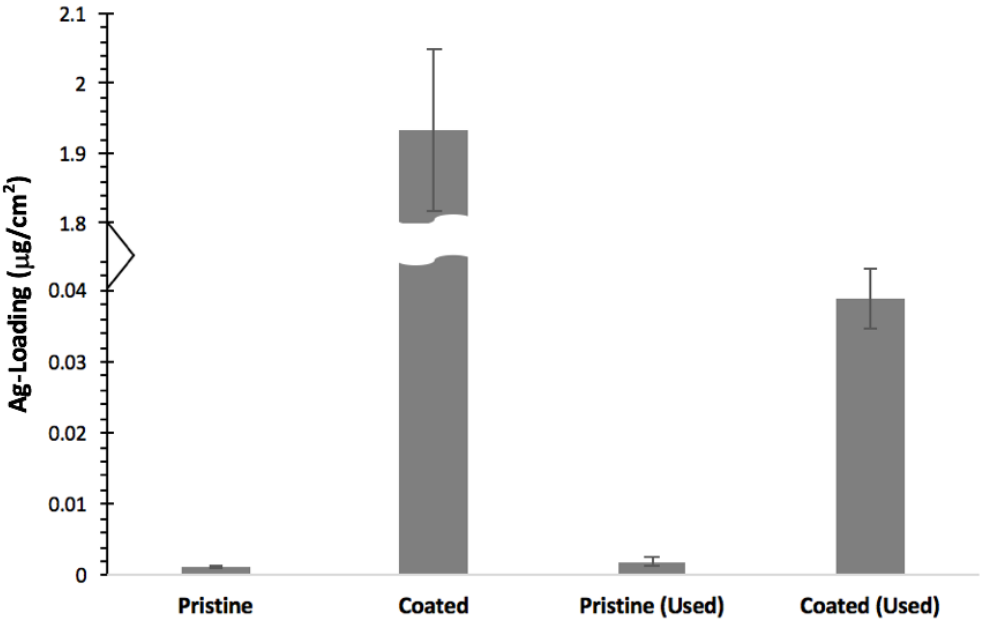

Figure 3.13: Silver Loading Results from Reverse Osmosis Membrane Digestion, Before and After 51 Days of Use in Point of Use System

As illustrated in Figure 3.13 above, a pristine membrane did not contain any silver, as the results were below the detection limit of the ICP-MS analysis. A freshly-coated RO membrane is loaded on average with 1.93 ± 0.12 μg/cm^2. After 51 days of use in the Mobile NEWT Testbed, the uncoated membrane $0.002 \pm 8\text{x}10^{-4}$ μg/cm^2. The coated membrane after 51 days of use had on average 0.039 μg/cm^2 $\pm 4\text{x}10^{-2}$. These results show a 98% decrease in silver loading after 51 days of use.

Contact Angle Measurements

Figure 3.14 below depicts the results obtained from the contact angle measurements using the Sessile Drop Method for the polyamide RO membrane before and after 51 days of use in the Mobile NEWT Testbed POU system.

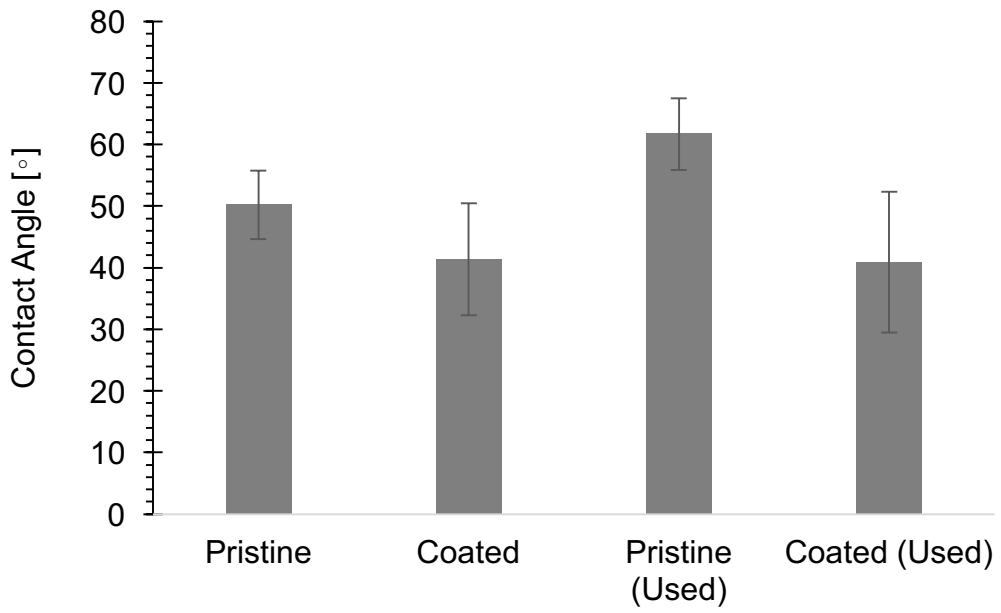

Figure 3.14: Spiral-Wound Polyamide RO Membrane Contact Angle, Before and After 51 Days of Use

The pristine RO membrane had an average contact angle of 50° ± 5°. After the silver coating was applied, the RO membrane had an average contact angle of 41° ± 9°. After 51 days of use, the pristine RO membrane had an average contact angle of 62° ± 6° and the silver-coated membrane had an average contact angle of 41° ± 11°. After conducting a student t-test, it was determined there was no statistically significant different between the contact angles of the coated and uncoated membranes. The pristine membrane and the silver-coated membrane showed a P-value of 0.08. After 51 days of use, the pristine membrane and the silver-coated membrane showed a P-value of 0.21. Because both these P-values are greater than the alpha value 0.05, the null hypothesis is accepted, showing no statistically significant difference.

Dynamic Leaching Test

a)

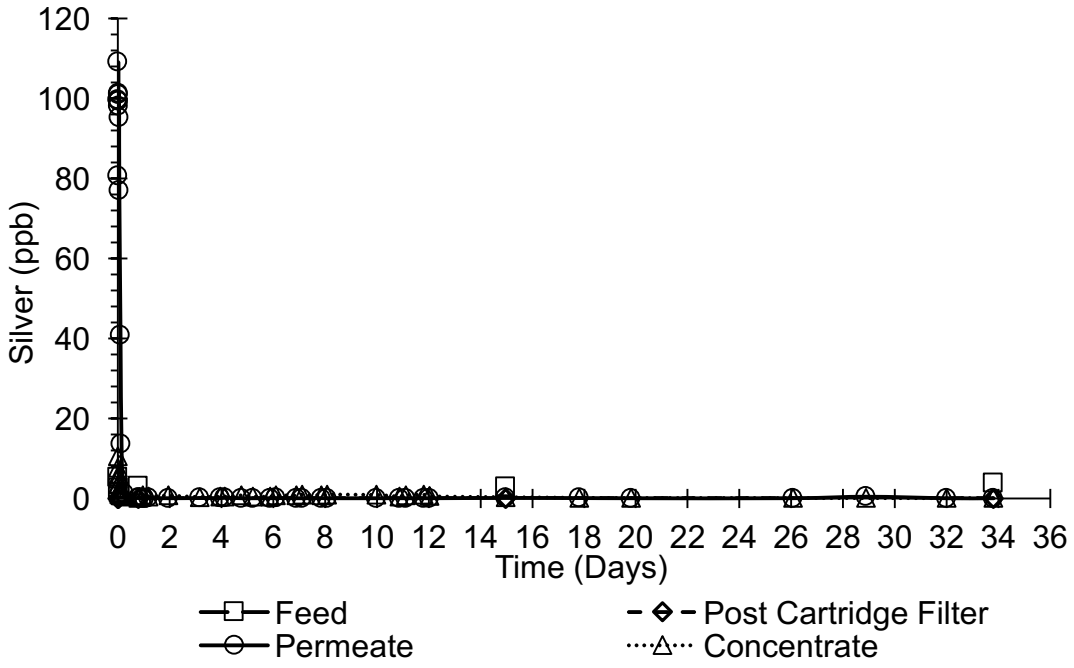

b)

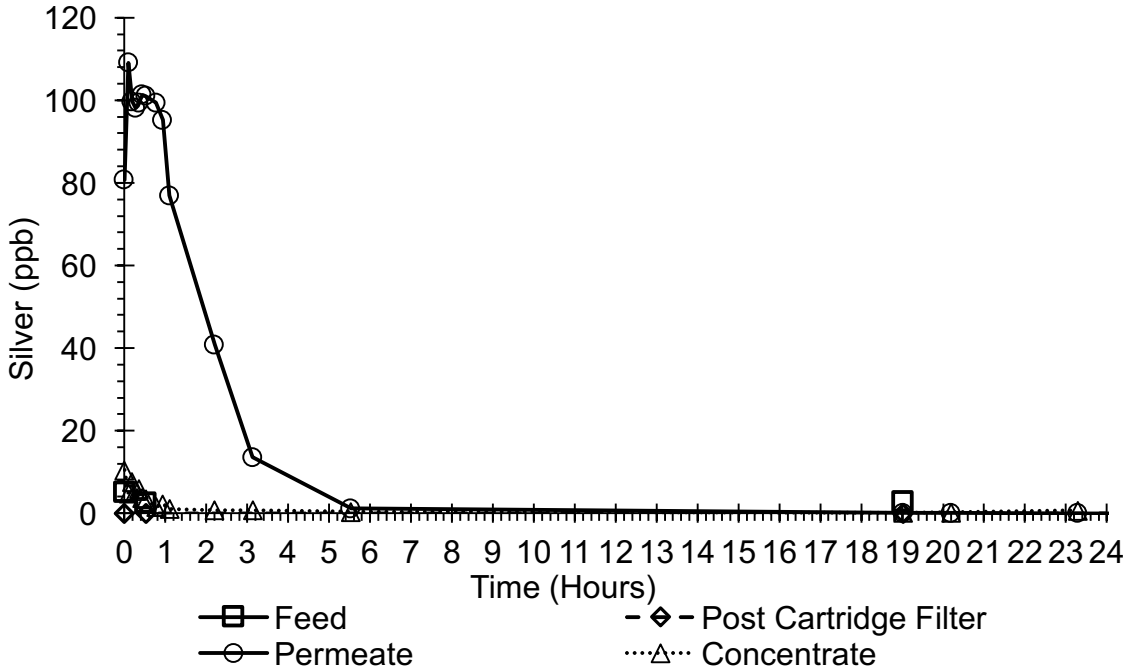

Figure 3.15: Dynamic Leaching Test Results Over (a) 34 Days and (b) 24 hours

Figure 3.15(a) above shows the silver released from the spiral-wound RO membrane over a period of 34 days. Within the first day, the permeate flow shows a release of silver at a maximum of 110 ppb, which then decreases to less than 5 ppb within the first day. The concentrate flow experienced a brief spike in silver concentration up 10 ppb within the first day, then subsequently decreased to less than 5 ppb. The feed water and effluent from the cartridge filter remained at a concentration below 5 ppb throughout the 34 days. Figure 3.15(b) shows the kinetics of silver released within the first 24 hours of operation. The silver released in the permeate flow reached a peak concentration of 110 ppb within the first five minutes of operation, then decreased to 95 ppb within the first hour, and 40 ppb within the first two hours. After three hours of operation, the silver concentration decreased to 14 ppb, and finally less than 5 ppb after five hours of operation. The feed, cartridge filter, and concentrate flows all remained under 5 ppb after the first five minutes of operation.

a)

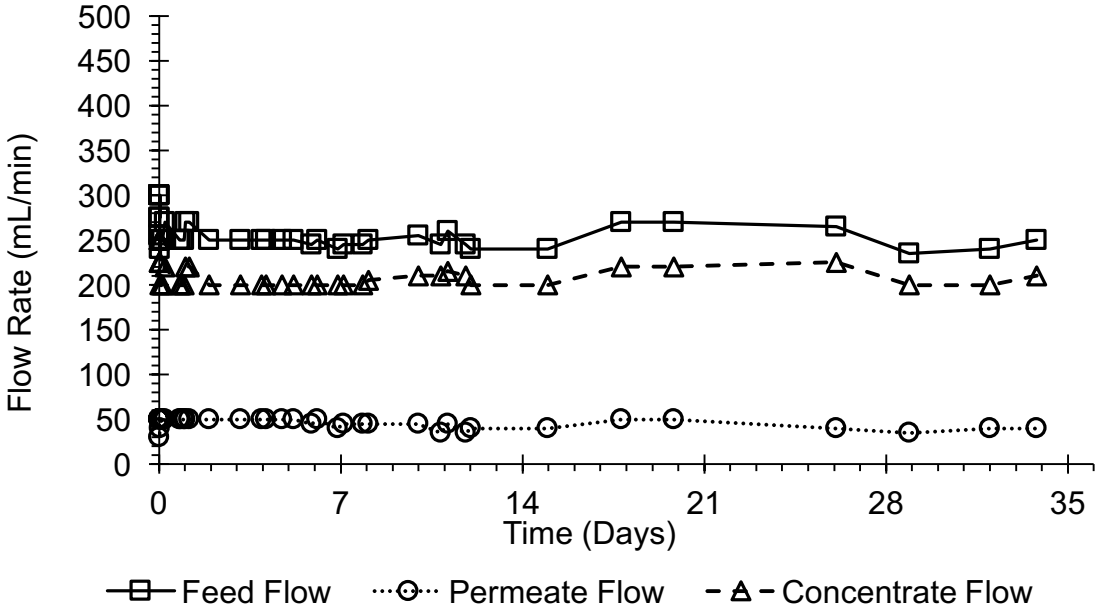

b)

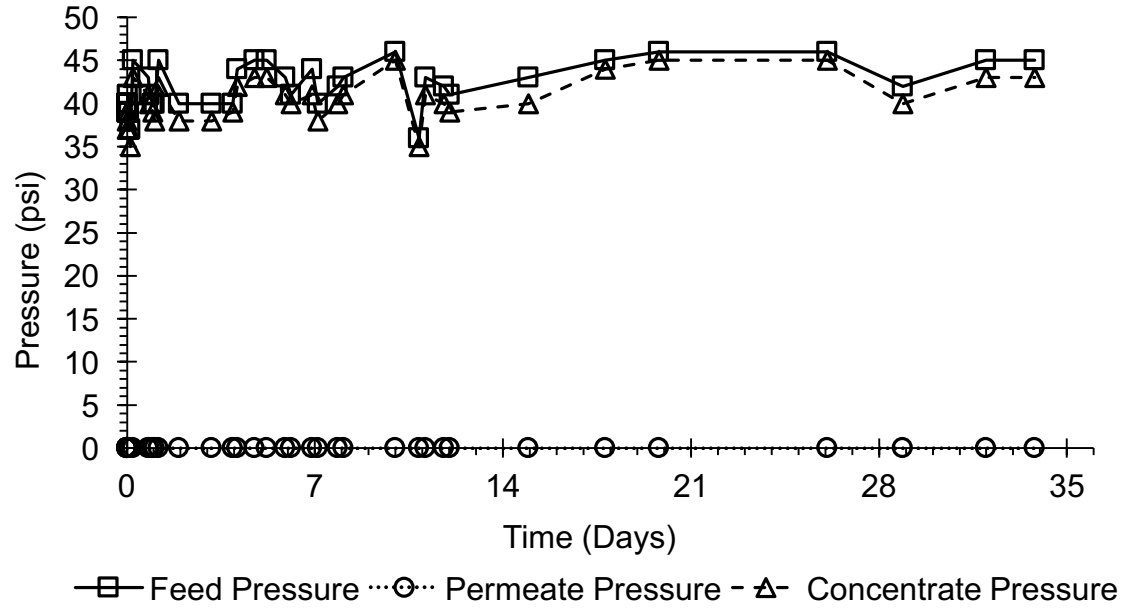

Figure 3.16: Operating Conditions During the Dynamic Leaching Test in Metrics of (a) Flow Rate and (b) Pressure

The flow rate during the dynamic leaching test was maintained around 250 mL/min, 200 mL/min, and 50 mL/min for the feed flow, concentrate flow, and permeate flow, respectively. The pressure during the dynamic leaching test was maintained around 45 psi for both the feed and concentrate flow, and 0 psi for the permeate flow. Fluctuations in the pressure were due to the source water being City of Tempe municipal water supply, which may experience fluctuations in flow and pressure due to varied use by customers.

Mobile NEWT Testbed

Run 1: Baseline Unit Comparison

Figure 3.17 below illustrates the flow and the flux results obtained from the baseline unit comparison run in the Mobile NEWT Testbed.

a)

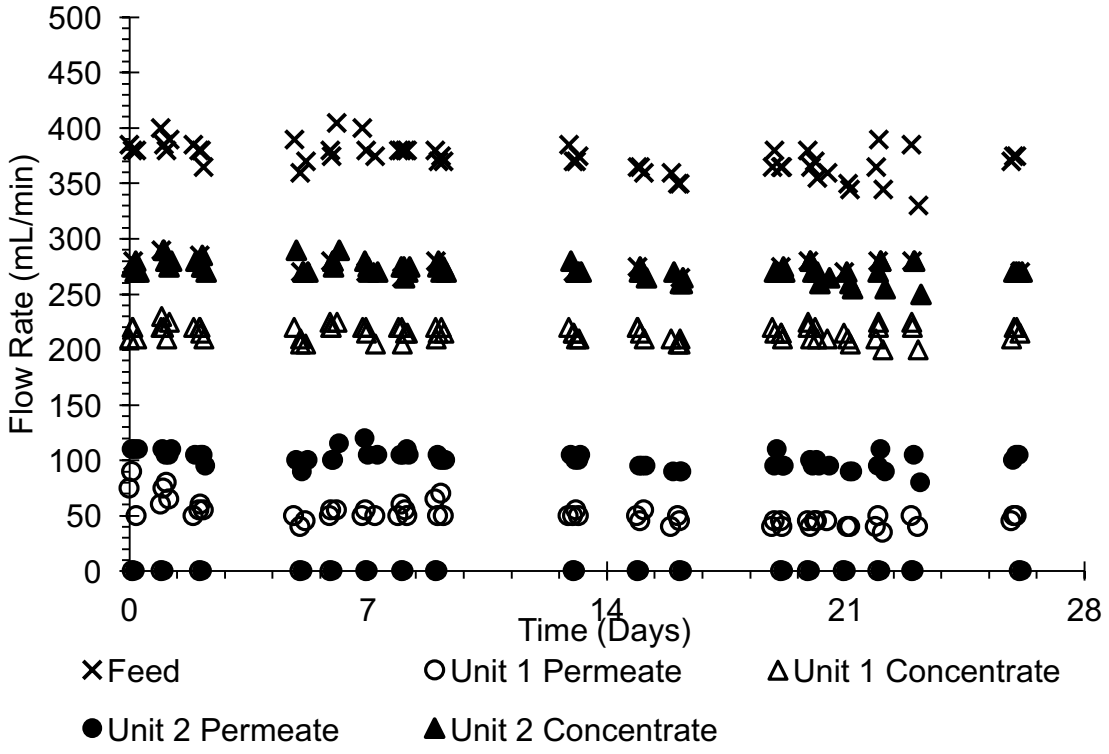

b)

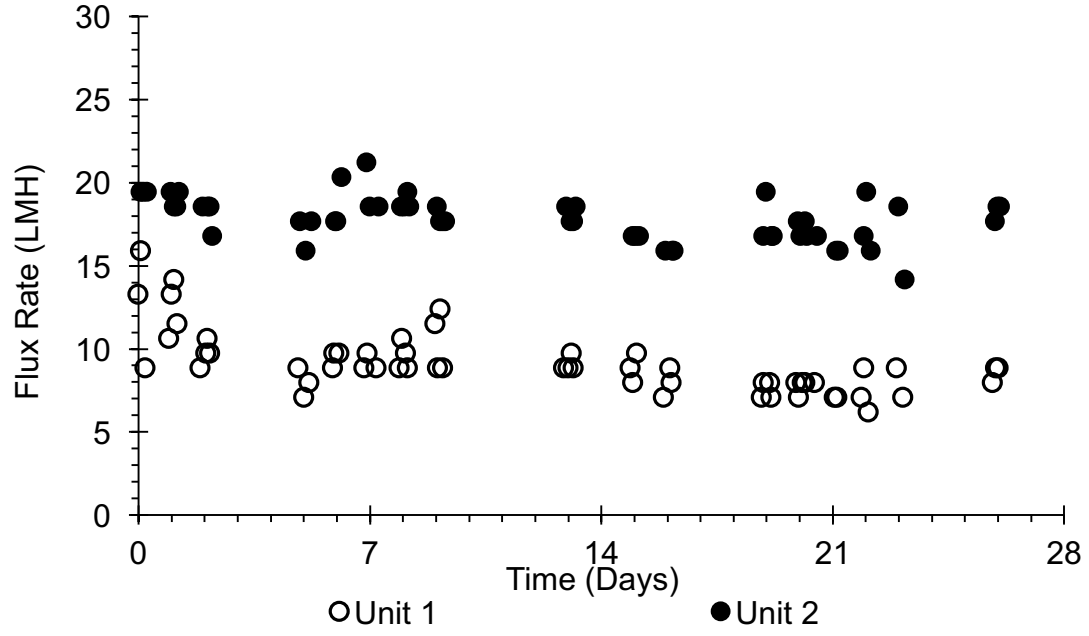

c)

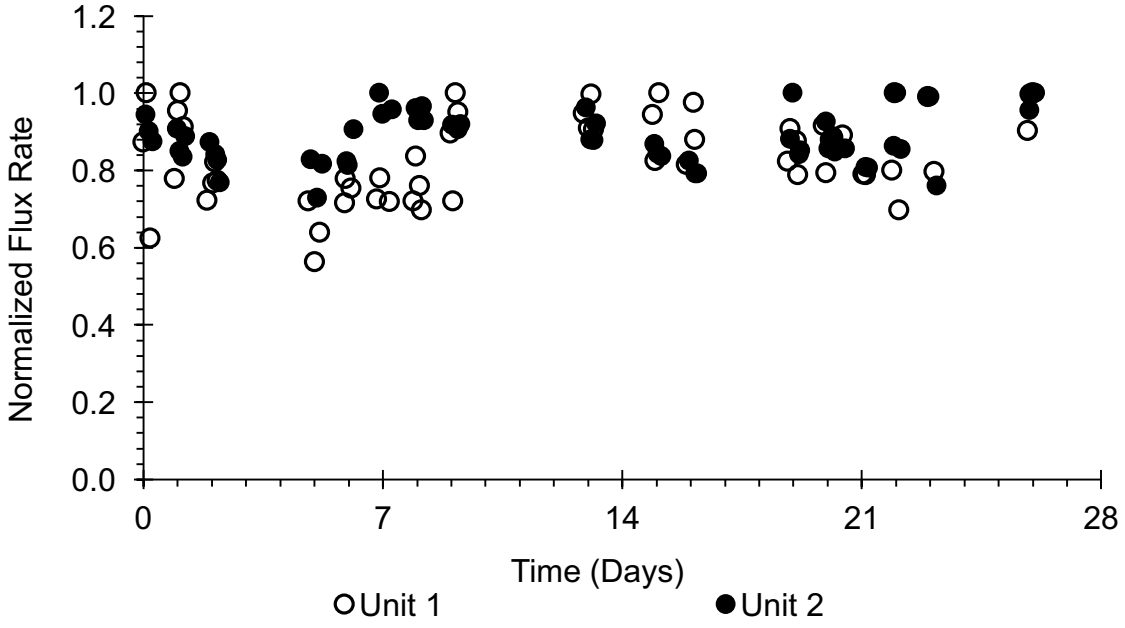

Figure 3.17: Baseline Unit Comparison Results for (a) Flow Rates, (b) Flux Rates, and (c) Normalized Flux Rate Over 26 Days

As illustrated in Figure 3.17(a), the average feed flow into the testbed was 373 ± 14 mL/min, not considering the data points where the testbed was not in operation (i.e. 0 mL/min feed flow). The average permeate and concentrate flow rates throughout the 26 days for Unit 1 were observed to be 51 ± 11 mL/min and 216 ± 10 mL/min, respectively. The average permeate and concentrate flow rates throughout the 26 days for Unit 2 were observed to be 101 ± 7 mL/min and 272 ± 8 mL/min, respectively.

Using Equation 3.2 below, the flux in LMH could be calculated from the permeate flow rates in mL/min, with a known membrane area of 3.7 square feet.

$$Flux\ (LMH)\ =\ Flow\ (\frac{mL}{min})\ x\ (\frac{60\ min}{1\ hr})\ x\ (\frac{1\ L}{1000\ mL})\ x\ (3.28^2\ \frac{ft^2}{m^2}) \quad (3.2)$$

Figure 3.17(b) shows the flux results obtained from the flow rate data in combination with Equation 3.2. The average flux rate over 26 days of operation for Unit 1 was 9 ± 2 LMH, while the average flux rate for Unit 2 was 18 ± 1 LMH.

Figure 3.18 below serves to illustrate the consistency in water quality measurements, such as temperature and pH. A common method to determine the amount of fouling that has occurred is to normalize the flux rate at any given time during an experiment (J_t) using the initial (or maximum) flux rate, J_0. Figure 3.17(c) illustrates the results obtained after normalizing the flux (i.e. J_t/J_0). As illustrated in the figure, the initial flux rate is the maximum flux rate around 1.0 for both units, however fluctuations due to changes in the pressure are observed, making it difficult to obtain a true flux-decline equation.

a)

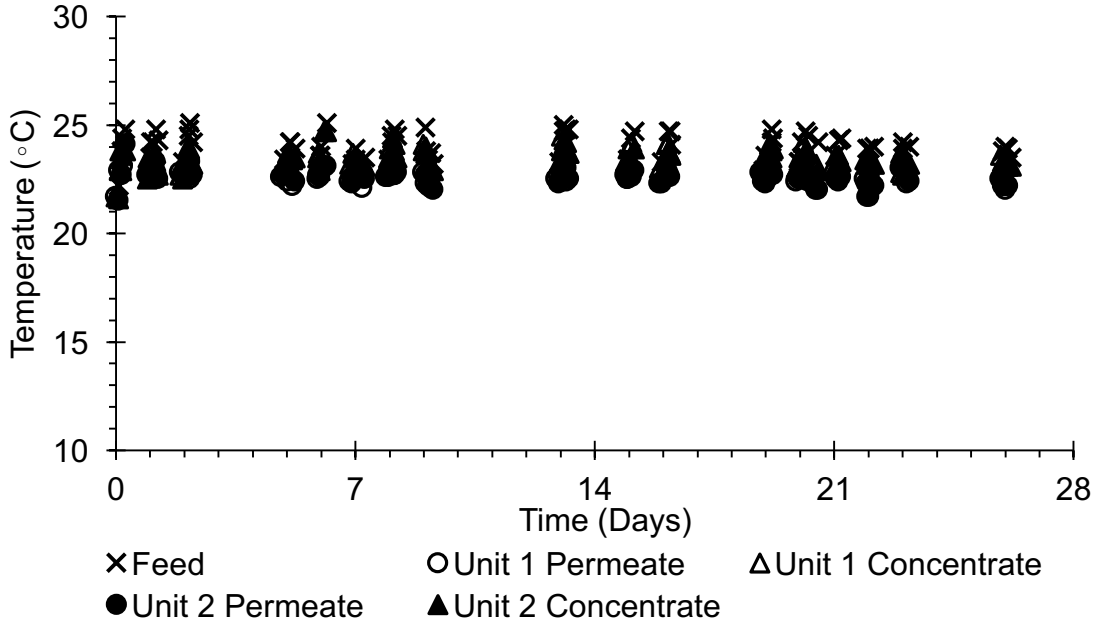

b)

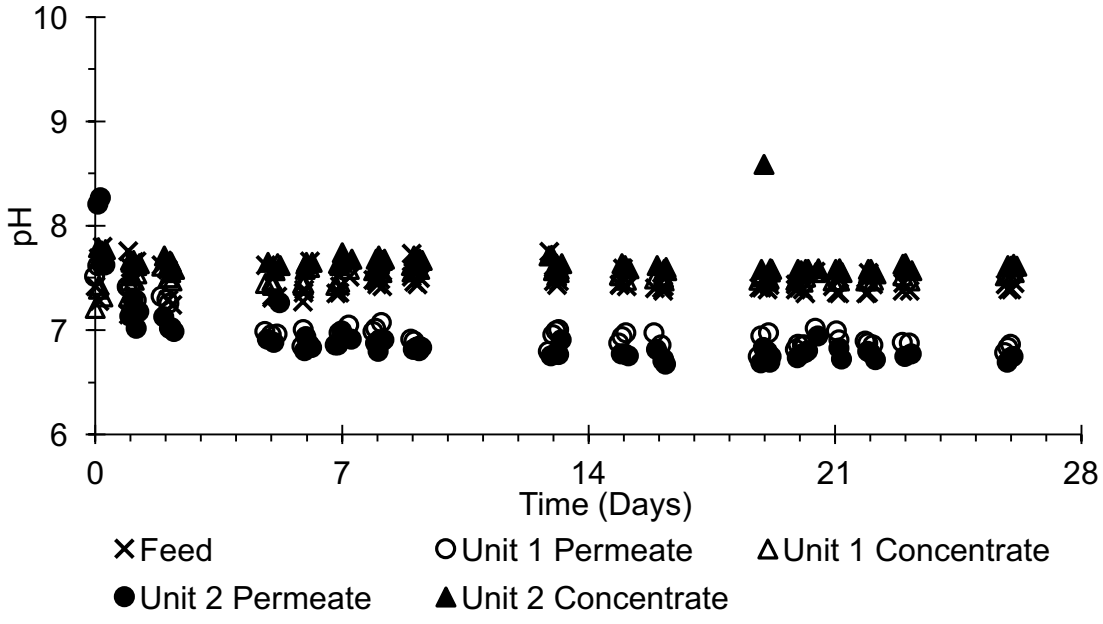

Figure 3.18: Water Quality Measurements During Baseline Unit Comparison for (a) Temperature and (b) pH

As shown in Figure 3.18(a), the average temperature measurements observed in the feed flow for the testbed over 26 days of operation was 24 ± 1 °C. The average temperatures observed in Unit 1 over 26 days of operation for the permeate and concentrate flow regimes were, 23.0 ± 0.3 °C and 23 ± 1 °C, respectively. The average temperatures observed in Unit 2 over 26 days of operation for the permeate and concentrate flow regimes were, 23.0 ± 0.4 °C and 23 ± 1 °C, respectively.

As shown in Figure 3.18(b), the average pH measurements observed in the feed flow for the testbed over 26 days of operation was 7.44 ± 0.17 pH units. The average pH measurements observed in Unit 1 over 26 days of operation for the permeate and concentrate flow regimes were, 6.99 ± 0.21 pH units and 7.50 ± 0.12 pH units, respectively. The average pH measurements observed in Unit 2 over 26 days of operation for the permeate and concentrate flow regimes were, 6.92 ± 0.31 pH units and 7.63 ± 0.14 pH units, respectively.

Figure 3.19 below illustrates the conductivity measurements and the subsequent salt rejection calculated in Unit 1 and Unit 2 of the testbed.

a)

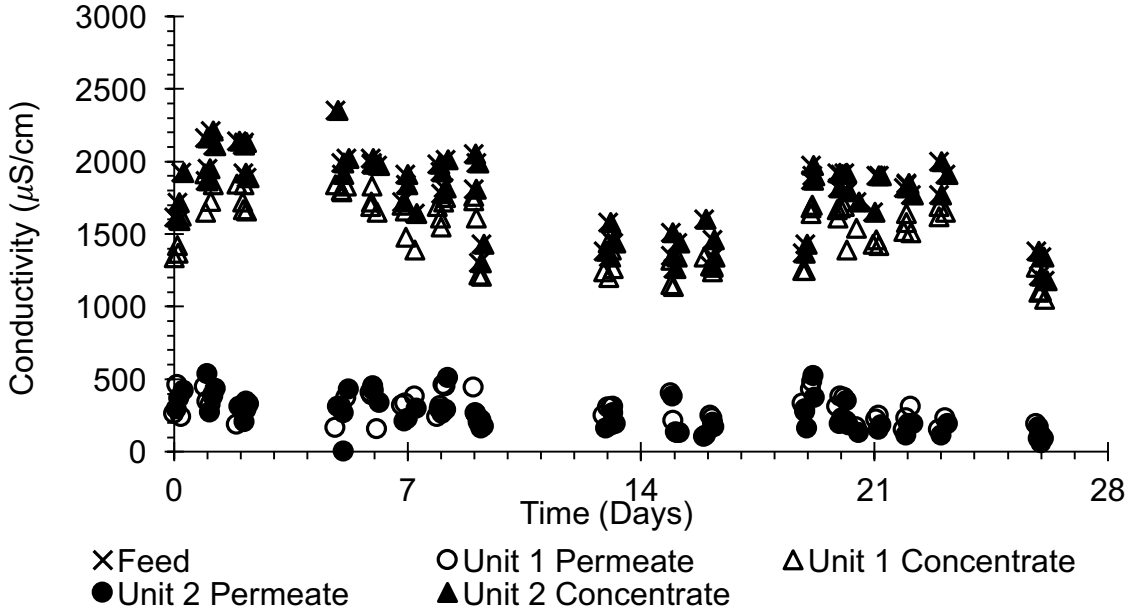

b)

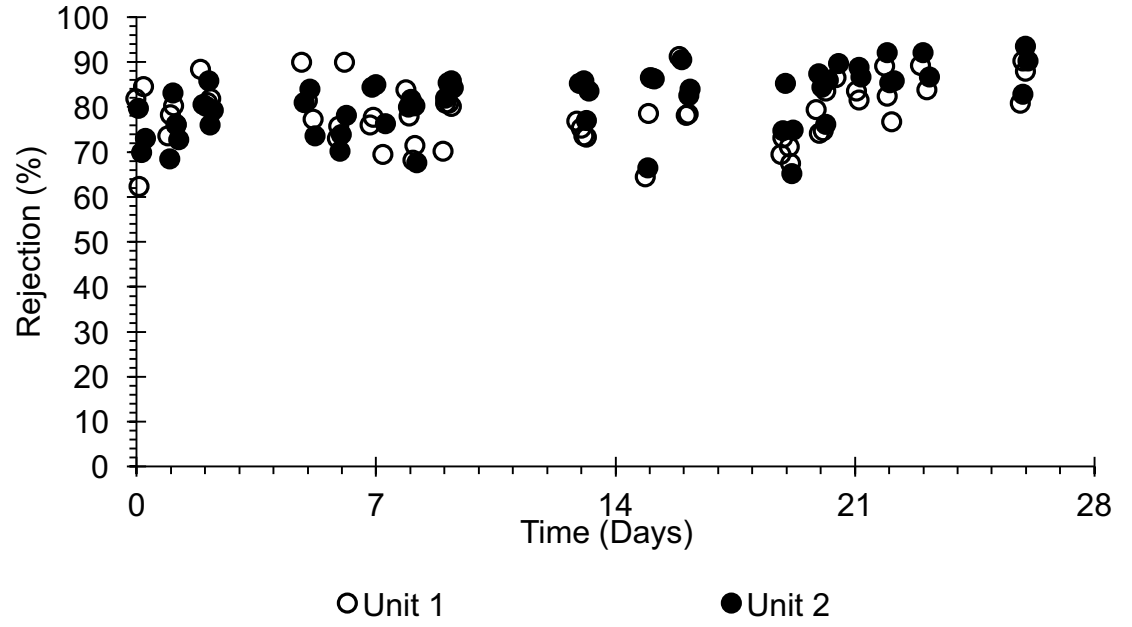

Figure 3.19: Baseline Unit Comparison Measurements for (a) Conductivity and (b) Calculated Salt Rejection

Figure 3.19(a) shows how the feed water conductivity measurements and the subsequent permeate and concentrate conductivity measurements can fluctuate during 26 days of operation. Fluctuations in the feed water conductivity could be attributed to fluctuations in source water quality and adjustments in water treatment parameters conducted at the City of Tempe Water Treatment Plant. The average feed conductivity over 26 days of operation was 1342 ± 205 µS/cm, fluctuating between a maximum and minimum conductivity of 1686 µS/cm and 910 µS/cm, respectively. The average conductivity for the permeate and concentrate flow regimes in Unit 1 was 287 ± 100 µS/cm and 1541 ± 219 µS/cm, respectively. The permeate conductivity measurements fluctuated between a maximum and minimum of 480 µS/cm and 90 µS/cm, respectively. The concentrate conductivity measurements fluctuated between a maximum and minimum of 1914 µS/cm and 1100 µS/cm, respectively. The average conductivity for the permeate and concentrate flow regimes in Unit 2 was 261 ± 117 µS/cm and 1771 ± 269 µS/cm, respectively. The permeate conductivity measurements fluctuated between a maximum and minimum of 534 µS/cm and 60 µS/cm, respectively. The concentrate conductivity measurements fluctuated between a maximum and minimum of 2350 µS/cm and 1210 µS/cm, respectively.

Due to the many fluctuations in source water conductivity, it is easier to model the performance of the membranes in terms of the percent of salts rejected, as shown in Figure 3.19(b). Over 26 days of operation, Unit 1 experienced an average salt rejection of 79 ± 7%, and Unit 2 experienced an average salt rejection of 81 ± 7%.

Run 2: Pristine Membrane vs. Silver-Coated Membrane Comparison

a)

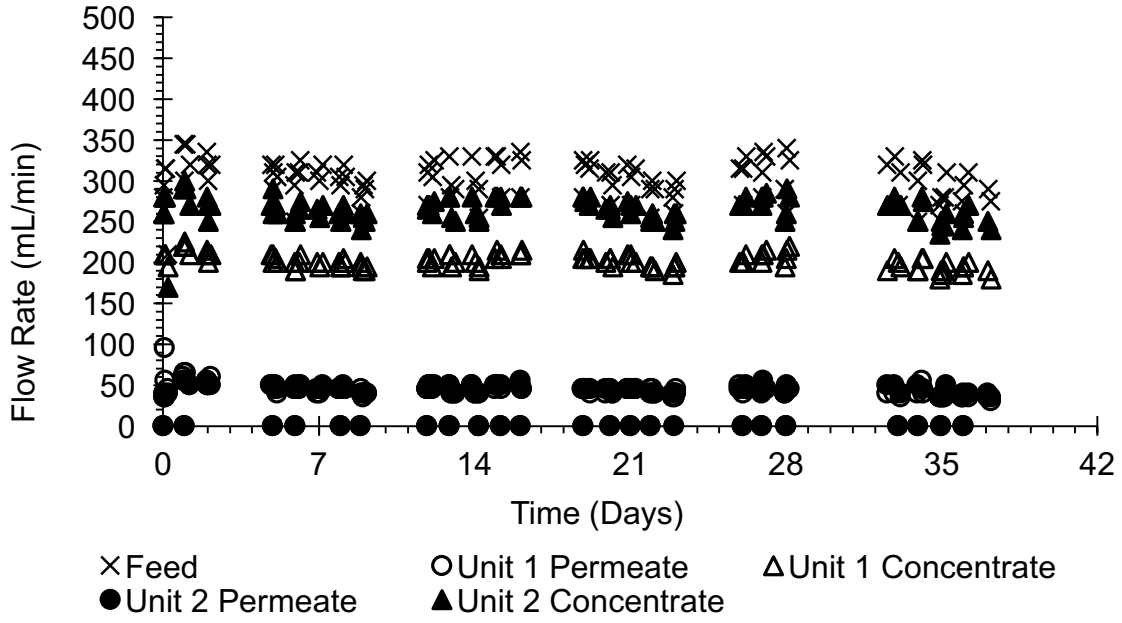

b)

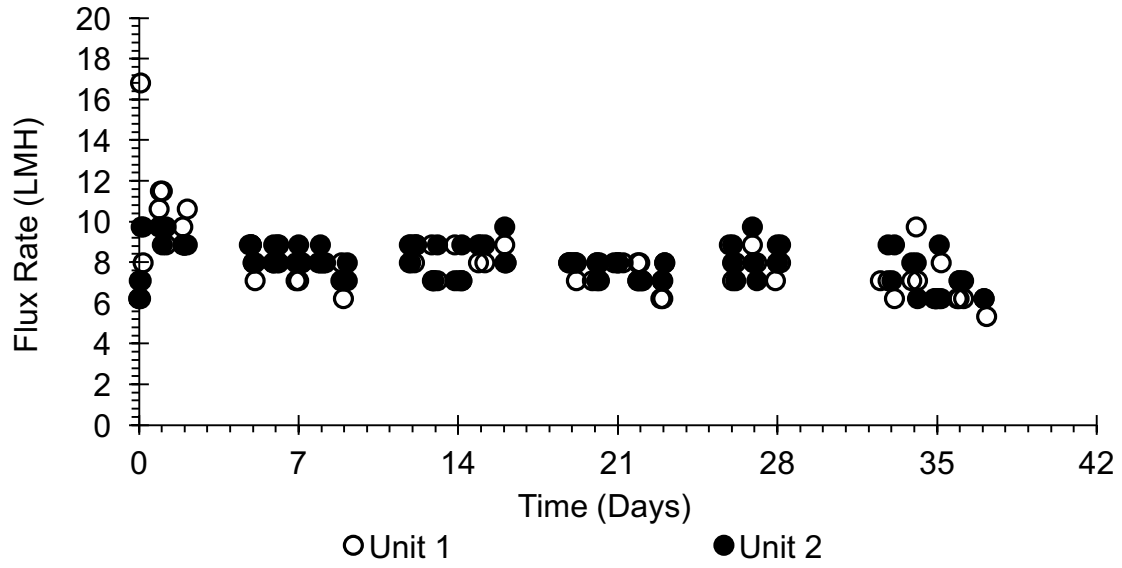

c)

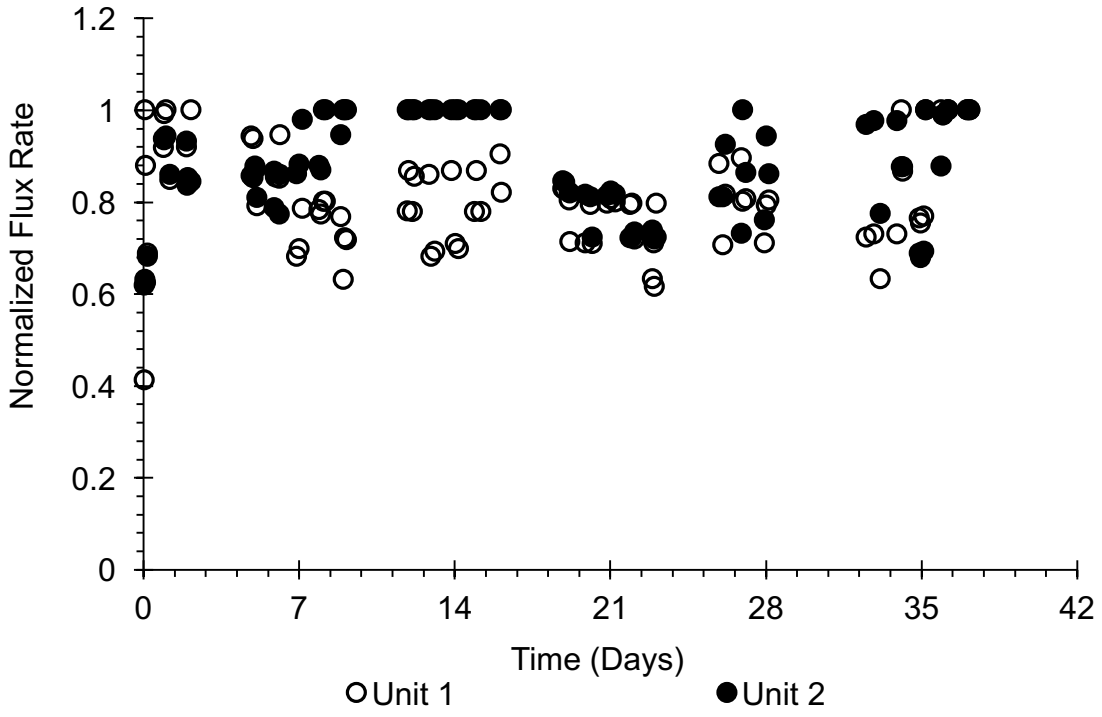

Figure 3.20: Pristine vs. Silver-Coated Membrane Comparison Results for (a) Flow Rates, (b) Flux Rates, and (c) Normalized Flux Rates Over 37 Days

As illustrated in Figure 3.20(a), the average feed flow into the testbed was 309 ± 20 mL/min, not considering the data points where the testbed was not in operation (i.e. 0 mL/min feed flow). The average permeate and concentrate flow rates throughout the 37 days for Unit 1 were observed to be 45 ± 9 mL/min and 201 ± 9 mL/min, respectively. The average permeate and concentrate flow rates throughout the 37 days for Unit 2 were observed to be 45 ± 5 mL/min and 264 ± 17 mL/min, respectively.

Using Equation 3.2, the flux in LMH could be calculated from the permeate flow rates in mL/min, with a known membrane area of 3.7 square feet. Figure 3.20(b) shows the flux results obtained from the flow rate data in combination with Equation 3.2. The

average flux rate over 37 days of operation for Unit 1 was 8 ± 1.5 LMH, while the average flux rate for Unit 2 was 8 ± 1.0 LMH. Figure 3.20(b) shows the normalized flux rate for both units, where the maximum flux rate for Unit 1 was the initial flux rate, and the maximum flux rate for unit 2 occurred during the second week of operation.

Figure 3.21 illustrates the consistency in water quality measurements, such as temperature and pH.

a)

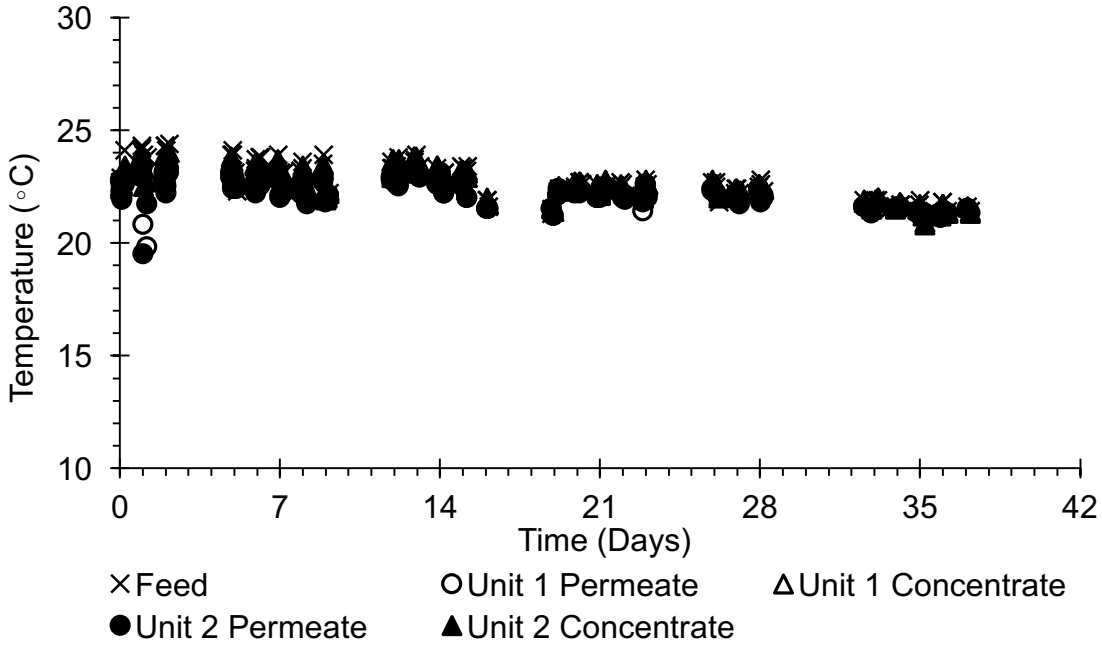

b)

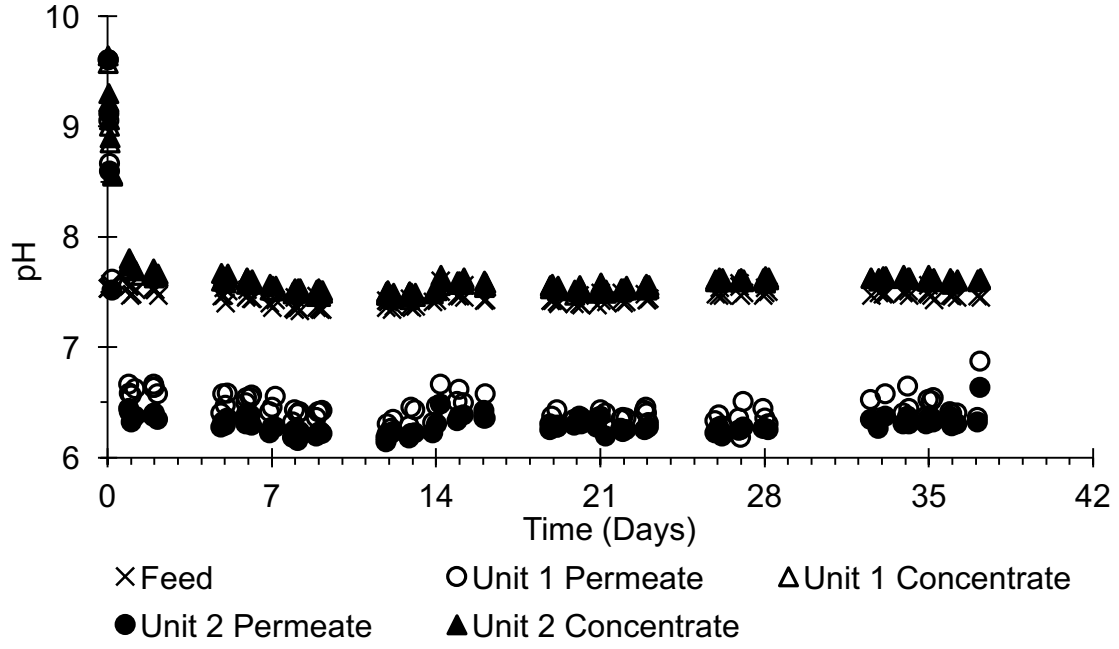

Figure 3.21: Water Quality Measurements During Pristine vs. Silver-Coated Membrane Comparison for (a) Temperature and (b) pH

As shown in Figure 3.21(a), the average temperature measurements observed in the feed flow for the testbed over 37 days of operation was 23 ± 0.9 °C. The average temperatures observed in Unit 1 over 37 days of operation for the permeate and concentrate flow regimes were, 22 ± 0.7 °C and 23 ± 0.8 °C, respectively. The average temperatures observed in Unit 2 over 37 days of operation for the permeate and concentrate flow regimes were, 22 ± 0.6 °C and 23 ± 0.7 °C, respectively.

As shown in Figure 3.21(b), the average pH measurements observed in the feed flow for the testbed over 37 days of operation was 7.45 ± 0.06 pH units. The average pH measurements observed in Unit 1 over 37 days of operation for the permeate and concentrate flow regimes were 6.54 ± 0.52 pH units and 7.61 ± 0.27 pH units,

respectively. The average pH measurements observed in Unit 2 over 37 days of operation for the permeate and concentrate flow regimes were, 6.40 ± 0.54 pH units and 7.64 ± 0.27 pH units, respectively.

Figure 3.22 below illustrates the conductivity measurements and the subsequent salt rejection calculated in Unit 1 and Unit 2 of the testbed.

a)

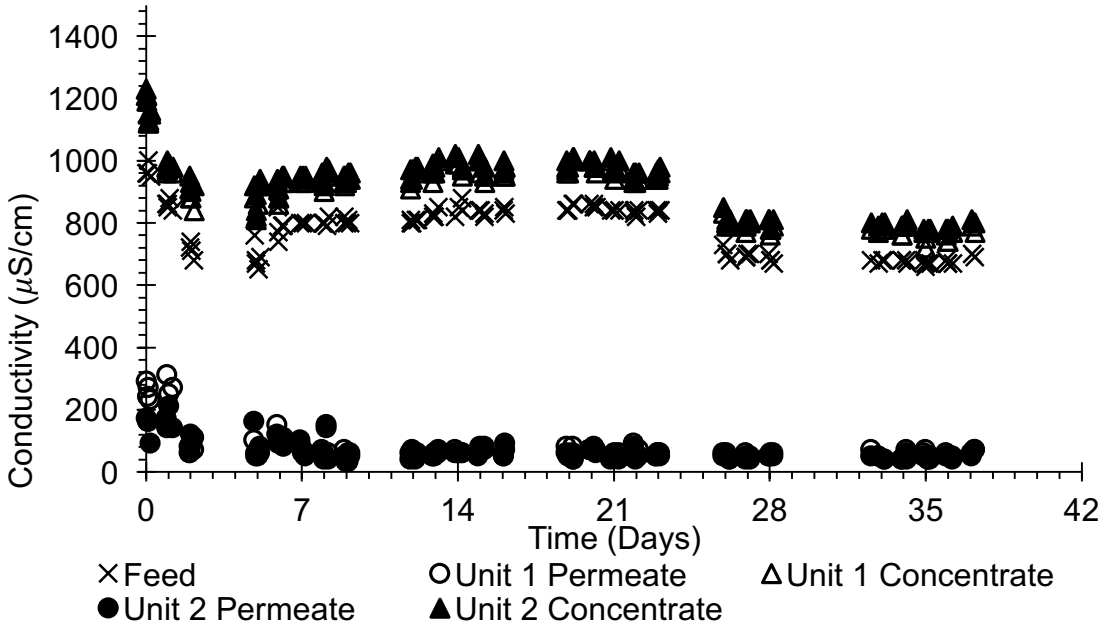

b)

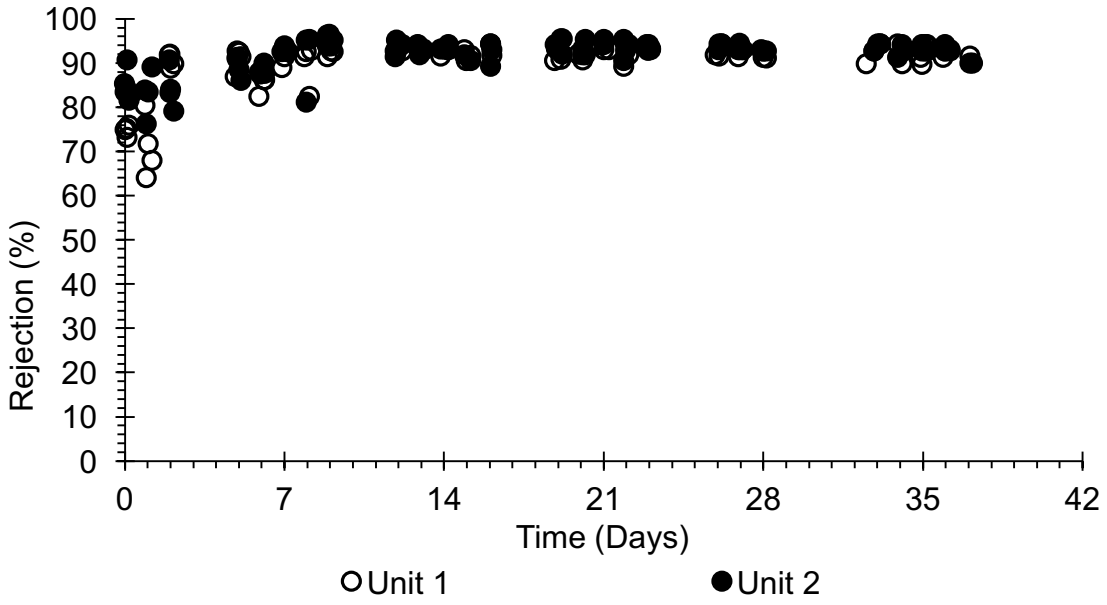

Figure 3.22: Pristine vs. Silver-Coated Membrane Comparison Measurements for (a) Conductivity and (b) Calculated Salt Rejection

Figure 3.22(a) again shows the feed water conductivity measurements and the subsequent permeate and concentrate conductivity measurements fluctuating during 37 days of operation. The average feed conductivity over 37 days of operation was 782 ± 86 µS/cm, fluctuating between a maximum and minimum conductivity of 1150 µS/cm and 650 µS/cm, respectively. The average conductivity for the permeate and concentrate flow regimes in Unit 1 was 82 ± 59 µS/cm and 902 ± 97 µS/cm, respectively. The permeate conductivity measurements fluctuated between a maximum and minimum of 310 µS/cm and 40 µS/cm, respectively. The concentrate conductivity measurements fluctuated between a maximum and minimum of 1210 µS/cm and 720 µS/cm, respectively. The average conductivity for the permeate and concentrate flow regimes in Unit 2 was 69 ±

37 µS/cm and 922 ± 93 µS/cm, respectively. The permeate conductivity measurements fluctuated between a maximum and minimum of 210 µS/cm and 30 µS/cm, respectively. The concentrate conductivity measurements fluctuated between a maximum and minimum of 1190 µS/cm and 770 µS/cm, respectively.

Due to the many fluctuations in source water conductivity, it is easier to model the performance of the membranes in terms of the percent of salts rejected, as shown in Figure 3.22(b). Over 37 days of operation, Unit 1 experienced an average salt rejection of 90 ± 6.0%, and Unit 2 experienced an average salt rejection of 91 ± 4.1%.

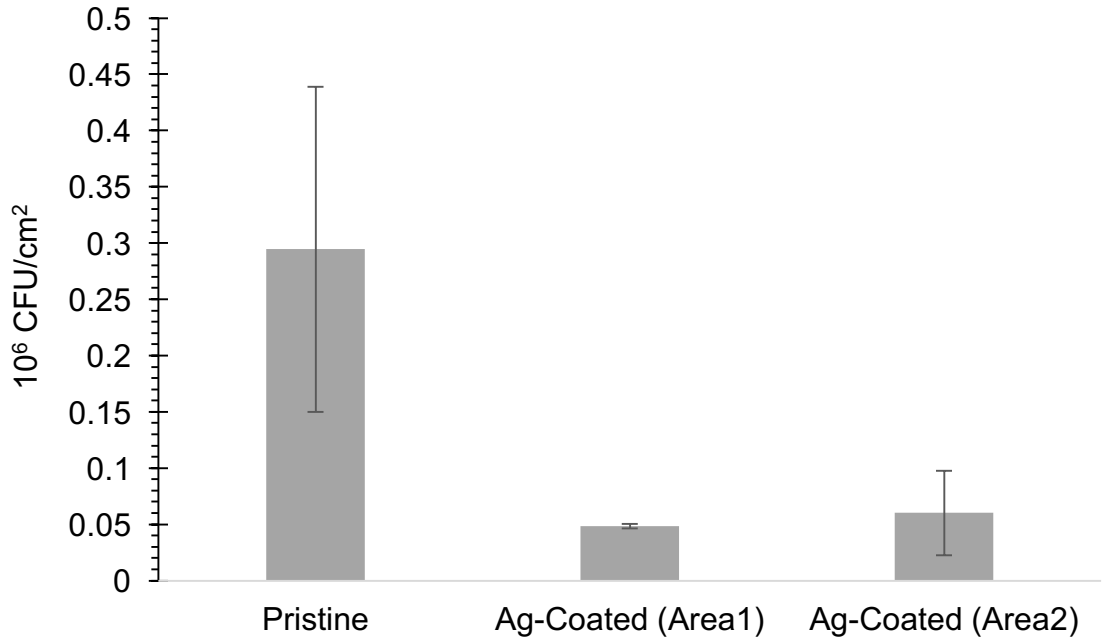

Figure 3.23: HPC Results from Pristine Membrane and Silver-Coated Membrane After Testbed Shut Down

As illustrated in Figure 3.23 above, the HPC results show greater average microbial growth on the pristine membrane compared to the silver-coated membrane. The pristine membrane had an average microbe count of 0.3 ± 0.1 x 10^6 CFU/cm^2. An area of

the silver-coated membrane that was stained a brownish-yellow color had an average microbe count of $0.048 \pm 0.002 \times 10^6$ CFU/cm^2. An area of the silver-coated membrane that was not stained had an average microbe count of $0.060 \pm 0.038 \times 10^6$ CFU/cm^2. After conducting a student t-test, the P-values obtained comparing all data ranged from $0.25 < P < 0.74$, which are all above the confidence value of 0.05, showing no statistically significant difference.

Run 3: Contaminant Removal Efficiency Using Hexavalent Chromium

a)

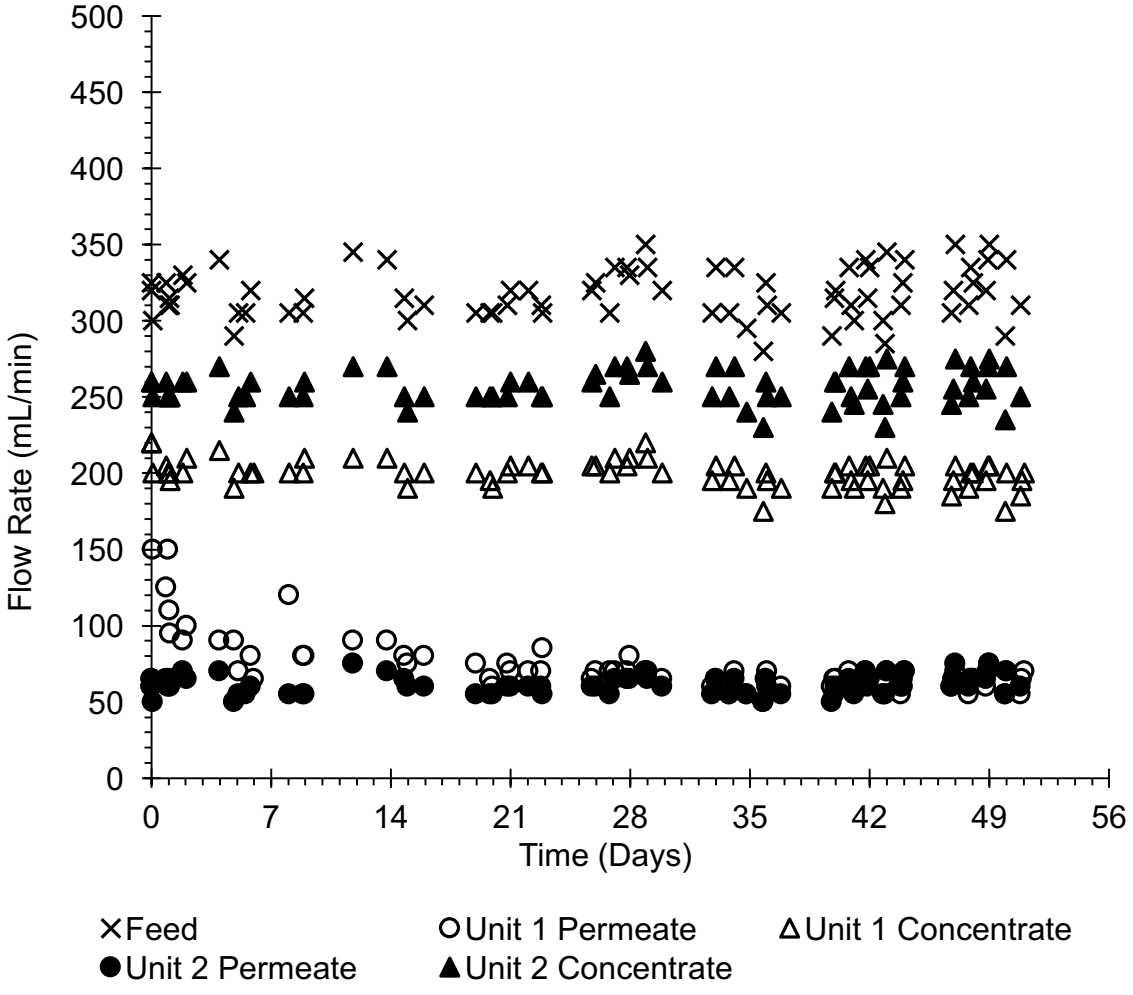

b)

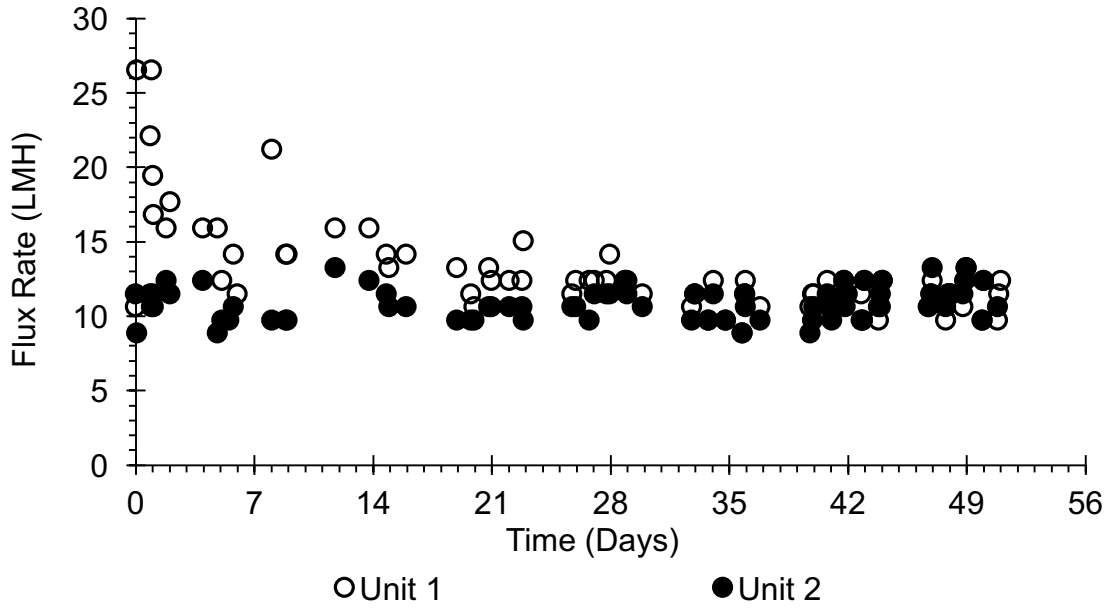

c)

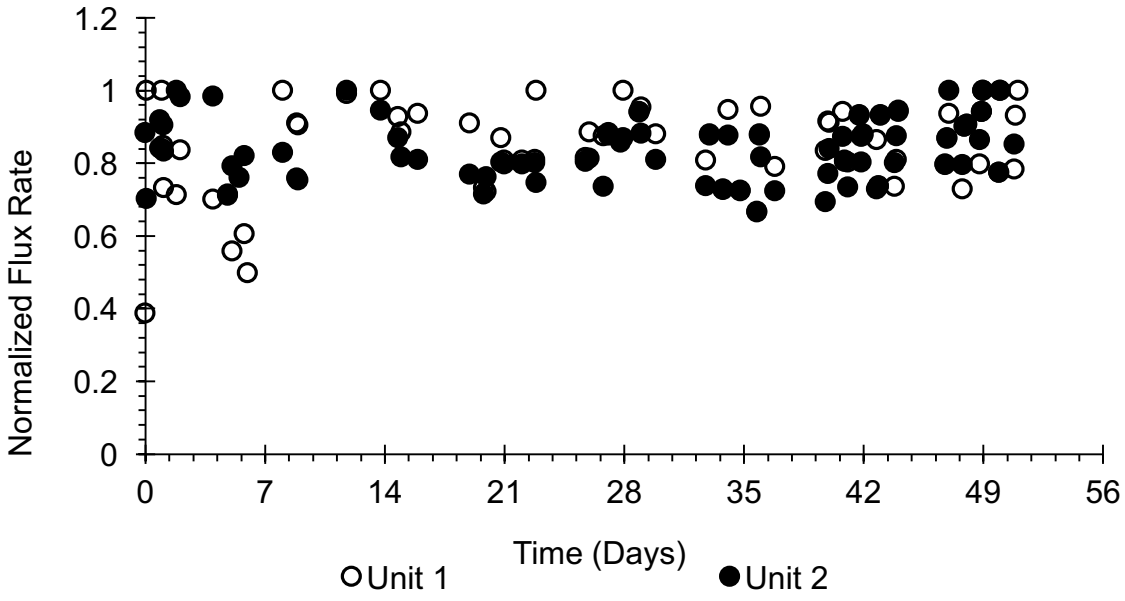

Figure 3.24: Contaminant Removal Comparison for Pristine vs. Silver-Coated Membrane Results for (a) Flow Rates, (b) Flux Rates, and (c) Normalized Flux Rates Over 51 Days

As illustrated in Figure 3.24(a), the average feed flow into the testbed was 318 ± 16 mL/min, not considering the data points where the testbed was not in operation (i.e. 0 mL/min feed flow). The average permeate and concentrate flow rates throughout the 51 days for Unit 1 were observed to be 73 ± 19 mL/min and 200 ± 9 mL/min, respectively. The average permeate and concentrate flow rates throughout the 51 days for Unit 2 were observed to be 61 ± 6 mL/min and 257 ± 11 mL/min, respectively.

Using Equation 3.2, the flux in LMH could be calculated from the permeate flow rates in mL/min, with a known membrane area of 3.7 square feet. Figure 3.24(b) shows the flux results obtained from the flow rate data in combination with Equation 3.2. The average flux rate over 51 days of operation for Unit 1 was 13 ± 3.3 LMH, while the average flux rate for Unit 2 was 11 ± 1.1 LMH. Figure 3.24(c) illustrates the normalized flux comparison for both units. As illustrated in the figure, the maximum flux rate is achieved initially for both Units 1 and 2, however, fluctuations in pressure within the distribution system make it difficult to determine a true flux-decline equation.

Figure 3.25 below serves to illustrate the consistency in water quality measurements, such as temperature and pH.

a)

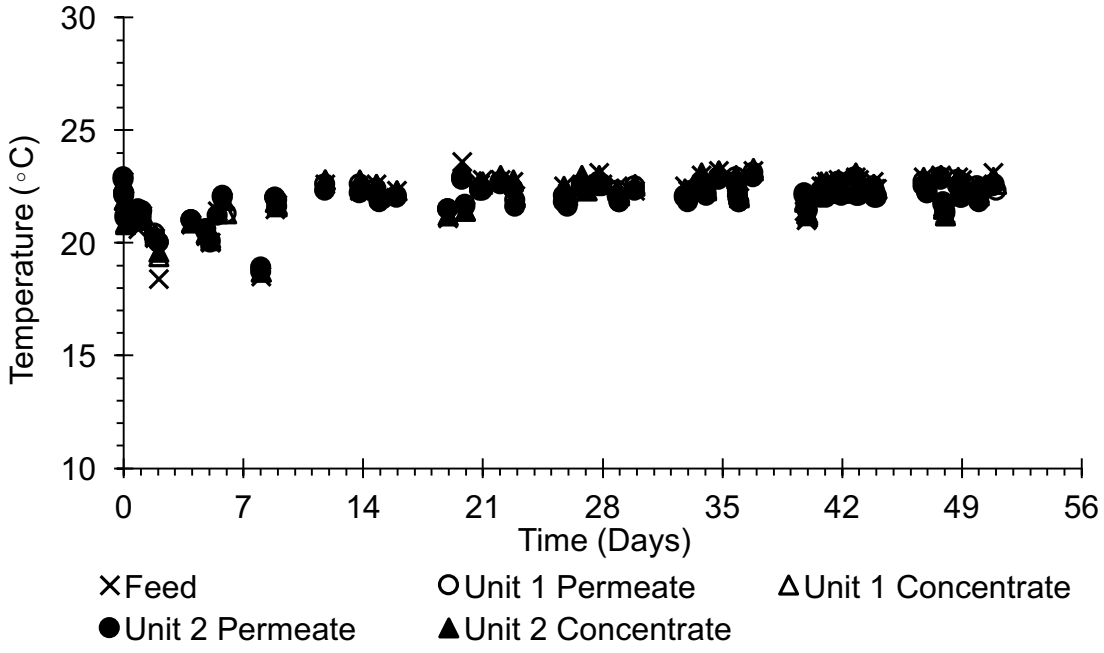

b)

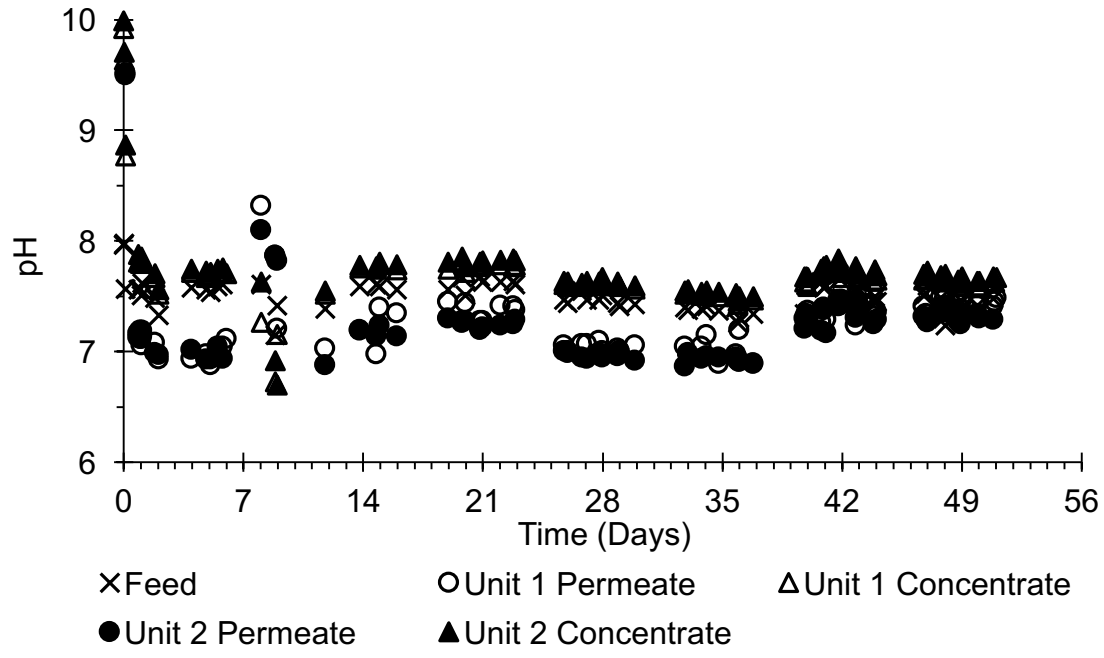

Figure 3.25: Water Quality Measurements During Contaminant Removal Comparison for Pristine vs. Silver-Coated Membrane for (a) Temperature and (b) pH

As shown in Figure 3.25(a), the average temperature measurements observed in the feed flow for the testbed over 51 days of operation was 22 ± 1.0 °C. The average temperatures observed in Unit 1 over 51 days of operation for the permeate and concentrate flow regimes were, 22 ± 0.7 °C and 22 ± 0.9 °C, respectively. The average temperatures observed in Unit 2 over 51 days of operation for the permeate and concentrate flow regimes were, 22 ± 0.7 °C and 22 ± 0.9 °C, respectively.

As shown in Figure 3.25(b), the average pH measurements observed in the feed flow for the testbed over 51 days of operation was 7.50 ± 0.14 pH units. The average pH measurements observed in Unit 1 over 51 days of operation for the permeate and concentrate flow regimes were 7.36 ± 0.59 pH units and 7.70 ± 0.40 pH units, respectively. The average pH measurements observed in Unit 2 over 51 days of operation for the permeate and concentrate flow regimes were, 7.31 ± 0.61 pH units and 7.74 ± 0.41 pH units, respectively.

Figure 3.26 below illustrates the conductivity measurements and the subsequent salt rejection calculated in Unit 1 and Unit 2 of the testbed.

a)

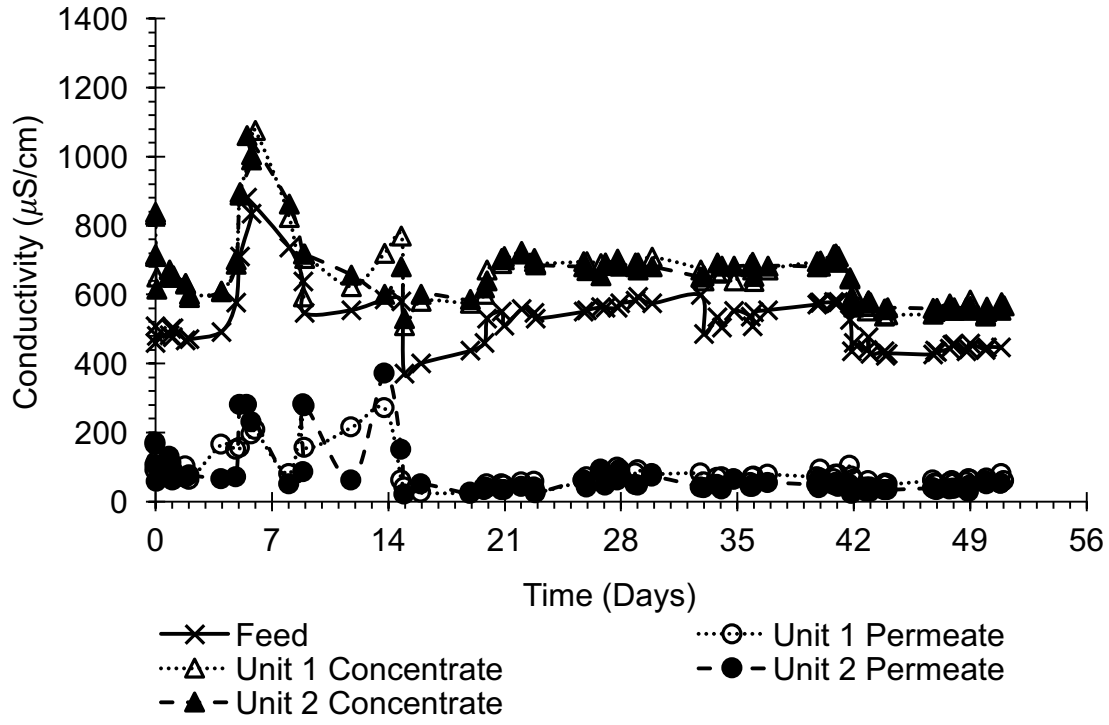

b)

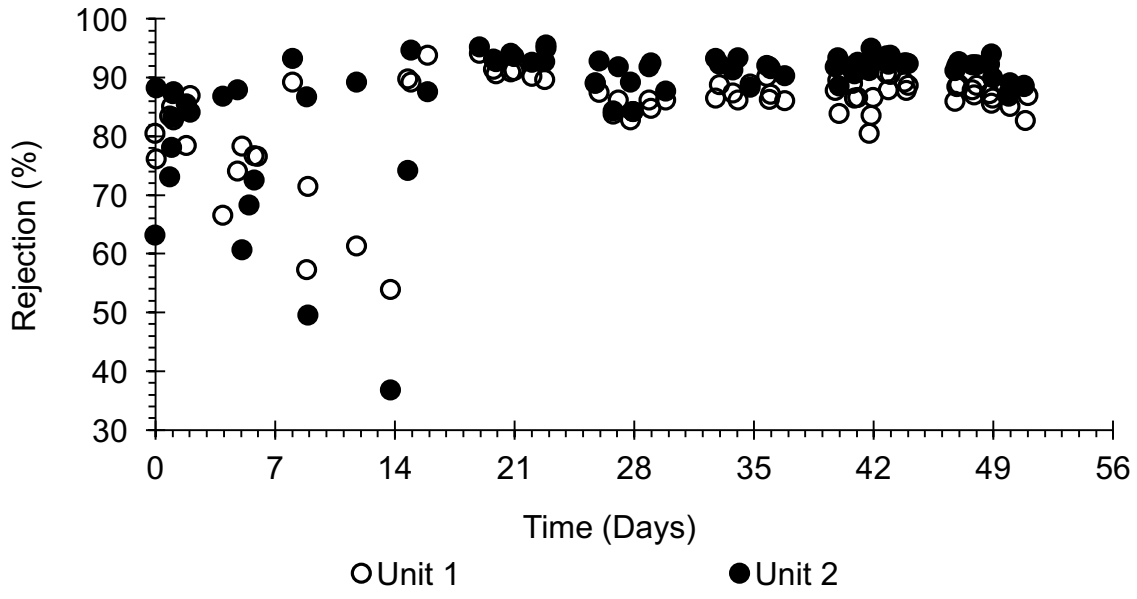

Figure 3.26: Contaminant Removal Comparison for Pristine vs. Silver-Coated Membrane Measurements for (a) Conductivity and (b) Calculated Salt Rejection

Figure 3.26(a) again shows the feed water conductivity measurements and the subsequent permeate and concentrate conductivity measurements fluctuating during 51 days of operation. The average feed conductivity over 51 days of operation was 520 ± 89 μS/cm, fluctuating between a maximum and minimum conductivity of 880 μS/cm and 370 μS/cm, respectively. The average conductivity for the permeate and concentrate flow regimes in Unit 1 was 82 ± 50 μS/cm and 655 ± 98 μS/cm, respectively. The permeate conductivity measurements fluctuated between a maximum and minimum of 281 μS/cm and 25 μS/cm, respectively. The concentrate conductivity measurements fluctuated between a maximum and minimum of 1075 μS/cm and 510 μS/cm, respectively. The average conductivity for the permeate and concentrate flow regimes in Unit 2 was 68 ± 65 μS/cm and 653 ± 94 μS/cm, respectively. The permeate conductivity measurements fluctuated between a maximum and minimum of 370 μS/cm and 20 μS/cm, respectively. The concentrate conductivity measurements fluctuated between a maximum and minimum of 1060 μS/cm and 530 μS/cm, respectively.

Due to the many fluctuations in source water conductivity, it is easier to model the performance of the membranes in terms of the percent of salts rejected, as shown in Figure 3.26(b). Over 51 days of operation, Unit 1 experienced an average salt rejection of 85 ± 7.5%, and Unit 2 experienced an average salt rejection of 88 ± 10.1%.

Figure 3.27 below shows the kinetics of the silver being released from Unit 1 and Unit 2 during the contaminant removal efficiency test.

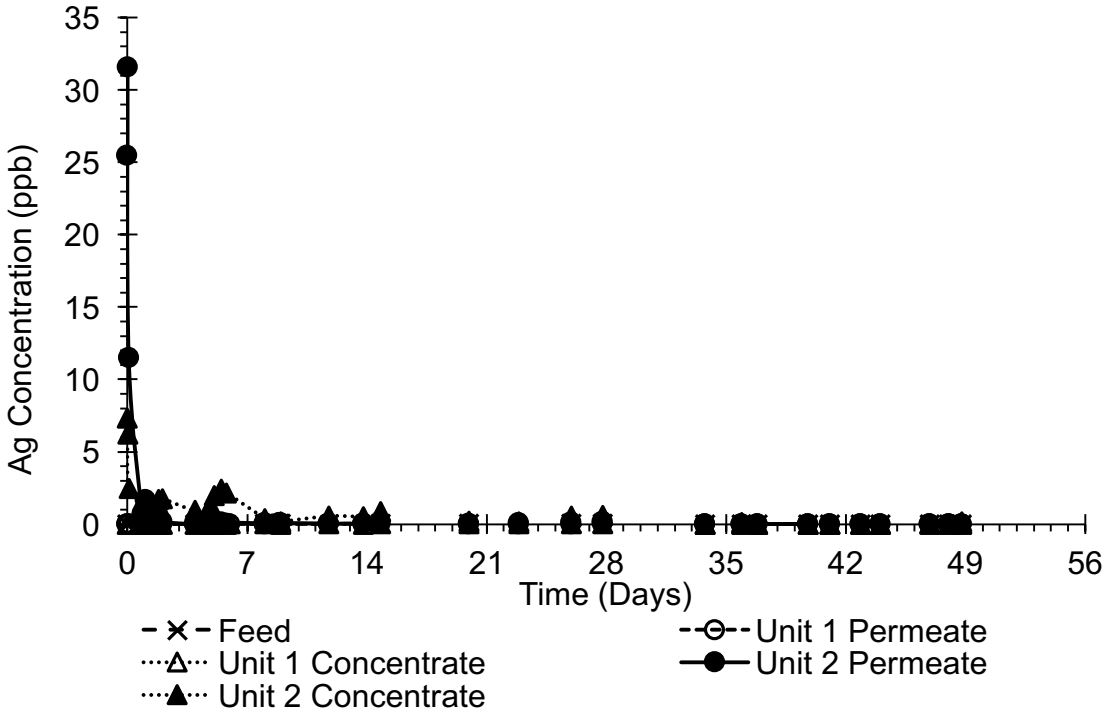

Figure 3.27: Silver Released Over 51 Days of Operation During the Contaminant Removal Comparison for Pristine vs. Silver-Coated Membranes

As illustrated in Figure 3.27 above, little to no silver (i.e. < 5 ppb) is released from the pristine membrane in Unit 1. Initially, silver is released from both the permeate and concentrate flow regimes of the silver-coated membrane in Unit 2 at maximum concentrations of 31 ppb and 7 ppb, respectively. After two hours of operation, the concentration of silver in the permeate and concentrate flow regimes decreased to 11 ppb and 2 ppb, respectively. After a day of operating, little to no silver (i.e. < 5 ppb) was found in both the permeate and concentrate flow regimes of Unit 2.

Figure 3.28 below illustrates the chromium concentrations in the feed, permeate, and concentrate flow regimes of Unit 1 and Unit 2, and the subsequent chromium removal efficiencies calculated.

a)

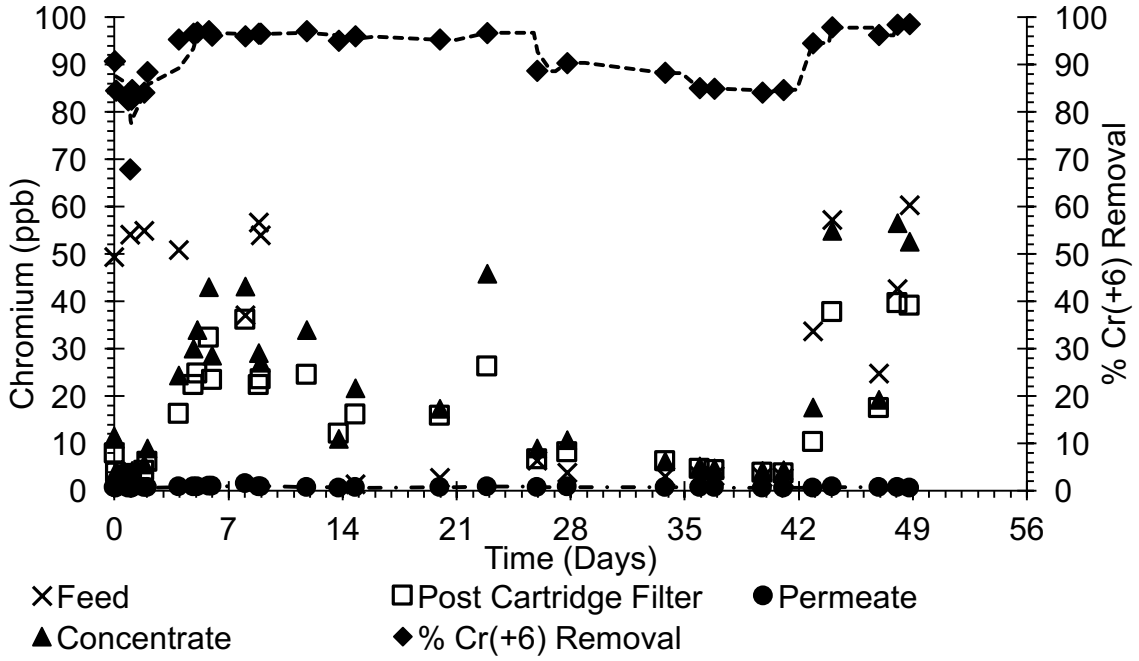

b)

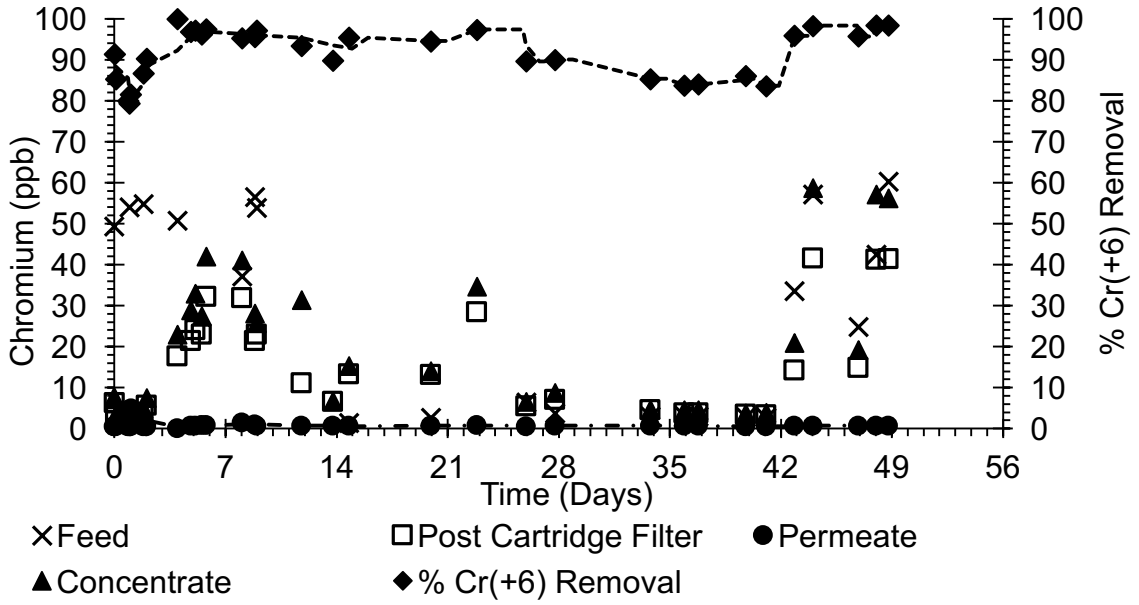

Figure 3.28: Chromium Concentrations and Removal Efficiency Comparison of (a) Pristine in Unit 1 vs. (b) Silver-Coated Membrane in Unit 2

As illustrated in Figures 3.28(a) and 3.28(b), the concentration of chromium in the feed water ranged from 1 ppb to 60 ppb. The concentration of chromium that the membranes received was from the water after the cartridge filters, which ranged from 3 - 40 ppb in Unit 1, and from 3 - 42 ppb in Unit 2. The average concentration of chromium in the permeate flow regimes for Unit 1 and Unit 2 was 0.73 ± 0.17 ppb and 0.78 ± 0.76 ppb, respectively. The average chromium removal efficiency of Unit 1 and Unit 2 over 51 days of operation was 91 ± 7%, and 92 ± 6%, respectively.

Run 4: Induced Fouling Test

a)

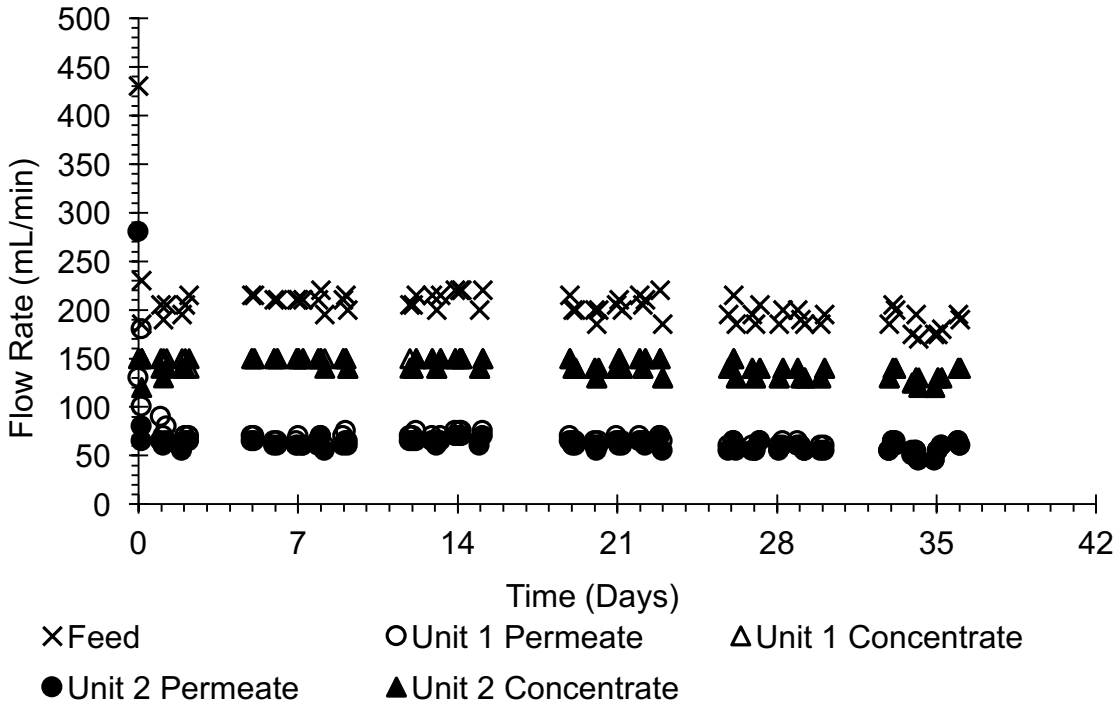

b)

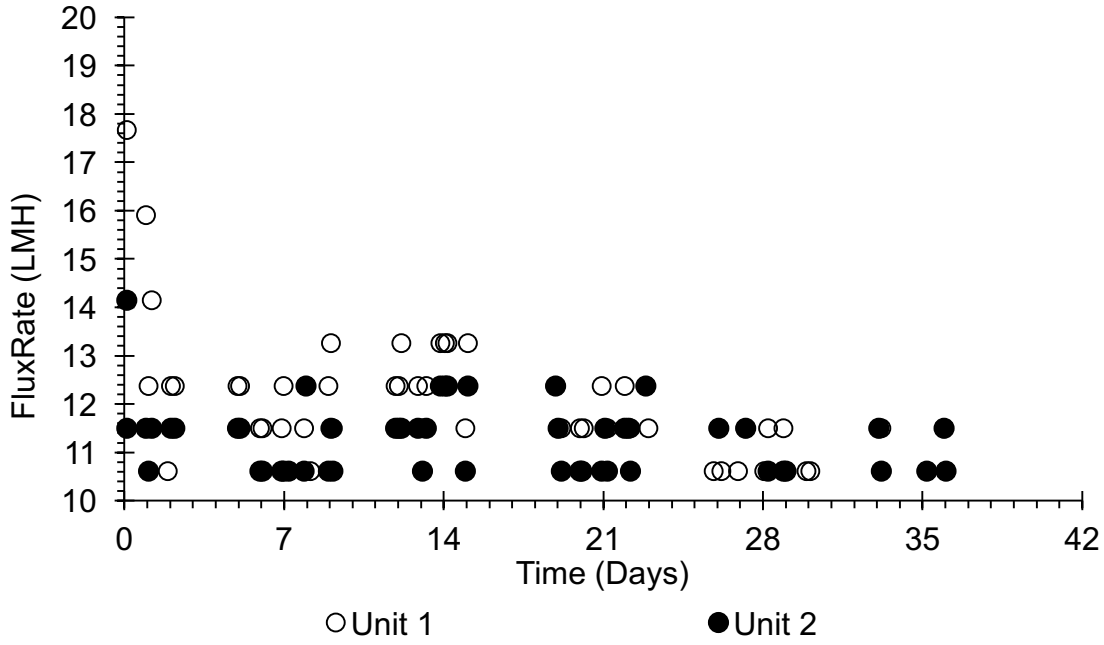

c)

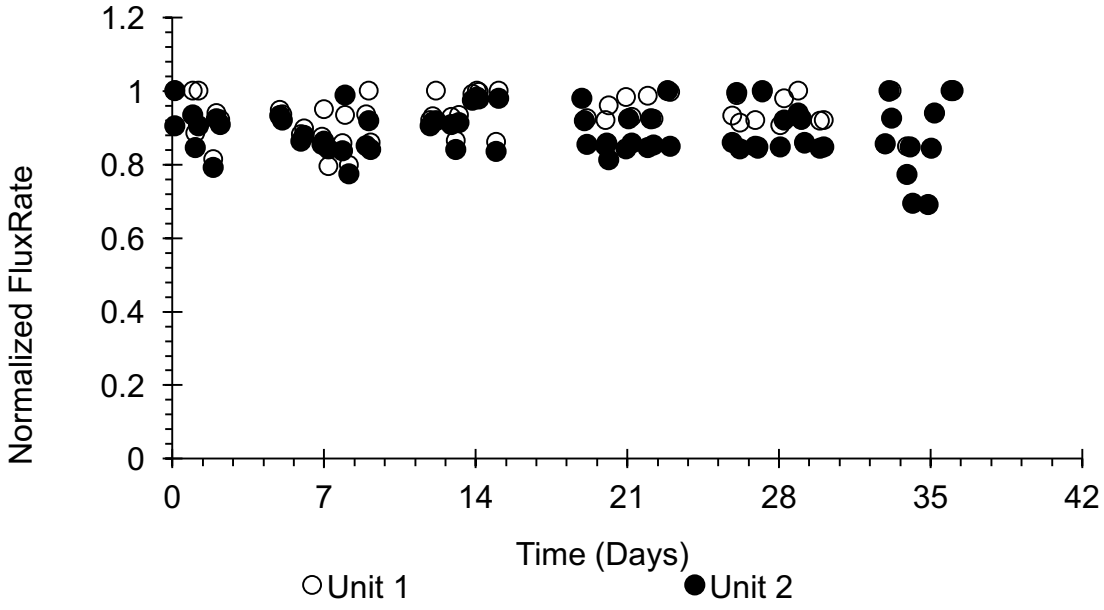

Figure 3.29: Induced Fouling Test Results for (a) Flow Rates, (b) Flux Rates, and (c) Normalized Flux Rates Over 36 Days

As illustrated in Figure 3.29(a), the average feed flow into the testbed was 205 ± 30 mL/min, not considering the data points where the testbed was not in operation (i.e. 0 mL/min feed flow). The average permeate and concentrate flow rates throughout the 36 days for Unit 1 were observed to be 68 ± 18 mL/min and 142 ± 8 mL/min, respectively. The average permeate and concentrate flow rates throughout the 36 days for Unit 2 were observed to be 64 ± 27 mL/min and 141 ± 9 mL/min, respectively.

Using Equation 3.2, the flux in LMH could be calculated from the permeate flow rates in mL/min, with a known membrane area of 3.7 square feet. Figure 3.28(b) shows the flux results obtained from the flow rate data in combination with Equation 3.2. The average flux rate over 36 days of operation for Unit 1 was 12 ± 2.8 LMH, while the average flux rate for Unit 2 was 11 ± 1.1 LMH. Figure 3.28(c) illustrates the normalized flux comparison for both units. As illustrated in the figure, the maximum flux rate for both units is achieved multiple times during operation, due to fluctuating pressure in the distribution system.

Figure 3.30 below serves to illustrate the consistency in water quality measurements such as temperature and pH during the induced fouling test.

a)

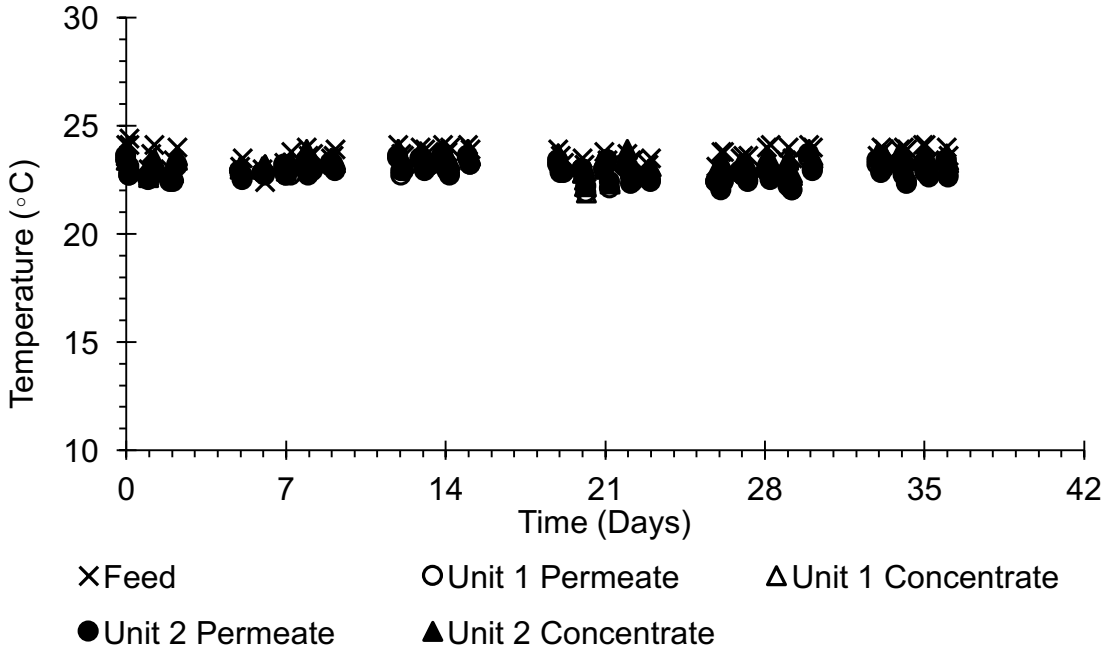

b)

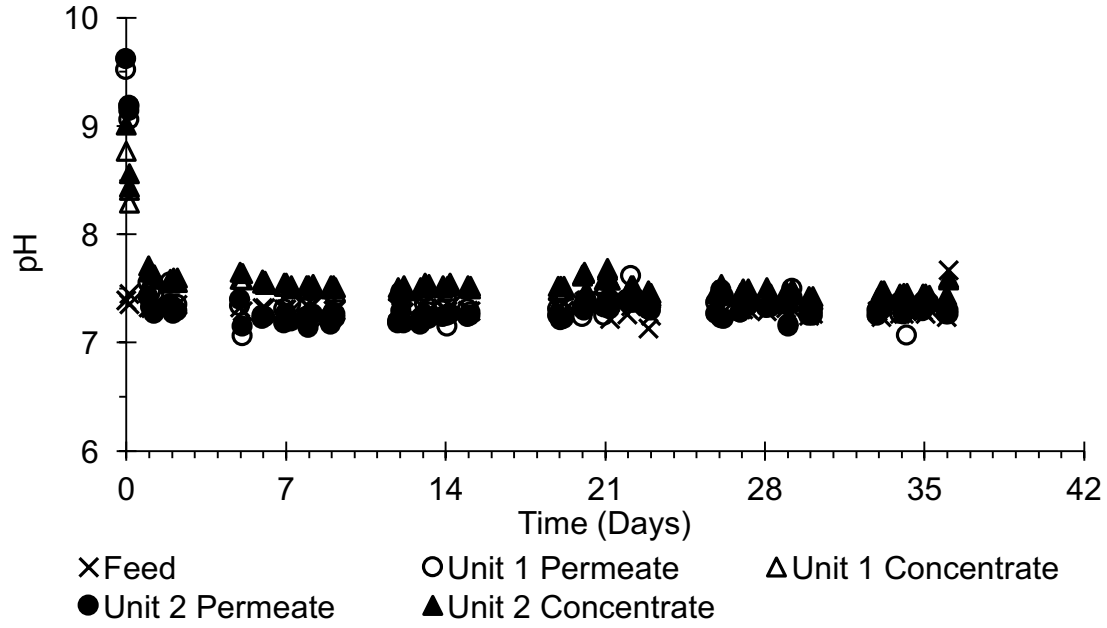

Figure 3.30: Water Quality Measurements During Induced Fouling Test for Pristine vs. Silver-Coated Membrane for (a) Temperature and (b) pH

As shown in Figure 3.30(a), the average temperature measurements observed in the feed flow for the testbed over 36 days of operation was 24 ± 0.4 °C. The average temperatures observed in Unit 1 over 36 days of operation for the permeate and concentrate flow regimes were, 23 ± 0.4 °C and 23 ± 0.4 °C, respectively. The average temperatures observed in Unit 2 over 36 days of operation for the permeate and concentrate flow regimes were, 23 ± 0.4 °C and 23 ± 0.4 °C, respectively.

As shown in Figure 3.30(b), the average pH measurements observed in the feed flow for the testbed over 36 days of operation was 7.32 ± 0.07 pH units. The average pH measurements observed in Unit 1 over 36 days of operation for the permeate and concentrate flow regimes were 7.40 ± 0.41 pH units and 7.53 ± 0.22 pH units, respectively. The average pH measurements observed in Unit 2 over 36 days of operation for the permeate and concentrate flow regimes were, 7.37 ± 0.42 pH units and 7.57 ± 0.25 pH units, respectively.

Figure 3.31 below illustrates the conductivity measurements and the subsequent salt rejection calculated in Unit 1 and Unit 2 of the testbed.

a)

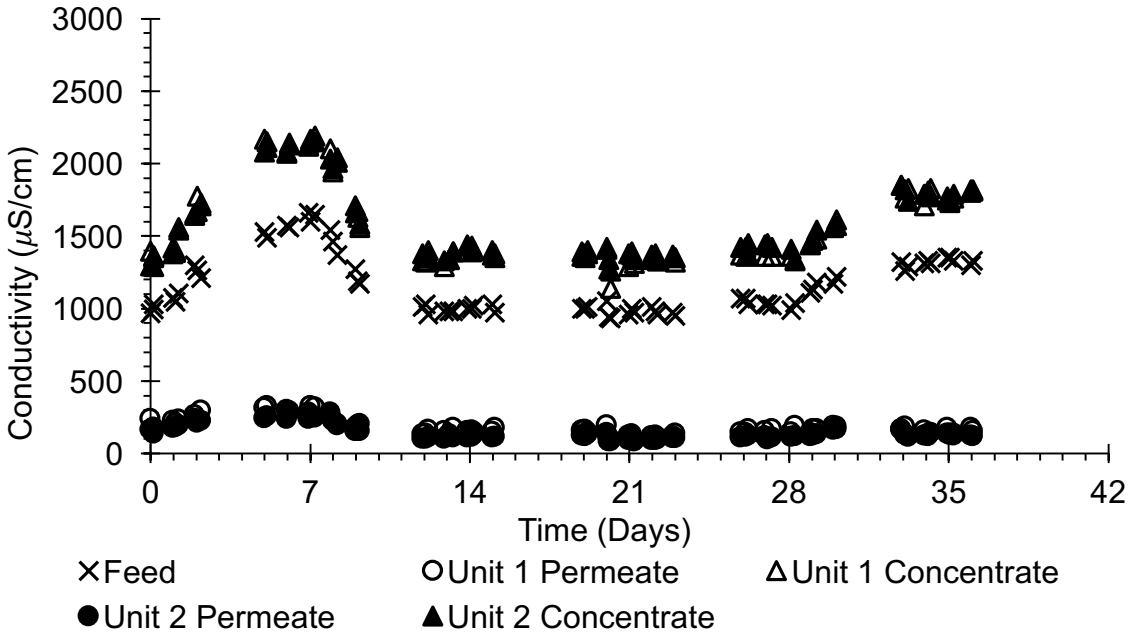

b)

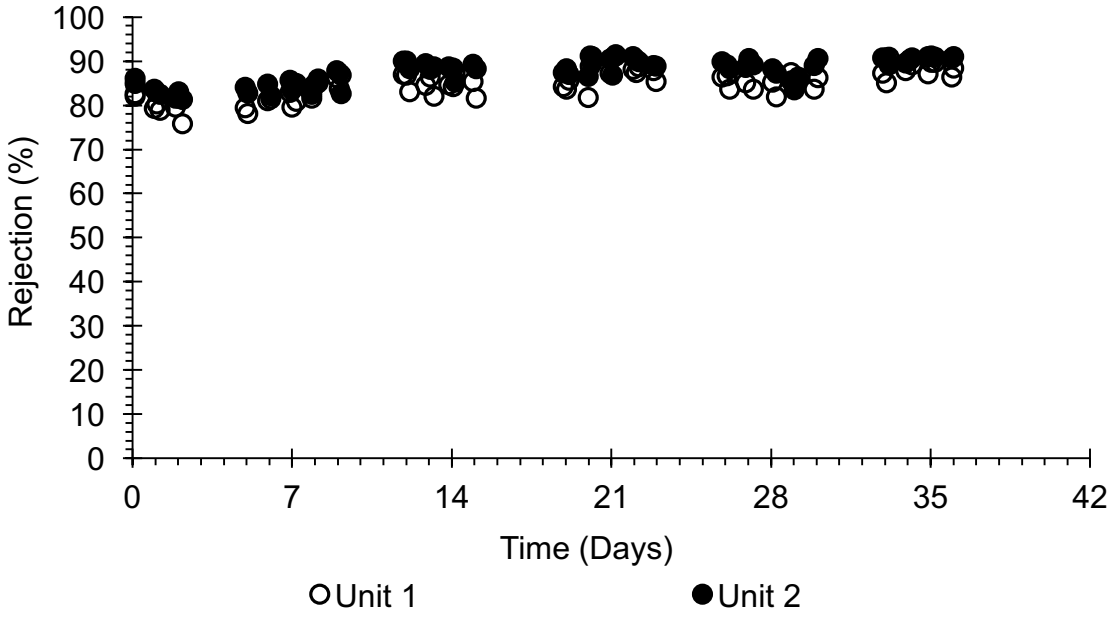

Figure 3.31: Induced Fouling Test Measurements for (a) Conductivity and (b) Calculated Salt Rejection

Figure 3.31(a) again shows the feed water conductivity measurements and the subsequent permeate and concentrate conductivity measurements fluctuating during 36 days of operation. The average feed conductivity over 36 days of operation was 1159 ± 202 μS/cm, fluctuating between a maximum and minimum conductivity of 1660 μS/cm and 930 μS/cm, respectively. The average conductivity for the permeate and concentrate flow regimes in Unit 1 was 178 ± 60 μS/cm and 1571 ± 279 μS/cm, respectively. The permeate conductivity measurements fluctuated between a maximum and minimum of 328 μS/cm and 84 μS/cm, respectively. The concentrate conductivity measurements fluctuated between a maximum and minimum of 2190 μS/cm and 1140 μS/cm, respectively. The average conductivity for the permeate and concentrate flow regimes in Unit 2 was 148 ± 52 μS/cm and 1575 ± 263 μS/cm, respectively. The permeate conductivity measurements fluctuated between a maximum and minimum of 280 μS/cm and 83 μS/cm, respectively. The concentrate conductivity measurements fluctuated between a maximum and minimum of 2150 μS/cm and 1260 μS/cm, respectively.

Due to the many fluctuations in source water conductivity, it is easier to model the performance of the membranes in terms of the percent of salts rejected, as shown in Figure 3.30(b). Over 36 days of operation, Unit 1 experienced an average salt rejection of 85 ± 3.5%, and Unit 2 experienced an average salt rejection of 87 ± 2.9%.

Figure 3.32 below shows additional water quality parameters in terms of organic content, including UV-254 and TOC measurements.

a)

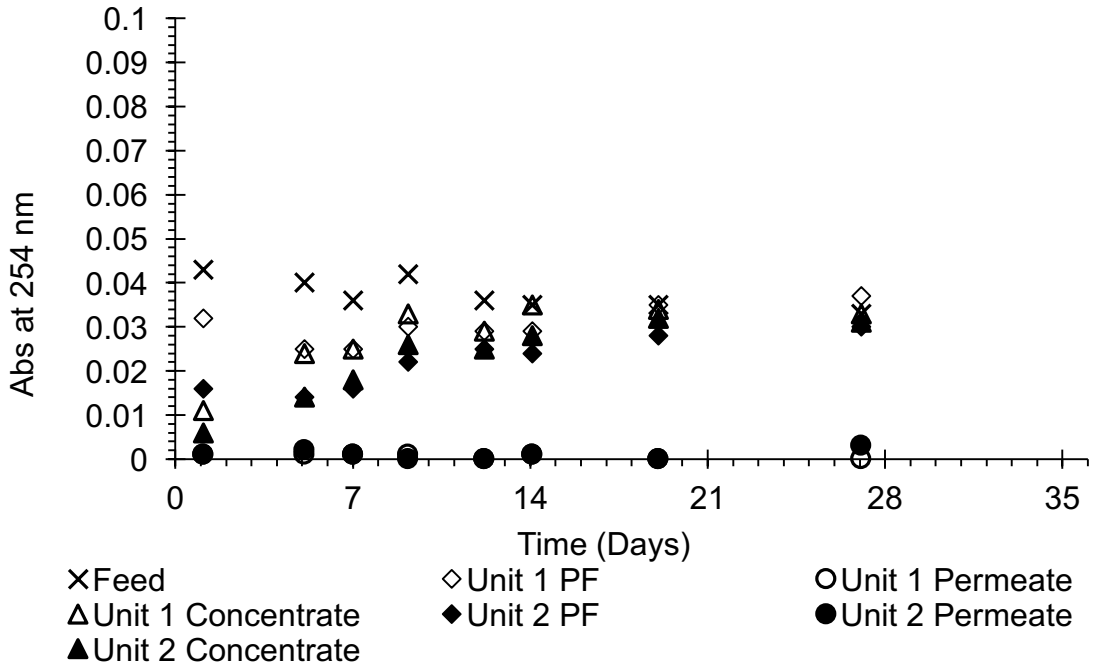

b)

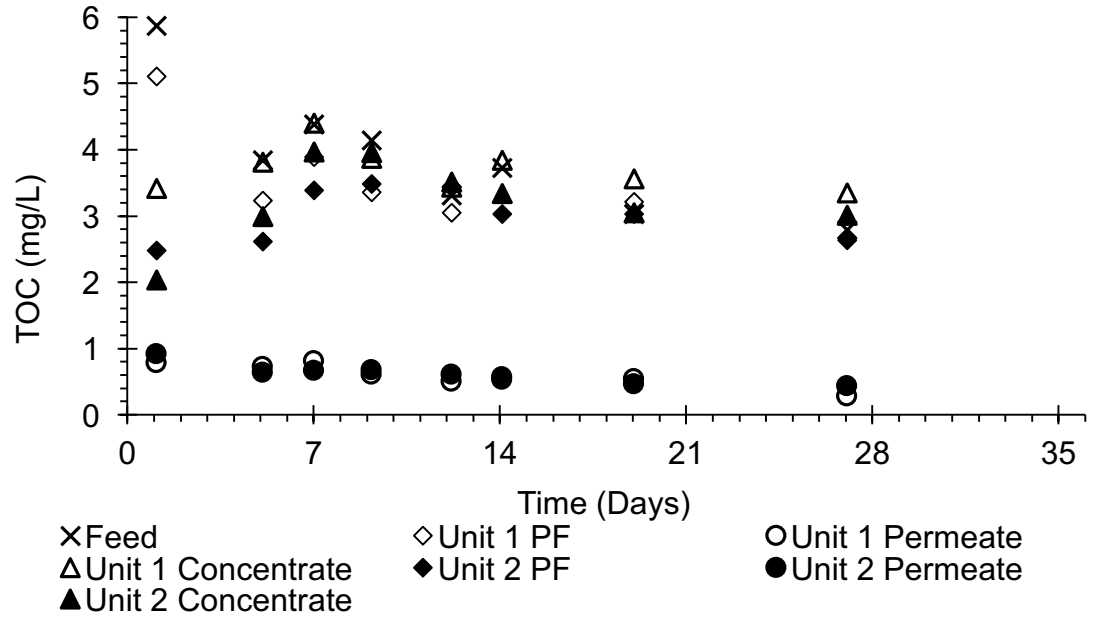

Figure 3.32: Induced Fouling Tests Organic Measurement Results for (a) UV-254 and (b) TOC

As illustrated in Figure 3.32(a) above, the average UV-254 abs in the feed water was 0.038 ± 0.004 abs. The average reduction observed in UV-254 abs for Unit 1 and Unit 2 was 98 ± 1.9% and 95 ± 5.2%, respectively. As illustrated in Figure 3.31(b) above, the average TOC concentration in the feed water was 3.89 ± 0.97 mg/L. The average reduction observed in TOC for both Unit 1 and Unit 2 was 84 ± 5%.

Figure 3.33 below shows the results obtained from the heterotrophic plate count after the testbed was shut down.

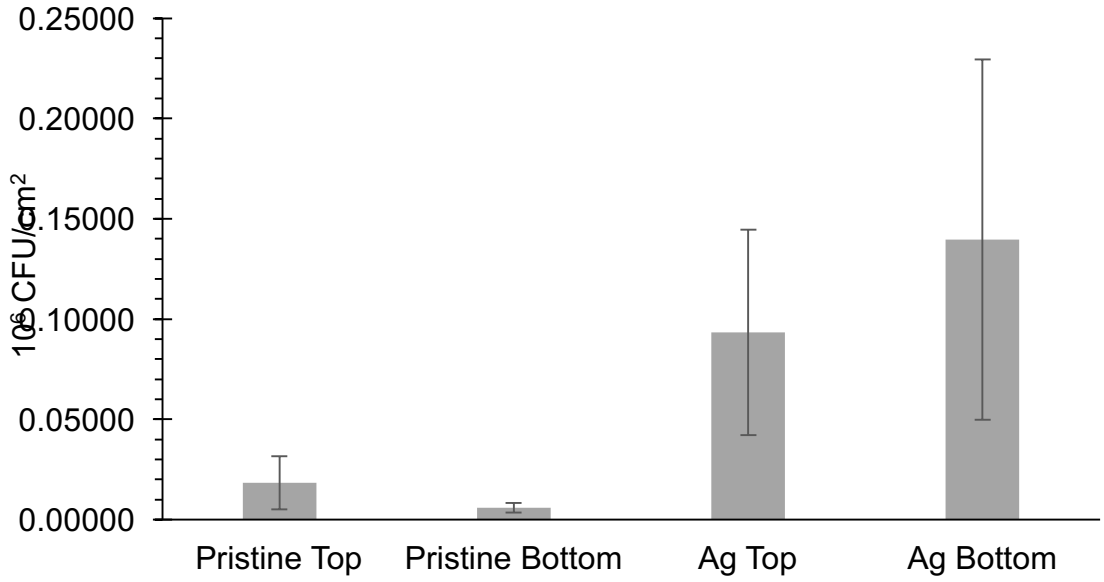

Figure 3.33: HPC Results from Pristine Membrane and Silver-Coated Membrane After Testbed Shut Down

As illustrated in Figure 3.33 above, the HPC results show greater average microbial growth on the silver-coated membrane compared to the pristine membrane. The pristine membrane top had an average microbe count of $0.018 \pm 0.013 \times 10^6$ CFU/cm^2. The pristine membrane top had an average microbe count of $0.006 \pm 0.002 \times 10^6$

CFU/cm^2. The silver-coated membrane top had an average microbe count of 0.093 ± 0.051 x 10^6 CFU/cm^2. The silver-coated membrane bottom had an average microbe count of 0.140 ± 0.090 x 10^6 CFU/cm^2. After conducting a student t-test to compare all data sets, the P-values obtained were all above the confidence value of 0.05, except for the silver top compared to the pristine bottom, which showed a P-value of 0.04. This indicates there is a statistically significant difference between these data sets.

Run 5: Deployment to Chandler Water Treatment Plant

a)

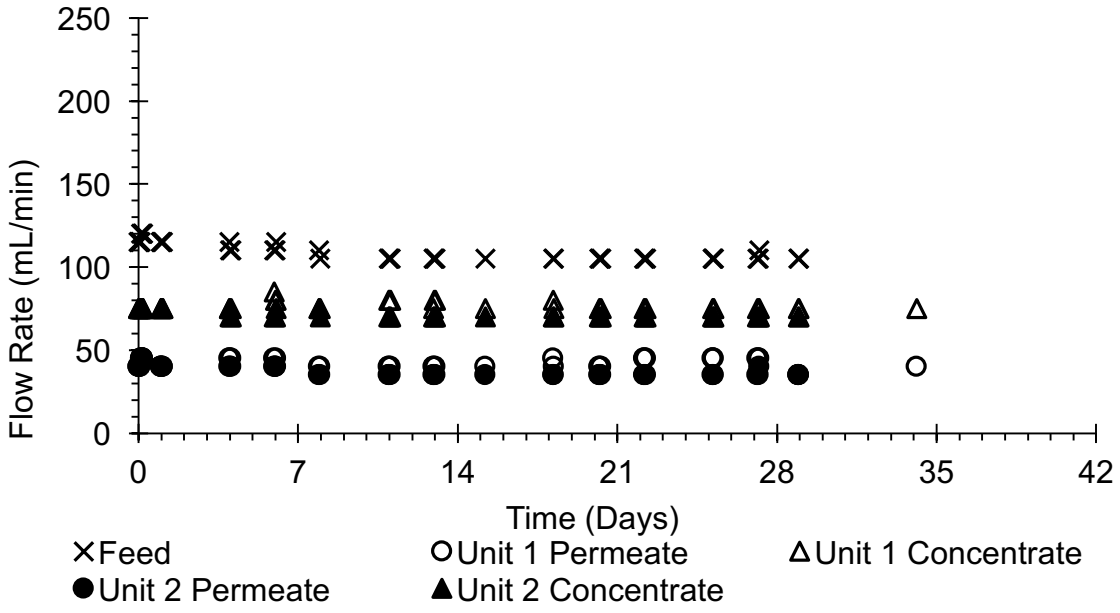

b)

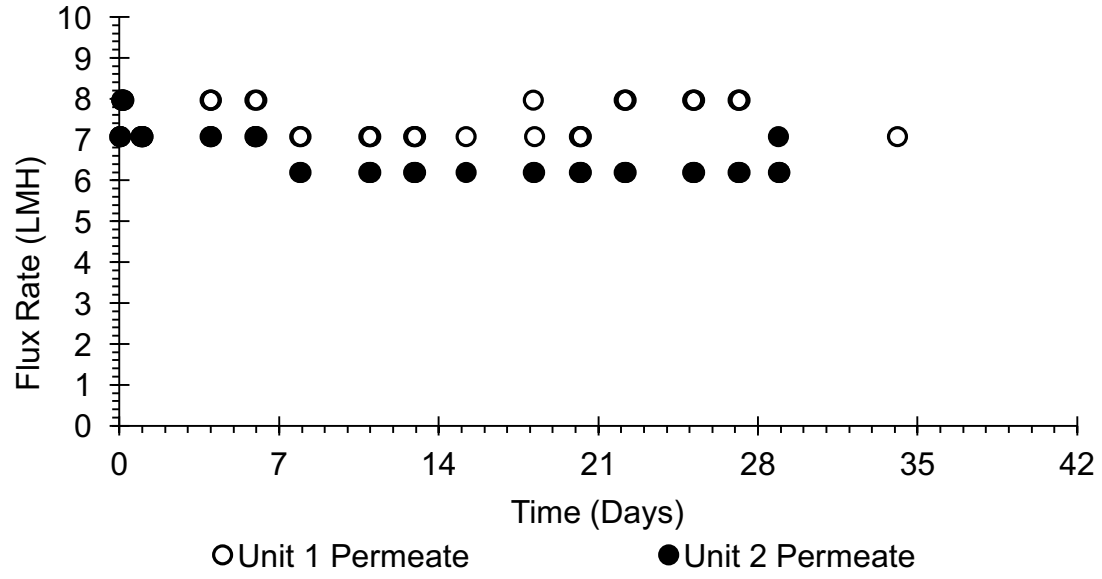

c)

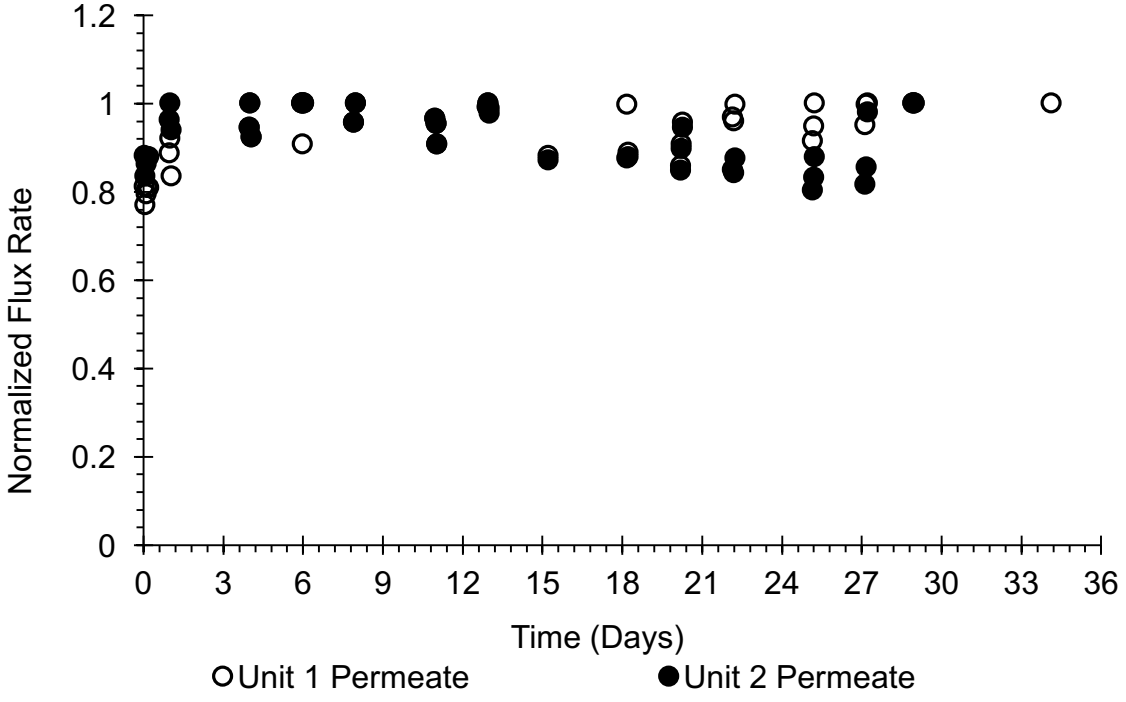

Figure 3.34: Testbed Deployment Test Results for (a) Flow Rates, (b) Flux Rates, and (c) Normalized Flux Rates Over 34 Days

As illustrated in Figure 3.34(a), the average feed flow into the testbed was 209 ± 5 mL/min, not considering the data points where the testbed was not in operation (i.e. 0 mL/min feed flow). The average permeate and concentrate flow rates throughout the 34 days for Unit 1 were observed to be 42 ± 3 mL/min and 76 ± 2 mL/min, respectively. The average permeate and concentrate flow rates throughout the 34 days for Unit 2 were observed to be 37 ± 3 mL/min and 71 ± 2 mL/min, respectively.

Using Equation 3.2, the flux in LMH could be calculated from the permeate flow rates in mL/min, with a known membrane area of 3.7 square feet. Figure 3.33(b) shows the flux results obtained from the flow rate data in combination with Equation 3.2. The average flux rate over 34 days of operation for Unit 1 was 7.4 ± 0.5 LMH, while the average flux rate for Unit 2 was 6.6 ± 0.6 LMH. Figure 3.34(c) illustrated the normalized flux results for Units 1 and 2. As illustrated in the figure, the maximum flux rate is achieved several times throughout operation. This can be attributed to the fluctuations in feed pressure observed in the distribution system, making it difficult to obtain a tru flux-decline equation.

Figure 3.35 below serves to illustrate the consistency in water quality measurements such as temperature and pH during the testbed deployment in Chandler, AZ.

a)

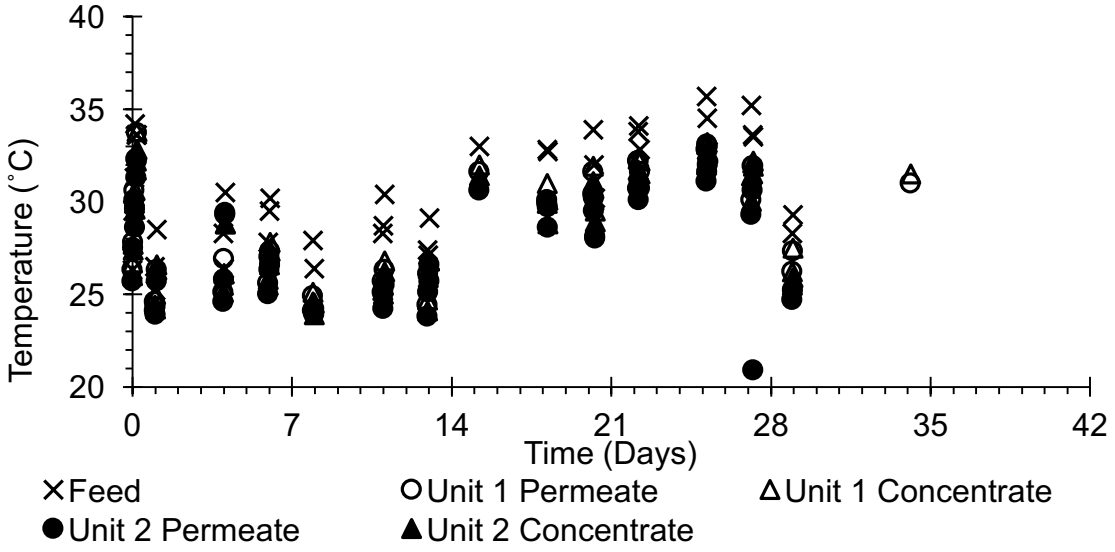

b)

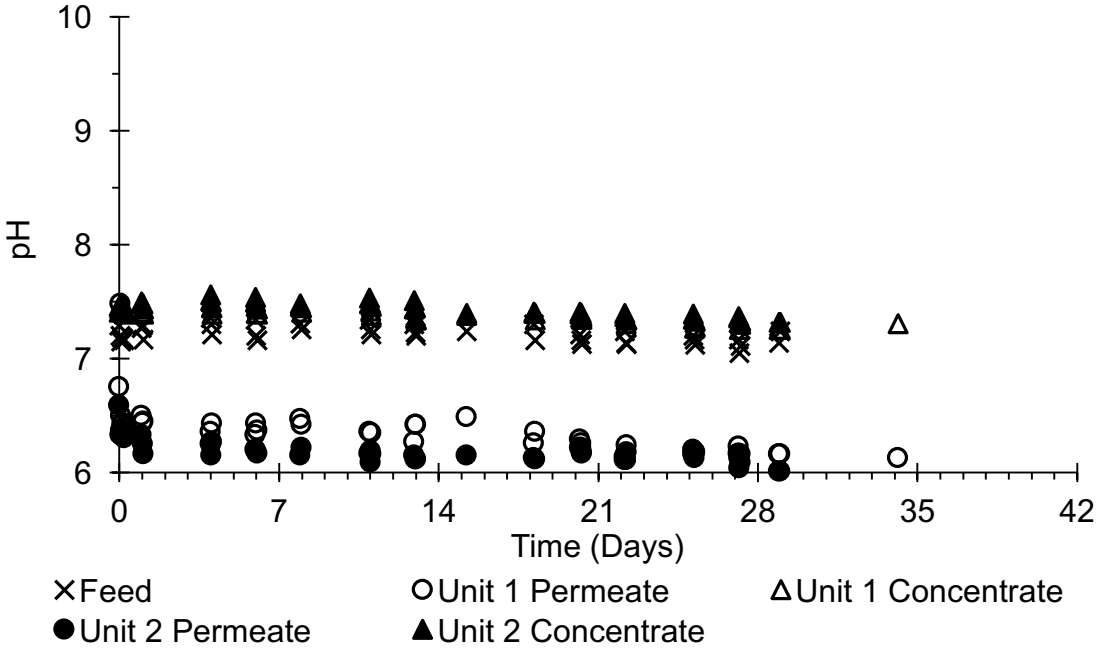

Figure 3.35: Water Quality Measurements During Testbed Deployment in Chandler, AZ for (a) Temperature and (b) pH

As shown in Figure 3.35(a), the average temperature measurements observed in the feed flow for the testbed over 34 days of operation was 30.8 ± 3.0 °C. The average temperatures observed in Unit 1 over 34 days of operation for the permeate and concentrate flow regimes were, 28.6 ± 3.0 °C and 28.9 ± 3.0 °C, respectively. The average temperatures observed in Unit 2 over 34 days of operation for the permeate and concentrate flow regimes were, 27.5 ± 2.9 °C and 28.3 ± 2.9 °C, respectively.

As shown in Figure 3.35(b), the average pH measurements observed in the feed flow for the testbed over 34 days of operation was 7.21 ± 0.07 pH units. The average pH measurements observed in Unit 1 over 34 days of operation for the permeate and concentrate flow regimes were 6.35 ± 0.22 pH units and 7.38 ± 0.07 pH units, respectively. The average pH measurements observed in Unit 2 over 34 days of operation for the permeate and concentrate flow regimes were, 6.19 ± 0.11 pH units and 7.42 ± 0.07 pH units, respectively.

Figure 3.36 below illustrates the conductivity measurements and the subsequent salt rejection calculated in Unit 1 and Unit 2 of the testbed.

a)

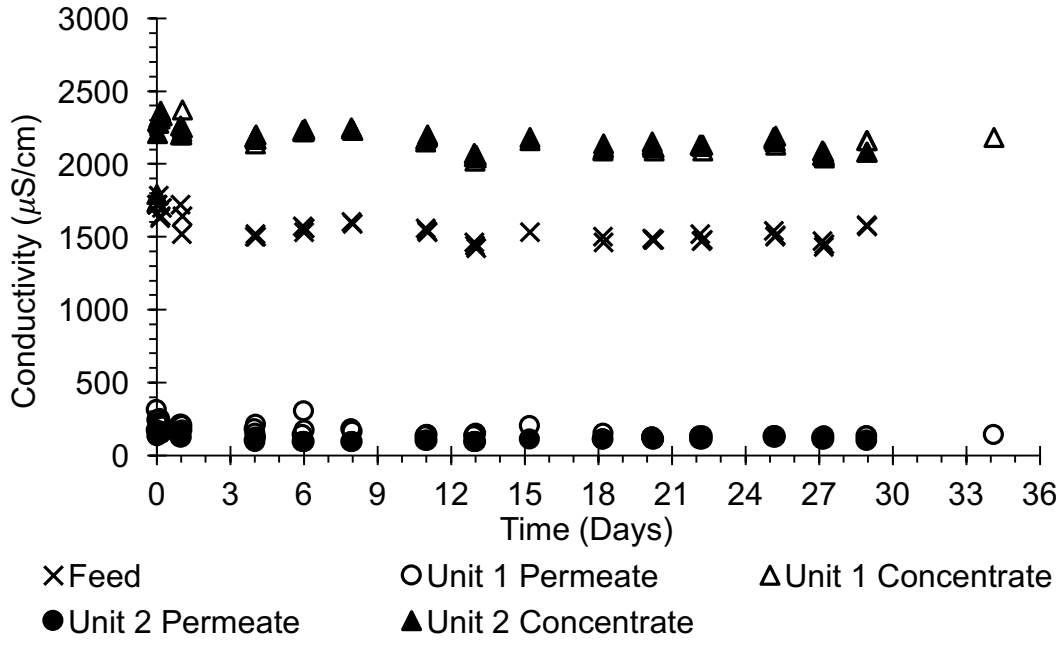

b)

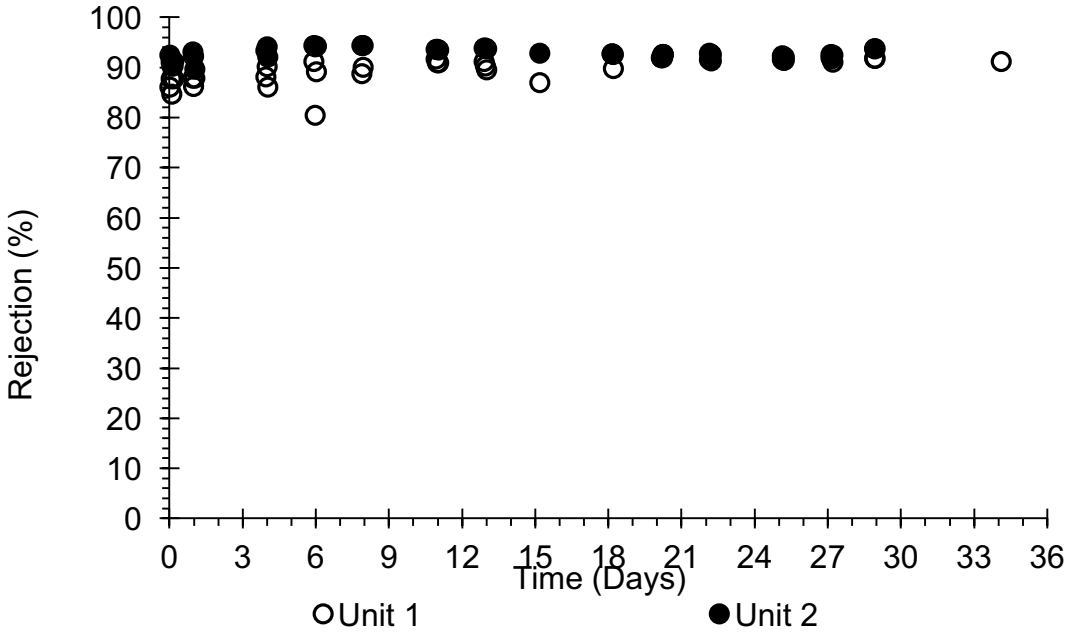

Figure 3.36: Testbed Deployment Measurements for (a) Conductivity and (b) Calculated Salt Rejection

Figure 3.36(a) shows the average feed conductivity at the Chandler Water Treatment Plant over 34 days of operation was 1547 ± 88 μS/cm, fluctuating between a maximum and minimum conductivity of 1780 μS/cm and 1420 μS/cm, respectively. The average conductivity for the permeate and concentrate flow regimes in Unit 1 was 164 ± 50 μS/cm and 2163 ± 111 μS/cm, respectively. The permeate conductivity measurements fluctuated between a maximum and minimum of 310 μS/cm and 110 μS/cm, respectively. The concentrate conductivity measurements fluctuated between a maximum and minimum of 2370 μS/cm and 1740 μS/cm, respectively. The average conductivity for the permeate and concentrate flow regimes in Unit 2 was 114 ± 23 μS/cm and 2160 ± 97 μS/cm, respectively. The permeate conductivity measurements fluctuated between a maximum and minimum of 170 μS/cm and 90 μS/cm, respectively. The concentrate conductivity measurements fluctuated between a maximum and minimum of 2360 μS/cm and 1790 μS/cm, respectively.

Due to the many fluctuations in source water conductivity, it is easier to model the performance of the membranes in terms of the percent of salts rejected, as shown in Figure 3.36(b). Over 34 days of operation, Unit 1 experienced an average salt rejection of 89.7 ± 2.6%, and Unit 2 experienced an average salt rejection of 93.0 ± 1.2%.

Figure 3.37 below illustrates the kinetics of the silver released from the silver-coated membrane in Unit 2 during the Testbed Deployment Test at the Chandler Water Treatment Plant.

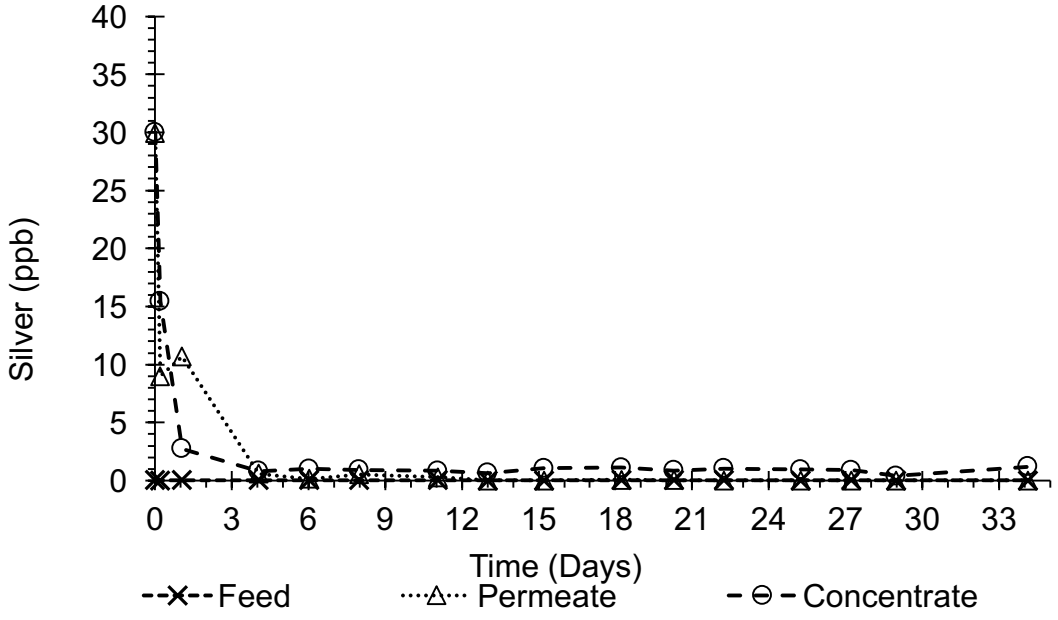

Figure 3.37: Silver Released Over 34 Days of Operation During the Contaminant Removal Comparison for Pristine vs. Silver-Coated Membranes

As illustrated in Figure 3.37 above, no silver was found in the feed water. Initially, silver is released from both the permeate and concentrate flow regimes of the silver-coated membrane in Unit 2 at maximum concentrations of 30 ppb for both. After five hours of operation, the concentration of silver in the permeate and concentrate flow regimes decreased to 9 ppb and 15 ppb, respectively. After a day of operating, the permeate and concentrate silver concentrations decreased to 11 ppb and 3 ppb, respectively. Afterwards, little to no silver (i.e. < 5 ppb) was detected in both the permeate and concentrate flow regimes of Unit 2. After integrating the area under the curves, it was found that approximately 1.31 μg-Ag/cm^2 was released in the first day, or approximately 75% of the silver loaded.

Figure 3.38 below shows additional water quality parameters in terms of organic content, including UV-254 and TOC measurements.

a)

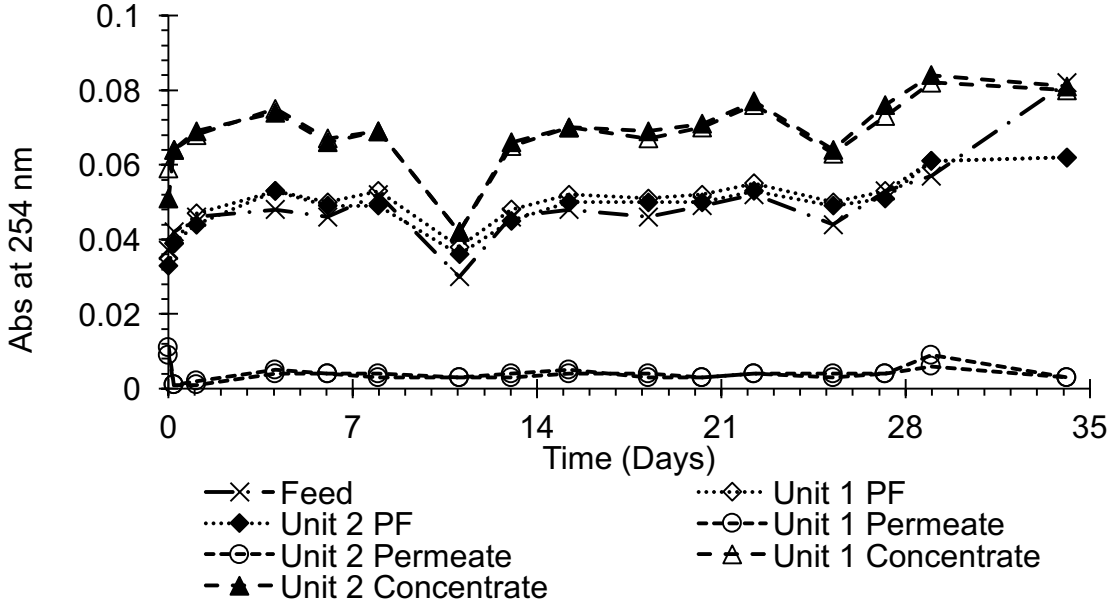

b)

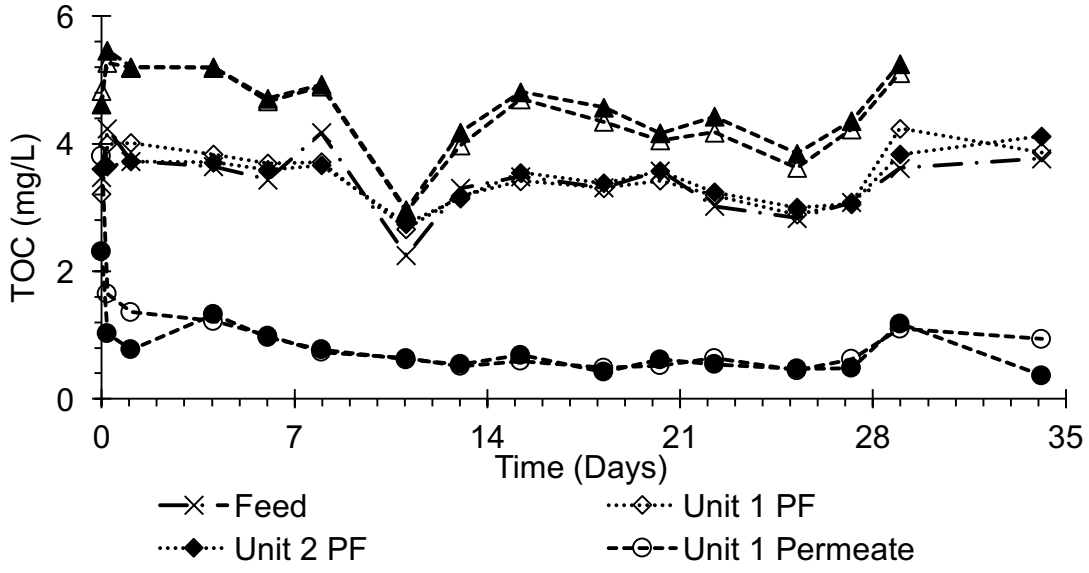

Figure 3.38: Testbed Deployment in Chandler Water Treatment Plant Organic Measurement Results for (a) UV-254 and (b) TOC

As illustrated in Figure 3.38(a) above, the average UV-254 abs in the feed water was 0.049 ± 0.011 abs. The average reduction observed in UV-254 abs for Unit 1 and Unit 2 was 91.7 ± 6.5% and 91.4 ± 5.8%, respectively. As illustrated in Figure 3.31(b) above, the average TOC concentration in the feed water was 3.43 ± 0.49 mg/L. The average reduction observed in TOC for both Unit 1 was 71.0 ± 25.0%. and Unit 2 was 76.7 ± 12.9%.

During the ICP-MS analysis, other constituents were tested to compare the removal efficiencies of the pristine and silver-coated membranes. Figure 3.39 below shows the results from these analyses.

a)

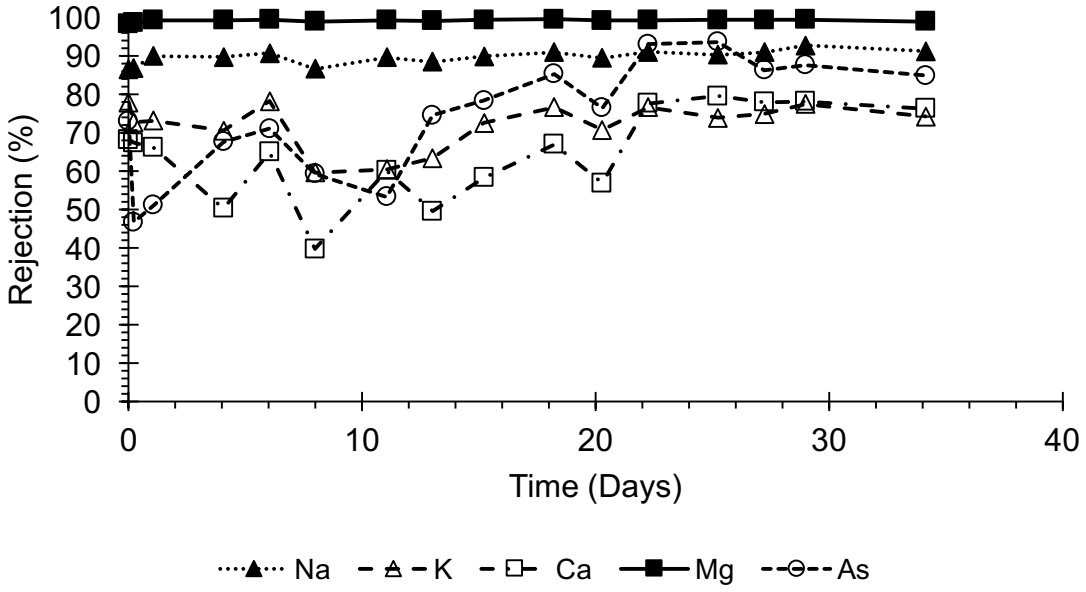

b)

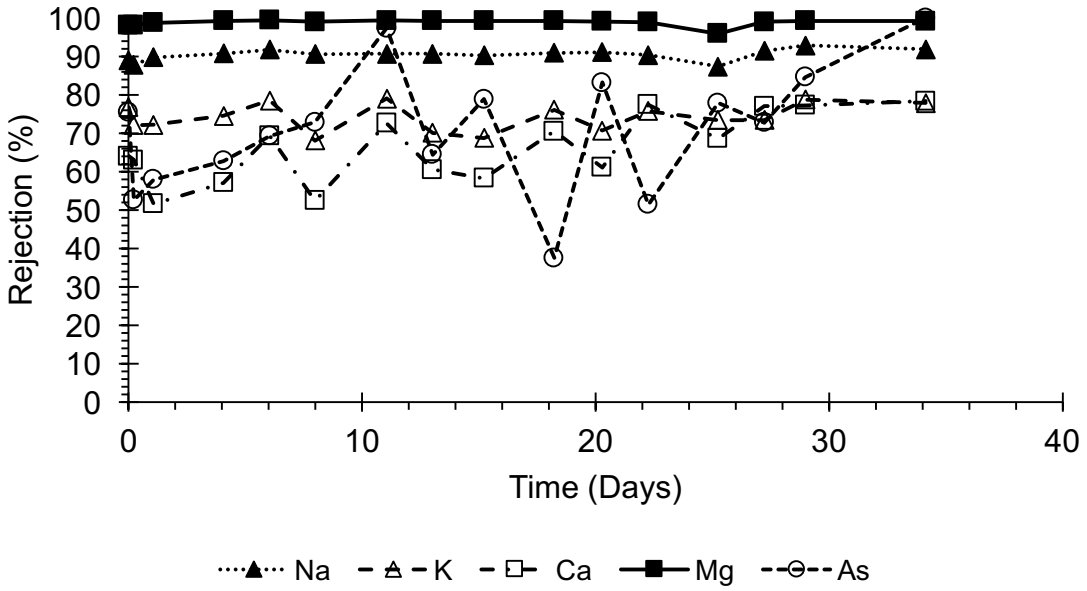

Figure 3.39: Multiple Constituent Removal Efficiencies of the (a) Pristine and (b) Silver-Coated Membrane During the Testbed Deployment at the Chandler Water Treatment Plant

As illustrated in Figures 3.39(a) and 3.39(b), the removal efficiencies of some constituents are more constant than others, where magnesium has a consistently high removal efficiency and arsenic has a fluctuating removal efficiency. The average feed concentrations for Na^+, K^+, Ca^{2+}, Mg^{2+}, and As were found to be 211 ± 46 mg/L, 6.98 ± 1.32 mg/L, 64 ± 14 mg/L, 17 ± 4 mg/L, and 1.57 ± 0.29 µg/L, respectively. Figure 3.37(a) illustrates the average removal efficiencies in the pristine membrane for Na^+, K^+, Ca^{2+}, Mg^{2+}, and As as 90 ± 2%, 72 ± 6%, 65 ± 12%, 99 ± 0%, and 74 ± 15%, respectively. Figure 3.37(b) illustrates the average removal efficiencies in the silver-coated membrane for Na^+, K^+, Ca^{2+}, Mg^{2+}, and As as 90 ± 1%, 69 ± 22%, 66 ± 9%, 99 ± 1%, and 71 ± 17%, respectively.

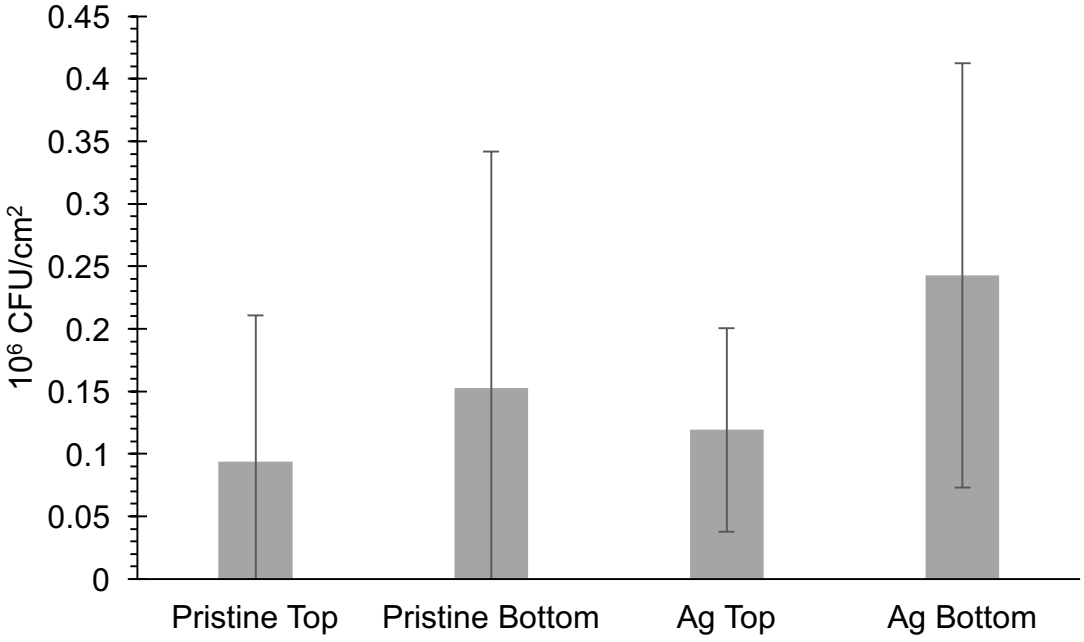

Figure 3.40: HPC Results After Testbed Shutdown in Chandler Water Treatment Plant

As illustrated in Figure 3.40 above, the HPC results show greater average microbial growth on the silver-coated membrane compared to the pristine membrane. The pristine membrane top had an average microbe count of $0.094 \pm 0.117 \times 10^6$ CFU/cm^2. The pristine membrane bottom had an average microbe count of $0.153 \pm 0.189 \times 10^6$ CFU/cm^2. The silver-coated membrane top had an average microbe count of $0.119 \pm 0.081 \times 10^6$ CFU/cm^2. The silver-coated membrane bottom had an average microbe count of $0.243 \pm 0.170 \times 10^6$ CFU/cm^2. After conducting a student t-test to compare all data sets in the HPC analysis, it was found that the P-values ranged from $0.29 < P < 0.80$, suggesting there is no statistically significant difference between the data sets.

Remote Data Acquisition

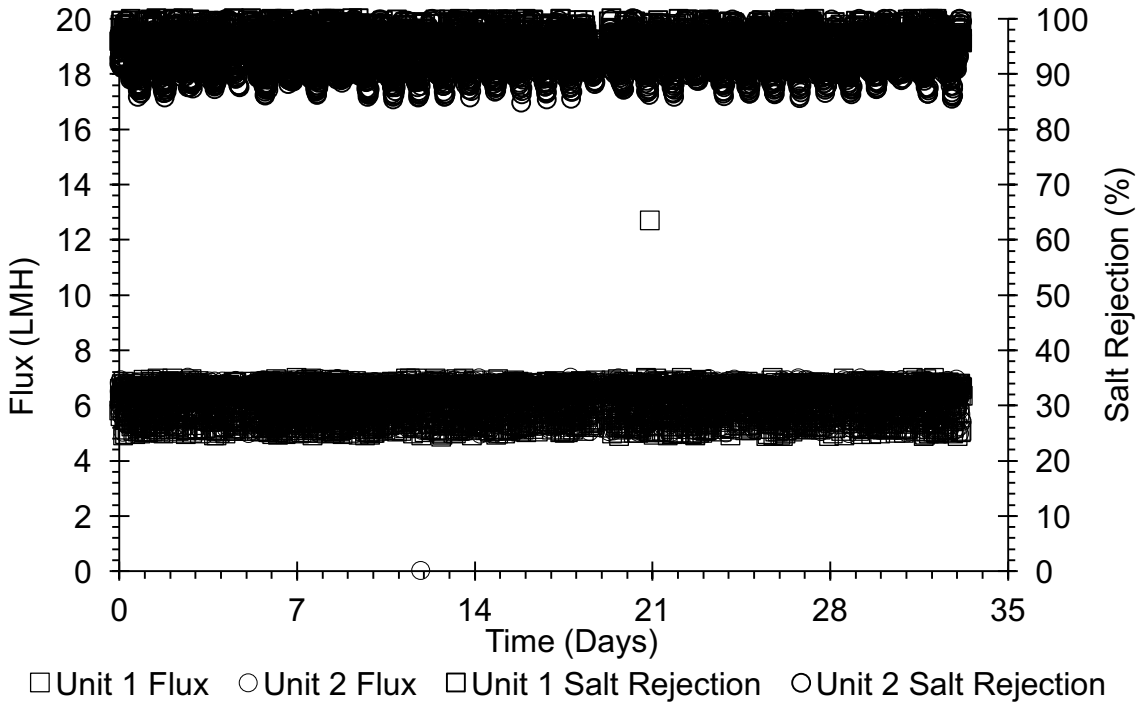

Figure 3.41: Flux Data and Salt Rejection Data from the Remote Data Acquisition System Over 34 Days of Operation at Chandler Water Treatment Plant

Figure 3.41 above illustrates the calculated flux and salt rejection data obtained using the remote data acquisition system in the Mobile NEWT Testbed. The flux data was calculated using Equation 3.2 based on the flow data obtained. The salt rejection was calculated based on the conductivity data obtained for the feed flow and the permeate flow sensors. The average flux for the pristine membrane in Unit 1 and the silver-coated membrane in Unit 2 was 6.9 ± 8.4 LMH and 6.8 ± 6.7 LMH, respectively. The average salt rejection for the pristine membrane and the silver-coated membrane was 95.5 ± 2.5% and 93.0 ± 3.0%, respectively.

Figure 3.42 below illustrates the data obtained by the temperature, conductivity, and pressure sensors used in the remote data acquisition system.

a)

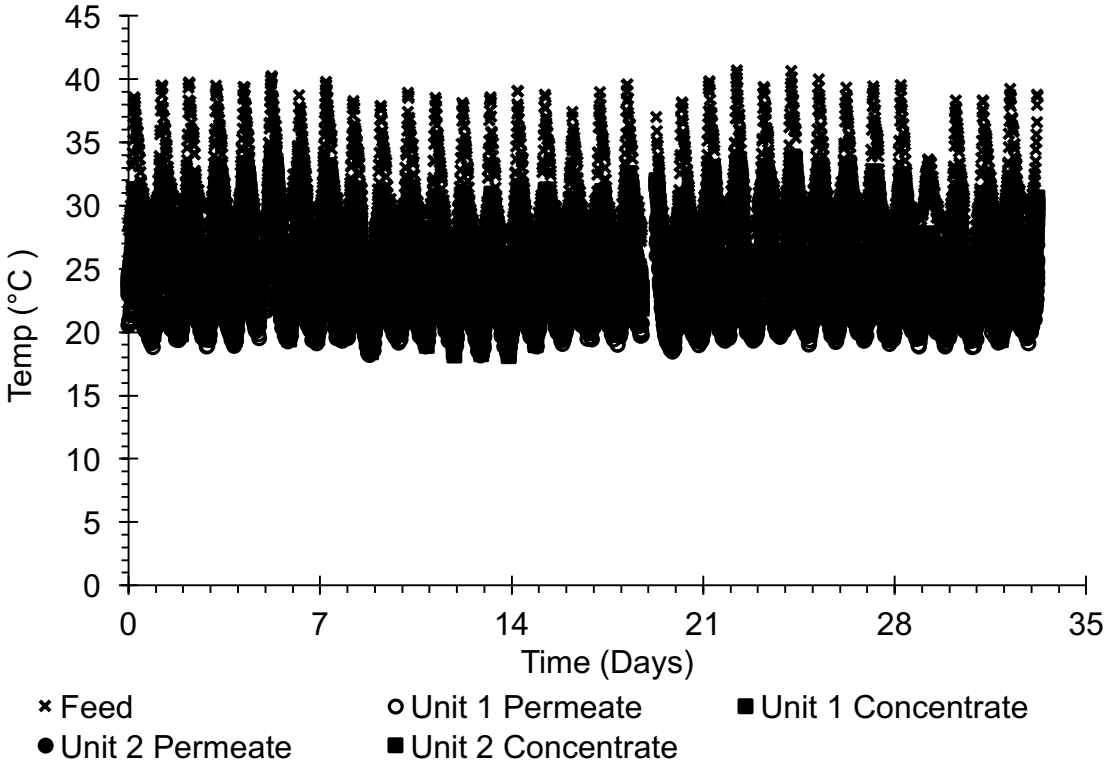

b)

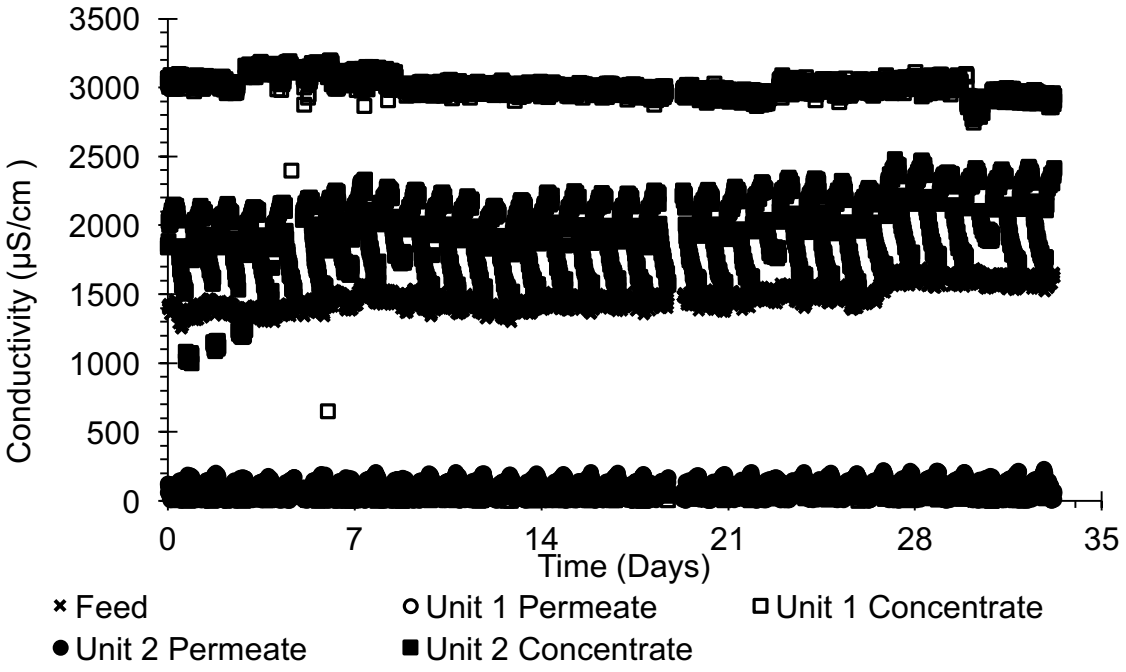

c)

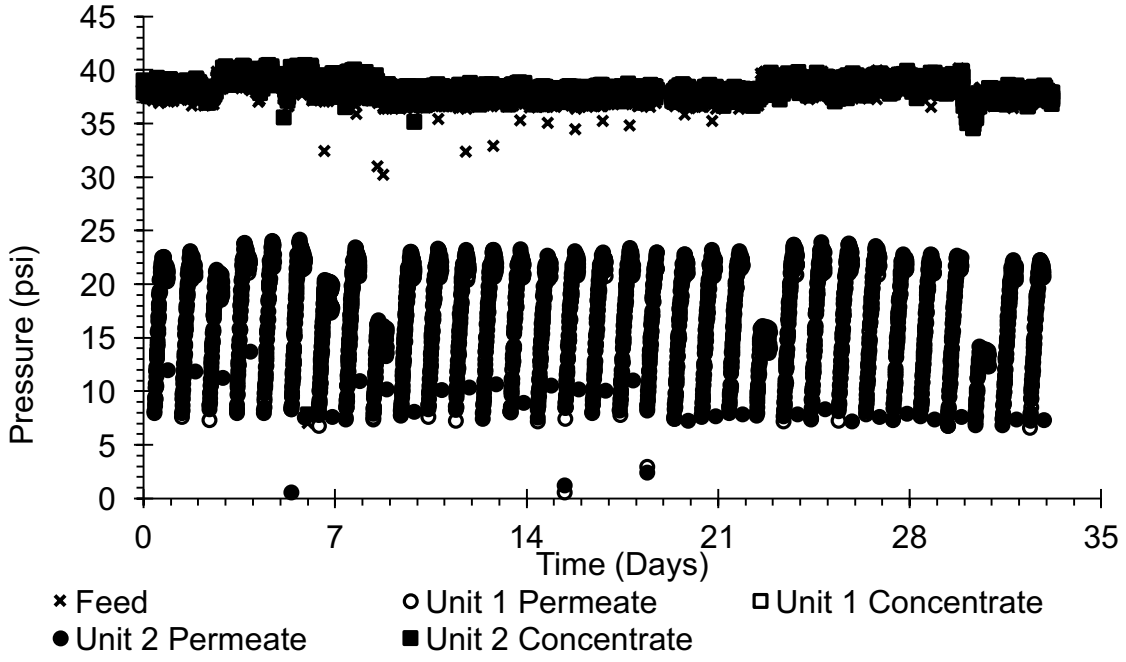

Figure 3.42: Remote Data Acquisition System Data from (a) Temperature, (b) Conductivity, and (c) Pressure Sensors

As illustrated in Figure 3.40 above, the remote data acquisition system acquired data with similar fluctuation patterns compared to the manual data obtained. The remote DAQ takes data points every 15 minutes, making the data set very populated.

Table 3.3 below summarizes the key performance data for pristine membranes and silver-coated membranes in the five testbed runs conducted, including the remote data acquisition data from the testbed deployment run. As illustrated by the results obtained from the student t-test, the flux results from all testbed runs had statistically significant differences between the pristine and silver-coated membranes, with P-values less than 0.05 except for Run 2. However, after 2 weeks of run, the flux values showed there was no statistically significant difference, with P-values greater than 0.05. When comparing salt rejection, most runs showed no statistically significant difference, except for Runs 4 and 5 showing P-values less than 0.05.

Table 3.3: Membrane Average Performance Summary from Testbed Runs

	Pristine		Silver-Coated		Student T-Test P-Values	
Run	Flux (LMH)	Salt Rejection (%)	Flux (LMH)	Salt Rejection (%)	Flux	Salt Rejection
1	9 ± 1.9	79 ± 6.7	18 ± 1.3	81 ± 7.0	0.00	0.55
2	8 ± 1.5	90 ± 6.0	8 ± 1.0	91 ± 4.1	0.99	0.07
3	13 ± 3.3	85 ± 7.5	11 ± 1.1	88 ± 10.1	0.00	0.06
4	12 ± 2.8	85 ± 3.5	11 ± 1.1	87 ± 2.9	0.00	0.00
5	7.4 ± 0.5	89.7 ± 2.6	6.6 ± 0.6	93.0 ± 1.2	0.00	0.00
DAQ	6.9 ± 8.4	95.5 ± 2.5	6.8 ± 6.7	93.0 ± 3.0	X	X

Table 3.4 below summarizes the amount of silver remaining and the percent silver released from the silver-coated membranes after each testbed run. Because Run 1 did not utilize a silver-coated membrane, it was intentionally excluded from the table. The percent silver released was calculated based on the previous membrane digestion, where 1.93 μg-Ag/cm^2 was loaded on the spiral-wound RO membranes. For each membrane used, three coupons were digested by agitating in 2% HNO_3 for 24 hours to obtain the standard deviation.

Table 3.4: Silver Remaining on Spiral Wound Membranes After Use and Percent Released Based upon Initial Loading

Testbed Run	Days of Operation	Silver Remaining ($\mu g\text{-}Ag/cm^2$)	% Silver Released
2	37	0.04 ± 0.01	98
3	51	0.08 ± 0.02	96
4	36	0.04 ± 0.01	98
5	34	0.55 ± 0.04	72

As illustrated in Table 3.4 above, after long-term operation, more than 90% of silver is released, except during Run 5. The lesser silver release observed in Run 5 could be attributed to the source water and Chandler WTP. The water there was not the finished water, meaning there was no chlorine added for disinfection. One speculation is that the presence of chlorine in tap water may promote silver release and promote the precipitation of silver in the form of silver chloride (AgCl). However, this has not been confirmed.

CHAPTER 4

DISCUSSION

In this chapter, the results provided in the previous chapter are discussed and speculations are made about reasons certain results were observed.

Permeability Tests

During the flat sheet membrane permeability tests, it was apparent that the higher flux rates achieved correlated with membranes with larger pore-sizes. The primary goal of the permeability tests was to observe the amount of water recovery (i.e. flux) lost due to the silver coating. For the Nylon MF membrane, a 3.7% average flux decline was observed due to the silver coating when filtering nanopure water, and a 15.9% average flux decline was observed when filtering tap water. For the PVDF MF membrane, an 8.6% average flux decline was observed when filtering nanopure water, and a 11.6% average flux decline was observed when filtering tap water. For the Regenerated Cellulose UF membrane, a 6.5% average flux decline was observed due to the silver coating when filtering nanopure water, and a 3.4% increase in average flux was observed when filtering tap water. For the PES UF membrane, a 9.2% average flux decline was observed due to the silver coating when filtering nanopure water, and a 5.6% increase in average flux was observed when filtering tap water. For the Polyamide RO membrane, a 12.5% average flux decline was observed due to the silver coating when filtering nanopure water, and a 16.7% average flux decline was observed when filtering tap water.

On average, the flux decline due to the silver coating when filtering tap water for all membrane types was 8.1%, and when filtering tap water was 7.0%. The flux decline

was expected, due to the presence of silver particles on the membrane surface and in the pores of the membrane. However, due to the small nature of the silver nanoparticles, the flux decline was minimal and even negligible in some cases, where pore-blockage did not occur.

Static Leaching Test

During the static leaching tests, it was hypothesized that there would be an inverse relationship between pH and silver leached (i.e. a decrease in pH would result in an increase in silver release). While this hypothesis was found to be true with regards to the Nylon MF and Polyamide RO membrane, it was disproved with the PVDF MF, Regenerated Cellulose UF, and PES UF membranes. For these membranes, the pH 6.0 solution caused the most silver release where both UF membranes experienced nearly 100% more silver release for pH 6.0 solutions compared to pH 2.0 solutions. Therefore, it may be possible that silver release is not dependent upon the pH of the solution, but more a function of the composition or chemical properties of the surface the silver is bound to. However, for all membrane types, the pH 2.0 solution released substantially more silver than the pH 8.0 solution, ranging between 15% – 79% more silver released. The pH 2.0 solution was designed to represent a CIP protocol that may take place during membrane rejuvenation, the pH 6.0 solution was designed to represent slight decreases in water quality during operation, and pH 8.0 solution was designed to represent ambient pH experienced during normal operation.

SEM/EDX

For the MF membranes, high quality images showing the pore-structures and sizes were obtained. The UF membranes did not appear to have visible pores, as the pore-sizes are on the nano-scale. Additionally, the Regenerated Cellulose membrane was easily damaged before high-resolution images could be captured. The Polyamide RO membrane showed complex surface properties with no visible pores, due to the semi-permeable nature of the membrane. It was hypothesized that silver peaks would be apparent during the elemental analyses, however most of the membranes did not have silver peaks in the EDX results. Upon further investigation, it was determined that the 10,000x magnification the EDX analysis was conducted at was analyzing approximately 127 μm^2 of membrane surface. Therefore, when considering the average silver-loading rate of 1.93 $\mu g/cm^2$ of membrane surface, it was determined that the EDX was analyzing approximately 2.44×10^{-8} μg of silver, which would not be enough mass to create elemental peaks during analyses.

Silver Loading on Spiral-Wound RO Membrane

As mentioned earlier, the silver loaded onto the spiral-wound RO membrane during the In-Situ coating procedure was on average 1.93 ± 0.12 $\mu g/cm^2$. After the membrane was operated in a POU system, 98% of the silver was released. However, the amount of silver required to have beneficial antimicrobial properties is very low, and the HPC counts performed support that the silver maintains antimicrobial properties at this concentration. Additionally, if the silver was completely depleted after an extended

operating period, it would be possible to repeat the In-Situ coating procedure to add more silver nanoparticles.

Mobile NEWT Testbed

During the Mobile NEWT Testbed evaluations, each test run served a different purpose. The primary metrics used for analyses were the flux rates and the salt rejection percentages, which were used to compare the pristine RO membrane to the silver-coated RO membrane. Secondary metrics were used for analyses depending on the tests being performed, such as chromium rejection. During Run 1, or the baseline unit comparison, Unit 1 observed a much lower flux rate than Unit 2, at about 100% less permeate production using the same feed flow and pressure. Upon addressing minor leaks in the Unit 1 POU system, it was determined that Unit 1 was suffering due to a lower quality feed water source. This lower quality feed water source was attributed to the positioning of the Unit, where Unit 2 was directly after the feed water inlet, and Unit 1 was placed at the end of the distribution system. At this location, the feed pipe was thought to have a "dead-zone", where water could sit stagnant for 12 hours during the night when the system was not operating, promoting microbial growth before turning back on. For this reason, a flushing system was installed, using a solenoid valve on a timer. The solenoid valve would turn on two times during the night for 30 minutes each time, with the purpose of flushing any stagnant water that may have accumulated overnight. After the installation, both units appeared to behave similarly with equal flux rates. The salt rejection for both units was also comparable, at 79% and 81% average rejection rates for Unit 1 and Unit 2, respectively ($P = 0.55$).

During Run 2, when the silver-coated spiral-wound RO membrane was first tested in comparison with a pristine RO membrane, the average flux rates and salt rejection rates were relatively the same. The average flux rate for both Unit 1 and Unit 2 was 8 LMH, while the average salt rejection for Unit 1 and Unit 2 was 90% and 91%, respectively. For Runs 3 through 5, a slight decrease in average flux rates was observed due to the silver coating, at about 8.9%. The salt rejection rates for the pristine membrane and the silver-coated membrane was virtually the same during all testbed runs.

During the Testbed Run 3 for the chromium spike, an issue was encountered with the dosing pump used to spike the potassium dichromate solution. During 1 week of operation, it was observed that the level of the solution in the feed tank was not decreasing. Upon further inspection, an air bubble was noticed in the feed line of the dosing pump, despite initially being purged of air. This is the reason the feed concentration of chromium ranged between 1 and 60 ppb, when the target concentration was 50 ppb. However, the average rejection rate for both the pristine and silver-coated membrane remained above 90%. Additionally, during the testbed Run 5 at the Chandler Water Treatment Plant, the rejection rate of major cations and arsenic were relatively the same between the pristine membrane and the silver-coated membrane. It was also observed that small amount of chromium was removed by the cartridge filters. The sediment filter and carbon blocks played a small role in adsorbing chromium, where the feed concentration was around 50 ppb, and the concentration after the cartridge filters was around 40 ppb, meaning 10 ppb was removed by direct filtration from the sediment filter or by adsorption into the carbon blocks,

During the induced fouling test (Run 4) and the testbed deployment (Run 5), UV-254 and TOC was monitored. These organic paramters are important to monitor and regulate, because their presence indicates a water samples ability to form disinfection byproducts after chlorination. However, both membranes showed promising rejection rates of both UV-254 abs and TOC.

To discuss the safety and sustainability of the silver-coated membrane, an examination of the kinetics of silver released was conducted several times. For the three times examined, consistent results were yielded. During the dynamic leaching test, silver was released at a higher concentration in the permeate flow than the concentrate flow. However, both flow regimes decreased to less than 5 ppb of silver within 3 hours. During the chromium spike test, silver was initially released from both the permeate and concentrate flow regimes at maximum concentrations of 31 ppb and 7 ppb, respectively. After two hours of operation, the concentration of silver in the permeate and concentrate flow regimes decreased to 11 ppb and 2 ppb, respectively. After a day of operating, little to no silver (i.e. < 5 ppb) was found in both the permeate and concentrate flow regimes of Unit 2. During the induced fouling test (Run 5), silver was initially released from both the permeate and concentrate flow regimes at maximum concentrations of 30 ppb for both. After five hours of operation, the concentration of silver in the permeate and concentrate flow regimes decreased to 9 ppb and 15 ppb, respectively. After a day of operating, the permeate and concentrate silver concentrations decreased to 11 ppb and 3 ppb, respectively. Afterwards, little to no silver (i.e. < 5 ppb) was detected in both the permeate and concentrate flow regimes of Unit 2. The EPA holds a secondary maximum

contaminant level (MCL) for silver at 100 ppb. Therefore, the silver-coated membrane meets the MCL, even during the peak silver-release within the first hours of operation.

The first HPC analysis conducted after the pristine membrane vs. the silver-coated membrane comparison test showed promising results, with much more microbial growth on the uncoated membrane compared to the coated membrane. However, the other two HPC analyses showed varying results, with one side of the silver-coated membrane having more microbial growth than the uncoated membrane, and the other side having less. While the HPC is a valuable tool, microbiological analysis can be misleading, due to the ease in which samples can be contaminated, misinterpreted, or invalid due to a lack of growth. For this reason, conclusions should not be made based on the HPC analyses alone.

Due to the high amount of silver leaching from the membranes, a literature review was conducted for comparison. The literature review examined papers from previous studies conducted on silver release from silver-embedded materials, such as textiles used for athletic clothing. Table 4.1 below illustrates the findings from this research compared to other studies, including silver-loading and percent silver released.

Table 4.1: Silver Loading and Release Comparison

Author of Paper	**Material Embedded with Silver**	**Initial Silver Loading (μg-Ag/cm^2)**	**Time of Use**	**Percent Released After Use (%)**
Thesis	RO Membrane	1.93	~ 35 Days	98%
Reed et al., 2016	Textiles for Athletic Clothing	0.34 in covalently tethered textile; 60.45 in commercial fabric	4 Washes with Detergent	76% in covalently tethered; 2.5% in commercial fabric
Mitrano et al., 2016	Textiles for Athletic Clothing	14 mg-Ag/kg-fabric	10 washes using color detergent and oxidizing detergent	22% with color detergent; 82% with oxidizing detergent
Hicks et al., 2015	Socks	Between 0.9 – 1,358 μg-Ag/g - textile	Washing in DI water for 1 – 24 hours	<1% for highest Ag-loading; 96 - 100% for most other socks
Mitrano et al., 2016	Textiles	Not Reported	1 wash cycle	10-25% for most detergents; 80% for industrial oxidizing detergent

While many studies report high percentage of silver release, the antimicrobial properties of silver remained, with one paper citing an inhibition > 99.9% of *E.coli* growth (Reed et al, 2016). This suggests that RO membranes coated with silver should also maintain high antimicrobial properties, despite the release of silver. Additionally, some papers indicate that smaller nanoparticles are released more than larger. One study

showed that after 10 washes using an oxidizing detergent, >35% of 100 nm Ag-particles remained on the fabric, while <20% of 60 nm Ag-particles remained on the fabric. This may suggest that larger nanoparticles are bound more efficiently to fabrics than their smaller counterparts (Mitrano et al., 2016).

CHAPTER 5

SUMMARY AND CONCLUSIONS

During the research conducted for this thesis, three main goals were addressed. The first goal was to analyze the performance and characteristics of silver-coated flat sheet membranes compared to pristine (uncoated) membranes. The second goal was to investigate the feasibility of scaling up the flat sheet In-Situ coating procedure into Spiral-Wound RO membranes for a POU system. And the third goal was to investigate the safety, sustainability, and performance of the In-Situ-synthesized Ag-NP spiral-wound RO membranes in terms of silver release, flux, salt rejection, and biofouling control. The major conclusions regarding the three primary goals and supplementary analyses presented within this thesis include:

- An initial flux decline around 17% was observed due to the silver-coating in the flat sheet membranes, which was consistent with previous studies.
- The surface characteristics of flat sheet membranes after the silver-coating was applied remained unchanged (i.e. surface charge remained negative, contact angle showed surface remained hydrophilic).
- The In-Situ silver-coating method is fast, easy, and effective, with the ability to load 1.93 μg of silver per cm^2 of membrane area.
- The In-Situ method does not require membranes to be fabricated, but rather can be modified, making the coating process more feasible than inventing a new method of membrane fabrication.
- Membrane characteristics are unaffected due to silver coating (i.e. contact angle remains <90° and thus hydrophilic, PZC for all membrane types remain around

pH 3.0, etc.) These are critical parameters to remain unchanged, because the hydrophilicity of a membrane affects the amount of water flux through the membrane. Additionally, the surface charge of the membrane is critical due to the types of ions that can adsorb to the membrane surface at different surface charges. For instance, divalent cations such as $CaCl_2$ and Na_2SO_4 more readily adsorb to membranes that are negatively charged (Childress & Elimelech, 1996). If the surface charge of a membrane becomes positive after modifications, biofouling could occur at a faster rate due to the nature of microorganisms and viruses being negatively charged.

- For the spiral-wound membranes, a slight decrease in flux was observed initially due to the silver coating, however the long-term benefits could outweigh the slight loss of flux.
- Salt rejection and contaminant removal by the RO membranes are unaffected by the silver coating, with both uncoated and coated membranes achieving the same removal efficiencies for monovalent and divalent ions, as well for hexavalent chromium and arsenic.
- Silver is released from the membrane within the first two hours of operation at levels below the secondary MCL of 100 ppb defined by the EPA, and drops to less than 5 ppb after two hours on average.
- After long-term operation between 34 and 51 days, 98% of the silver loaded onto the membranes is released when operated in a typical POU configuration.
- The HPC analyses suggest there is no statistically significant difference in the amount of biofouling formation between pristine and silver-coated membranes

during long-term operation, which could be caused by the high amount of silver lost from the membrane.

While there are several methods that have investigated coating silver onto membranes for biofouling resistance, this is the first time an In-Situ coating method has been scaled-up to the household level in spiral-wound POU membrane elements. Silver-coated spiral-wound membranes used in a POU system could increase the lifespan of RO membranes, saving time, money, and waste streams from entering landfills. In-Situ coating of silver on spiral-wound membranes remains a cost-effective method of preventing the formation of biofouling, and future possibilities such as scaling up further to municipal water treatment facilities could be investigated.

Future Research for this Project

Additional work that could be conducted to further investigate this research could be in both operational and analytical aspects of the research. After successfully coating many different types of membranes used in drinking water treatment processes (i.e. MF, UF, and RO), investigations into coating membranes in different configurations could be performed. For example, hollow fiber membranes are commonly used in drinking water treatment processes and are susceptible to biofouling, making hollow fiber membranes a feasible treatment process to perform an In-Situ Ag-NP coating on.

Supplemental research pertaining to the long-term, scaled-up spiral-wound study could also performed. After the silver coating has been depleted, it could be beneficial to apply an additional coating. Therefore, further investigations into the time when the second coating should take place, as well as the effectiveness of an additional coating

could be undertaken. Additionally, a longer-term study could be conducted on these membranes since they typically last up to two years before replacement is necessary due to fouling. For analytical investigations, it could be interesting to determine the types of microorganisms that are deposited on the pristine membrane vs. the silver-coated membranes. For instance, it is possible that similar results in fouling were observed due to silver-resistant microbes colonizing on the silver-coated membrane, compared to the typical microbes found in potable drinking water.

REFERENCES

Baek, Y., Kang, J., Theato, P., & Yoon, J. (2012). Measuring hydrophilicity of RO membranes by contact angles via sessile drop and captive bubble method: A comparative study. *Desalination*, *303*(Supplement C), 23–28. https://doi.org/https://doi.org/10.1016/j.desal.2012.07.006

Ben-Sasson, M., Lu, X., Bar-Zeev, E., Zodrow, K. R., Nejati, S., Qi, G., … Elimelech, M. (2014). In situ formation of silver nanoparticles on thin-film composite reverse osmosis membranes for biofouling mitigation. *Water Research*, *62*(Supplement C), 260–270. https://doi.org/https://doi.org/10.1016/j.watres.2014.05.049

Childress, A. E., & Elimelech, M. (1996). Effect of solution chemistry on the surface charge of polymeric reverse osmosis and nanofiltration membranes. *Journal of Membrane Science*, *119*(2), 253–268. https://doi.org/https://doi.org/10.1016/0376-7388(96)00127-5

Deng, L., Guo, W., Ngo, H. H., Zhang, H., Wang, J., Li, J., … Wu, Y. (2016). Biofouling and control approaches in membrane bioreactors. *Bioresource Technology*, *221*(Supplement C), 656–665. https://doi.org/https://doi.org/10.1016/j.biortech.2016.09.105

Fritzmann, C., Löwenberg, J., Wintgens, T., & Melin, T. (2007). State-of-the-art of reverse osmosis desalination. *Desalination*, *216*(1), 1–76. https://doi.org/https://doi.org/10.1016/j.desal.2006.12.009

Greenlee, L. F., Lawler, D. F., Freeman, B. D., Marrot, B., & Moulin, P. (2009). Reverse osmosis desalination: Water sources, technology, and today's challenges. *Water Research*, *43*(9), 2317–2348. https://doi.org/https://doi.org/10.1016/j.watres.2009.03.010

Jiang, S., Li, Y., & Ladewig, B. P. (2017). A review of reverse osmosis membrane fouling and control strategies. *Science of The Total Environment*, *595*(Supplement C), 567–583. https://doi.org/https://doi.org/10.1016/j.scitotenv.2017.03.235

Kochkodan, V., & Hilal, N. (2015). A comprehensive review on surface modified polymer membranes for biofouling mitigation. *Desalination*, *356*(Supplement C), 187–207. https://doi.org/https://doi.org/10.1016/j.desal.2014.09.015

Wang, Y., Wang, Z., Han, X., Wang, J., & Wang, S. (2017). Improved flux and anti-biofouling performances of reverse osmosis membrane via surface layer-by-layer assembly. *Journal of Membrane Science*, *539*(Supplement C), 403–411. https://doi.org/https://doi.org/10.1016/j.memsci.2017.06.029

Millipore Corporation (2008). Ultrafiltration Membranes: Ultrafiltration Membranes for Macromolecule Processing. *Millipore Product Selection Guide.* https://www.lenntech.com/Data-sheets/Millipore-Ultrafiltration-Membranes-L.pdf

Hicks, A. L., Gilbertson, L. M., Yamani, J. S., Theis, T. L., & Zimmerman, J. B. (2015). Life Cycle Payback Estimates of Nanosilver Enabled Textiles under Different Silver Loading, Release, and Laundering Scenarios Informed by Literature Review. Environmental Science and Technology, 49(13), 7529–7542. https://doi.org/10.1021/acs.est.5b01176

Mitrano, D. M., Limpiteeprakan, P., Babel, S., & Nowack, B. (2016). Durability of nano-enhanced textiles through the life cycle: releases from landfilling after washing. Environ. Sci.: Nano, 3(2), 375–387. https://doi.org/10.1039/C6EN00023A

Mitrano, D. M., Lombi, E., Dasilva, Y. A. R., & Nowack, B. (2016). Unraveling the Complexity in the Aging of Nanoenhanced Textiles: A Comprehensive Sequential Study on the Effects of Sunlight and Washing on Silver Nanoparticles. Environmental Science and Technology, 50(11), 5790–5799. https://doi.org/10.1021/acs.est.6b01478

Reed, R. B., Zaikova, T., Barber, A., Simonich, M., Lankone, R., Marco, M., … Westerhoff, P. K. (2016). Potential Environmental Impacts and Antimicrobial Efficacy of Silver- and Nanosilver-Containing Textiles. Environmental Science and Technology, 50(7), 4018–4026. https://doi.org/10.1021/acs.est.5b06043